

# **An Experimental Study of Mechanical and Impact behaviour of Nanofiller Infused Kevlar based Composites**

## **A PROJECT REPORT**

*Submitted by*

**Soumitra Manish Dodkey**

**(18103086)**

**Rishi Suhas Karandikar**

**(18103096)**

**S Srinidhi**

**(18103104)**

*in partial fulfilment for the award of the degree  
of*

**BACHELOR OF TECHNOLOGY**

*in*

**AEROSPACE ENGINEERING**



**DEPARTMENT OF AEROSPACE ENGINEERING**

**SCHOOL OF AERONAUTICAL SCIENCES**

**HINDUSTAN INSTITUTE OF TECHNOLOGY AND SCIENCE**

**PADUR, CHENNAI – 603103**

**MAY, 2022**

**HINDUSTAN INSTITUTE OF TECHNOLOGY AND SCIENCE**  
**PADUR, CHENNAI - 603 103**

**BONAFIDE CERTIFICATE**

It is certified that this project report titled “**An Experimental Study of Mechanical and Impact behaviour of Nanofiller Infused Kevlar based Composites**” is the bonafide work of “**Soumitra Manish Dodkey (18103086), Rishi Suhas Karandikar (18103096) and S Srinidhi (18103104)**” who carried out the project work under my supervision. It is certified further that to the best of my knowledge the work reported here does not form part of any other project / research work on the basis of which a degree or award was conferred on an earlier occasion on this or any other candidate.

**HEAD OF THE DEPARTMENT**

Dr P. Vasanthakumar

Department of Aeronautical Engineering  
Hindustan Institute of Technology &  
Science, Padur

**SUPERVISOR**

Dr Piyush Gaur

Associate Professor

Department of Aeronautical Engineering  
Hindustan Institute of Technology &  
Science, Padur

The Project Viva-Voce Examination is held on **0 /05/2022**.

**INTERNAL EXAMINER**

**EXTERNAL EXAMINER**

## ACKNOWLEDGEMENT

We would like to place on record our sincere thanks to all those who contributed to the successful completion of our final year project work.

It's a matter of pride and privilege for us to express our deep gratitude to the management of Hindustan Institute of Technology and Science for providing us with the necessary facilities and support.

We express our deep sense of gratitude to our respected Chairperson **Dr. (Mrs.) Elizabeth Verghese** and Pro-Chancellor **Dr. Anand Jacob Verghese** for giving us an opportunity to do the project.

We would like to thank our Director **Mr Ashok Verghese** and Vice-Chancellor **Dr. S.N. Sridhara** for giving us moral support to complete this project.

We would like to express our gratitude to Dean (E&T) **Dr. Angelina Geetha** and Registrar **Dr. Pon. Ramalingam** for their support and encouragement.

We extend our sincere thanks to our Head of the Department **Dr. P Vasanthakumar** for inspiring and motivating us to complete this project.

We would like to thank our guide **Dr. Piyush Gaur** for continually guiding and actively participating in our project and giving valuable suggestions to complete our project.

We would like to thank all the faculty members of the School of Aeronautical Sciences, who have directly or indirectly extended their support.

Last, but not least, we are deeply indebted to our parents who have been our greatest support while we worked day and night for the project to make it a success.

## ABSTRACT

Composite materials are used in a variety of vital applications, including aerospace, defence, and marine. As a result, it is critical to investigate the failure of these materials-based components. Testing of these materials can provide information such as mechanical properties, fatigue life, and impact properties allowing their application to be better understood. The purpose of this study is to develop a lighter Kevlar-based material while also improving its mechanical strength, impact resistance, and toughness. The goal of this study is to determine the best combination of a set proportion of MWCNT and changing weight percent of Seashell & Alumina nanofillers to improve the mechanical properties of a Kevlar fibre-reinforced nanocomposite. This work involves the development of Kevlar fibre reinforced epoxy nanocomposite incorporating Multiwall Carbon Nanotubes (MWCNT), nano alumina, and nano seashell in various combinations that can be used in the lightweight structure of aircraft and armoured vehicles. The prevailing advancement covers the use of nanofillers in specific proportions in the Kevlar-based nanocomposite material which is generally used in lightweight applications in the aerospace and defence sector. The high need for nanofiller in advanced material engineering stems from the fact that their properties improve with greater research.

**Keywords:** Kevlar, Kevlar-based composites, Mechanical properties, Nanofillers, Alumina, Seashell, MWCNT, Impact Testing, Fatigue performance.

# TABLE OF CONTENTS

CHAPTER NO.	TITLE	PAGE NO.
	Abstract	i
	List of Tables	iv
	List of Figures	v
	List of Abbreviations	ix
<b>1</b>	<b>INTRODUCTION</b>	
	1.1. General Introduction	1
	1.2. Matrix Material	2
	1.3. Design of Composites	3
	1.4. Nanotechnology in Composites	4
	1.5. Aramid Fibres	5
	1.6. Summary	6
<b>2</b>	<b>LITERATURE REVIEW</b>	
	2.1. Literature Survey	7
	2.2. Research Gap	15
	2.3. Summary	15
<b>3</b>	<b>METHODOLOGY</b>	16
<b>4</b>	<b>SEASHELL + MWCNT</b>	
	4.1. Introduction	20
	4.2. Preparation of Nano Seashell	21
	4.3. Morphological Studies of Nano Seashell	23
	4.4. Fabrication of Plates	25
	4.5. Mechanical & Impact Analysis for Specimens	32
	4.6. Summary	60
<b>5</b>	<b>ALUMINA + MWCNT</b>	
	5.1. Introduction	61
	5.2. Morphological Studies of Nano Alumina	63
	5.3. Fabrication of Plates	65

	5.4. Mechanical & Impact Analysis for Specimens	65
	5.5. Summary	91
<b>6</b>	<b>CONCLUSION &amp; FUTURE WORKS</b>	
	6.1 Summary	92
	6.2 Conclusion	92
	6.3 Future Scope	93
<b>7</b>	<b>REFERENCES</b>	94

## LIST OF TABLES

<b>Table Number</b>	<b>Description</b>	<b>Page Number</b>
1.1	Properties of different types of Kevlar	6
4.1	Elemental Concentration of Nano Seashell	24
4.2	Comparative Analysis of UTM and Young's Modulus for different Seashell Nanofiller content	38
4.3	Flexural Stress Variation in different Seashell filler content	44
4.4	Flexural Strain Variation in different Seashell filler content	44
4.5	Flexural Strength Variation in different Seashell filler content	45
4.6	Comparative Analysis of Results obtained by 3 point bending test	46
4.7	Variation of Flexural Modulus for different Seashell Fillers content	50
4.8	Variation of Impact Strength with different Seashell filler content	53
5.1	Properties of Alumina Nano powder	62
5.2	Elemental Concentration of Nano Alumina	64
5.4	Comparative Analysis of UTM and Young's Modulus for different Alumina Nanofiller content	70
5.5	Flexural Strain Variation in different Alumina filler content	77
5.6	Flexural Strength Variation in different Alumina filler content	78
5.7	Comparative Analysis of Results obtained by 3 point bending test	79
5.8	Variation of Interlaminar Shear Strength for different Alumina Fillers content	83
5.9	Variation of Impact Strength of different Alumina nano filler content	85
5.10	Maximum Shear Stress for different nanofiller content	89

## LIST OF FIGURES

<b>Figure Number</b>	<b>Description</b>	<b>Page Number</b>
1.1	Epoxy Resin LY556 and Hardener HY951	3
1.2	Design considerations for composites	4
1.3	Composite design concurrence	4
1.4	Aramid Kevlar Fabric	6
4.1	Seashells	22
4.2	Hammered Seashells	22
4.3	Ball Milling Machine	22
4.4	Nano Seashell Powder	22
4.5	SEM Image of Nano Seashell	23
4.6	SEM Image of Nano Seashell	23
4.7	XRD of Nano Seashell	24
4.8	EDS of Nano Seashell	24
4.9	Kevlar Fabric of 320 mm × 320 mm	25
4.10	Epoxy LY556 measured	26
4.11	Applying Epoxy-Hardener Mixture	27
4.12	Dead weights for curing of composite plates	27
4.13	Fabricated Kevlar Composite Plate	27
4.14	Specimen sizing according to ASTM Standards of tests to be performed marked on Fabricated Kevlar Plate for Water Jet Cutting	28
4.15	Kevlar Fabric of 320 mm × 320 mm	29
4.16	Epoxy LY556 measured	29
4.17	MWCNT OF 0.25 g	29
4.18	Seashell Nanofiller	30
4.19	Sonification of Epoxy-nanofiller mixture	30
4.20	Applying Resin + Seashell nanofiller+ MWCNT Mixture on Kevlar plates	31
4.21	Dead weights for curing of composite plates	31
4.22	INSTRON Universal Testing Machine	33
4.23	Tensile Test Specimen fixed in UTM Fixture	33



4.24	Engineering Stress - Strain Graph for Neat Kevlar Specimens	34
4.25	Engineering Stress - Strain Graph for Seashell 1% + 0.25% MWCNT Specimens	35
4.26	Engineering Stress - Strain Graph for Seashell 3% + 0.25% MWCNT Specimens	36
4.27	Engineering Stress - Strain Graph for Seashell 7% + 0.25% MWCNT Specimens	37
4.28	Comparative Analysis of UTM and Young's Modulus for different Seashell Nanofiller content	38
4.29	Failed Tensile Test Specimens	39
4.30	Failed Tensile Test Specimens	39
4.31	SEM Image of Failed Tensile Test Specimen	40
4.32	SEM Image of Failed Tensile Test Specimen	40
4.33	3 Point Bending Test Setup	41
4.34	3 Point Bending Test of Specimen	41
4.35	Load v/s Cross Head Travel for Neat Kevlar Specimens	42
4.36	Load v/s Cross Head Travel for 1% Seashell + 0.25% MWCNT infused Kevlar Specimens	42
4.37	Load v/s Cross Head Travel for 3% Seashell + 0.25% MWCNT infused Kevlar Specimens	43
4.38	Load v/s Cross Head Travel for 7% Seashell + 0.25% MWCNT infused Kevlar Specimens	43
4.39	Flexural Stress Variation in different Seashell filler content	44
4.40	Flexural Strain Variation in different Seashell filler content	45
4.41	Flexural Strength Variation in different Seashell filler content	45
4.42	Failed 3 Point Bending Test Specimens	47
4.43	Failed 3 Point Bending Test Specimens	47
4.44	Load v/s Cross Head Travel for Neat Kevlar Specimens of ILSS	48
4.45	Load v/s Cross Head Travel for 1% Seashell + 0.25% MWCNT infused Kevlar Specimens of ILSS	48
4.46	Load v/s Cross Head Travel for 3% Seashell + 0.25% MWCNT infused Kevlar Specimens of ILSS	49
4.47	Load v/s Cross Head Travel for 7% Seashell + 0.25% MWCNT infused Kevlar Specimens of ILSS	49
4.48	Variation of Flexural Modulus for different Seashell Fillers content	50
4.49	Failed ILSS Test Specimen	51
4.50	Failed ILSS Test Specimen	51
4.51	Charpy Impact Testing Setup	52
4.52	Absorbed Energy Reader	53

4.53	Variation of Impact Strength for different Seashell Filler content	53
4.54	Failed Charpy Impact Test Specimen	54
4.55	Failed Charpy Impact Test Specimen	54
4.56	Universal Testing Machine for Shear Test	55
4.57	Shear testing fixture attached in UTM	55
4.58	Shear Test Specimen fixed in the testing fixture	56
4.59	Shear Stress vs Shear Strain Graph for Neat Kevlar Specimens	56
4.60	Shear Stress vs Shear Strain Graph for 1% Seashell + 0.25% MWCNT infused Kevlar Specimen	57
4.61	Shear Stress vs Shear Strain Graph for 3% Seashell + 0.25% MWCNT infused Kevlar Specimen	57
4.62	Shear Stress vs Shear Strain Graph for 7% Seashell + 0.25% MWCNT infused Kevlar Specimen	58
4.63	Variation of Maximum Shear Stress for different Seashell filler content	59
4.64	Failed Shear Test Specimen	59
4.65	Failed Shear Test Specimen	59
5.1	SEM Image of Nano Alumina	63
5.2	SEM Image of Nano Alumina	63
5.3	XRD Image of Nano Alumina	64
5.4	EDS of Nano Alumina	64
5.5	INSTRON Universal Testing Machine	66
5.6	Engineering Stress - Strain Graph for Neat Kevlar Specimens	67
5.7	Engineering Stress - Strain Graph for Alumina 1% + 0.25% MWCNT Specimens	68
5.8	Engineering Stress - Strain Graph for Alumina 3% + 0.25% MWCNT Specimens	69
5.9	Engineering Stress - Strain Graph for Alumina 6% + 0.25% MWCNT Specimens	70
5.10	Comparative Analysis of UTM and Young's Modulus for different Alumina Nanofiller content	71
5.11	Failed Tensile Test Specimen	72
5.12	Failed Tensile Test Specimen	72
5.13	SEM Image of Failed Tensile Test Specimen	73
5.14	SEM Image of Failed Tensile Test Specimen	73
5.15	3 Point Bending Test Setup	74
5.16	Load v/s Cross Head Travel for Neat Kevlar Specimens	75

5.17	Load v/s Cross Head Travel for 1% Alumina + 0.25% MWCNT infused Kevlar Specimens	75
5.18	Load v/s Cross Head Travel for 3% Alumina + 0.25% MWCNT infused Kevlar Specimens	76
5.19	Load v/s Cross Head Travel for 6% Alumina + 0.25% MWCNT infused Kevlar Specimens	76
5.20	Flexural Stress Variation in different Alumina filler content	77
5.21	Flexural Stress Variation in different Alumina filler content	77
5.22	Flexural Strength Variation in different Alumina filler content	78
5.23	Failed 3 Point Bending Test Specimens	80
5.24	Failed 3 Point Bending Test Specimens	80
5.25	Load v/s Cross Head Travel for Neat Kevlar Specimens of ILSS	81
5.26	Load v/s Cross Head Travel for 1% Alumina + 0.25% MWCNT infused Kevlar Specimens of ILSS	81
5.27	Load v/s Cross Head Travel for 3% Alumina + 0.25% MWCNT infused Kevlar Specimens of ILSS	82
5.28	Load v/s Cross Head Travel for 6% Alumina + 0.25% MWCNT infused Kevlar Specimens of ILSS	82
5.29	Variation of Flexural Modulus for different Alumina Fillers content	83
5.30	Failed ILSS Test Specimen	84
5.31	Failed ILSS Test Specimen	84
5.32	Charpy Impact Testing Setup	85
5.33	Variation of Impact Strength for different Alumina filler content	85
5.34	Failed Charpy Impact Test Specimen	86
5.35	Failed Charpy Impact Test Specimen	86
5.36	Universal Testing Machine for Shear Test	87
5.37	Shear Test Specimen fixed in the testing fixture	87
5.38	Shear Stress vs Shear Strain Graph for Neat Kevlar Specimens	87
5.39	Shear Stress vs Shear Strain Graph for 1% Alumina + 0.25% MWCNT infused Kevlar Specimens	88
5.40	Shear Stress vs Shear Strain Graph for 3% Alumina + 0.25% MWCNT infused Kevlar Specimens	88
5.41	Shear Stress vs Shear Strain Graph for 6% Alumina + 0.25% MWCNT infused Kevlar Specimens	89
5.42	Variation of Maximum Shear Stress for different Alumina filler content	90
5.43	Failed Shear Test Specimen	90
5.44	Failed Shear Test Specimen	90

## LIST OF ABBREVIATIONS

ABBREVIATIONS	DESCRIPTION
MMCs	Metal matrix composites
pMMCs	Particle-reinforced metal matrix composites
HC-1	Hybrid composite-1
PM	Powder metallurgy
PMCs	Polymer matrix composites
CMCs	Ceramic matrix composites
$\mu\text{m}$	Micro meter
SEM	Scanning electron microscope
HRSEM	High resolution scanning electron microscope
TEM	Transmission electron microscope
MWCNTs	Multi-walled carbon nano tubes
PSR	Particle size ratio
CNTs	Carbon nano tubes
MPa	Mega Pascal
EDS	Energy dispersive spectroscope
GPa	Gega Pascal
$\sigma_s$	Shear Stress
$\epsilon_f$	Shear Strain
$V_f$	Volume fractions of the reinforcement
$V_m$	Volume fractions of the matrix
$y_m$	The yield stress of the unreinforced matrix
ROM	Rule of mixture
ASTM	American society for testing and materials
G	Shear modulus of the matrix
UTM	Universal Testing Machine

UTS	Ultimate Tensile Strength
$\Delta\sigma$	Increase in yield strength
$\epsilon$	Strain
W	Normal load
Cm	Centimeter
mm	millimeter
g	Gram
M	Meter
min	Minute
s	second
m/s	Meter per second
mm/min	millimeter per minute
N	Newton
nm	Nano meter
S	Shearing Distance
Wt. %.	Weight percentage
Al <sub>2</sub> O <sub>3</sub>	Alumina
CaCO <sub>3</sub>	Seashell
<sup>o</sup> C	Degree Celsius
XRD	X-ray diffraction
$\lambda$	The wavelength of the X-ray

# **CHAPTER 1**

## **INTRODUCTION**

### **1.1 GENERAL INTRODUCTION**

Composites have emerged as a valuable class of engineering materials because they provide many attributes not attainable with different materials. Light weight, plus high stiffness, and selectable properties have fostered their use for several years in satellites, high performance aircraft and missiles further as submarines. Now, these materials demonstrate their worth within the mundane, but equally as demanding, consumer, infrastructure, and sports equipment arenas.

Designing a composite part is in some ways a designer's dream, with nearly infinite combinations of materials that will be utilized to achieve specific design goals. Composites have recently gained much attention because of their weight-adjusted (or specific) stiffness and strength, which allow for light weighting in fly- or drive-away implementations. Thus, aerospace companies are increasing the composite content in their products. Demand is increasing in other industries supported additional material properties available in composites. Because of how composites are produced, they're both heterogeneous and anisotropic. Composite materials are heterogeneous because they're composed of assorted materials with different physical, mechanical and electrical properties. Along different axes, composites have different mechanical and electrical properties because of which they need to be analysed in more rigour manner. Using mechanics of materials approach analysis of composites is carried out which is designers first choice.

Modem structural composites, frequently brought up as 'Advanced Composites', are a mix of two or more components, one amongst which is created of stiff, long fibres, and also the other, a binder or 'matrix' which holds the fibres in situ. The

fibres are strong and stiff relative to the matrix and are generally orthotropic (having different properties in two different directions). The fibre, for advanced structural composites, is long, with length to diameter ratios of over 100. The fibres strength and stiffness are usually much greater, perhaps several times more, than the matrix material. The matrix material can be polymeric (e.g. polyester resins, epoxies), metallic, ceramic or carbon. When the fibre and therefore the matrix are joined to create a composite they keep their individual identities and both directly influence the composite's final characteristics. The resulting composite will generally be composed of layers (laminate) of the fibres and matrix stacked to attain the required properties in one or more directions. It is well known that advanced composites show high strength to weight ratio and high stiffness to weight ratio.

## **1.2 MATRIX MATERIAL**

Besides having its own advantages, fibre has limits in its engineering applications, within which it cannot transmit the load from one to a different. The composite are include fibre and matrix material that are embedded together, where the matrix serves to bind and transfer the load to the fibre and protect them again environmental attack and damage because of handling. During this research, epoxy glue is that the variety of matrix that's visiting be accustomed fabricate fibre composites. Epoxy glue is nearly totally transparent when cured. Epoxy is employed as a structural matrix material or as structural glue within the aerospace industry. Resin may be a good resistance to most chemicals, good resistance to creep and fatigue, high strength and good electrical properties. To fabricate the composites, the hand lay-up construction method are employed in this research. There are major advantages of using hand lay-up methods; low moulding costs, it's widely and commonly used, it's possible for big products small series products.



**Figure 1.1** Epoxy Resin LY556 and Hardener HY951

The Matrix possesses these functions and requirements:

- Keep the fibres in place within the structure;
- Help to distribute or transfer loads;
- Protect the filaments, both within the structure and before and thru fabrication;
- Control the electrical and chemical properties of the composite;
- Carry interlaminar shear loads.

The desired properties of the matrix that depend on the purpose of the structure are to minimize moisture absorption, have low shrinkage, it should be wet and should bond to fibre. It should have elongation greater than fibre which would result in appreciable strength and modulus. During curing process matrix should penetrate the fibre bundles and should avoid voids. Matrix should be elastic in nature to be able to transfer load to fibres. It should have good chemical and dimensional stability. The main aim of the composite manufacturing process are to achieve a uniform product by controlling fibre thickness, fibre volume, fibre directions and by minimizing voids.

### **1.3 DESIGN OF COMPOSITES**

The design process for composites involves both laminate design and component design and must also include considerations of the manufacturing process and



eventual environmental exposure. These steps are all interdependent with composites and therefore the most effective design must involve true concurrent engineering.

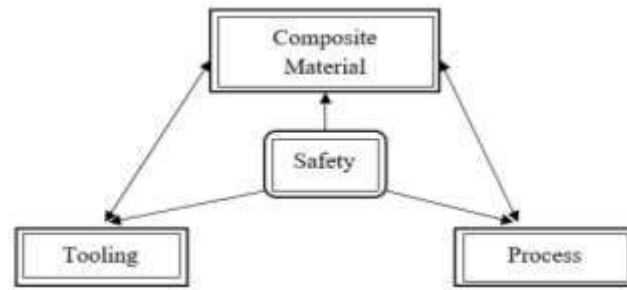


**Figure 1.2** Design considerations for composites

The design of composite structures is complicated by the actual fact that each different material property used must be defined as shown in figure 4.2. Composites cannot be designed without concurrence. Design details rely on tooling and processing and assembly & inspection. Good structural design may be a compromise between design requirements and constraints. As shown in figure 4.3, the event process for any component consists of design, analysis and manufacturing process.

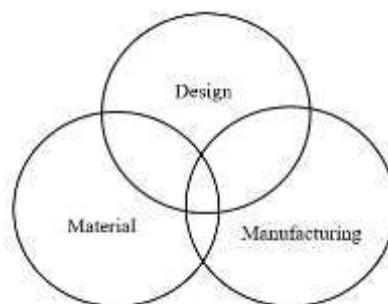


**Figure 1.3** Composite design concurrence

## 1.4 NANOTECHNOLOGY IN COMPOSITES

Nanotechnology is one of the foremost popular areas in current research and development in all technical disciplines. It shows great promise for providing many breakthroughs within the near future. This can change the direction of technological advances during a wide selection of applications. It may be defined because

the science and engineering involved within the design, synthesis, characterization, and application of materials and devices whose smallest functional organization in a minimum of one dimension is on the scale of nano meter. Nanotechnology is additionally defined because the manipulation of materials, measuring 100 nm or less in a minimum of one dimension where the physical, chemical, and biological properties are fundamentally different from those of the majority material. The major advantages of nano composites involves improvement of mechanical properties with increased stiffness without flexibility loss and dimensional stability being improved. With nano composites better scratch resistance can be achieved and considerably better thermal and chemical stability.

## **1.5 ARAMID FIBRES**

Aramid fibre is that the generic term for a selected form of 'aromatic polyamide fibre.' Kevlar aramid, an organic fibre with high specific tensile modulus and strength. This was the primary organic fibre to be used as a reinforcement in advanced composites. Aramid fibre is manufactured by extruding a polymer solution through a spinneret. The organic fibre Kevlar, also called aramid, essentially revolutionized pressure vessel technology thanks to its great lastingness and consistency as well as denseness leading to weigh more weight effective designs for rocket motors. Aramid composites have relatively poor shear and compression properties; careful design is requires for his or her use in structural applications that involve bending or compression. Excellent vibration-damping characteristics are achieved for composites reinforced with aramid fibres. Aramid fibre is comparatively flexible and difficult. Composites with aramid was initially being implemented for its applications intended to weight saving was critical like in outer space vehicles, components of aircraft, missile structure and helicopter parts. Aramid showed its armour applications by the superior ballistic and performance of structure.



**Figure 1.4** Aramid Kevlar Fabric

**Table 1.1** Properties of different types of Kevlar

Nominal Properties of Aramid Fibre				
Tensile Property	Unit	Type of Kevlar		
		29	49	149
Modulus	GPA	83	124	173
Strength	GPA	3.6	3.85	3.4

## 1.6 SUMMARY

In this chapter we have discussed about

- Composites in general, advanced composites and need of Nanotechnology in composites.
- We have also given brief overview of Matrix and Fabric in composites, its role and advantages.
- Design consideration for composite manufacturing is also been covered in this chapter.
- General description about Aramid Fibre with some basic properties and difference between majorly used different types of Kevlar in ballistic applications.

## **CHAPTER 2**

### **LITERATURE REVIEW**

#### **2.1 LITERATURE SURVEY**

Raghavendra et *al.* (2015) studied the influence of micro/nano alumina ( $\text{Al}_2\text{O}_3$ ) on the mechanical properties of epoxy/jute fiber (J)/glass fiber (G) laminates was studied. It was also found that nanofiller-added composites show better results when compared with and without microfiller-added composites. The morphology of the surfaces was examined by scanning electron microscopy to have better insight into the flexural and tensile mechanism.

Nidhi Sharma et *al.* (2019) studied the influence of MWCNT addition on such properties as the density, hardness, fracture toughness, and wear behavior of both conventionally sintered and SPSeD  $\text{Al}_2\text{O}_3$ –MWCNT composite. The plots suggest that the wear resistance of  $\text{Al}_2\text{O}_3$ –MWCNT composites improves significantly when MWCNT is introduced into the  $\text{Al}_2\text{O}_3$  matrix up to a low loading level of 3 vol%.  $\text{Al}_2\text{O}_3$ -based composites are potential engineering materials possessing superior mechanical as well as tribological properties.

Zhang Hui et *al.* (2010) has investigated the mechanical properties of nano-alumina-filled E-54/4, 4-diaminodiphenylsulphone (DDS) epoxy resins prepared by combining high-speed mixing and three-roll milling. Transmission electron microscopy revealed a homogeneous dispersion of nano-alumina with small agglomerates in epoxy resin (TEM). The addition of nano-alumina fillers increased the nanocomposites' static/dynamic modulus, tensile strength, and fracture tough-

ness all at the same time. When compared to the unfilled epoxy resin, nanocomposite filled with 18.4 wt percent alumina nanofillers increased KIC and GIC by about 50% and 80%, respectively. Furthermore, scanning electron microscopy (SEM) and atomic force microscopy (AFM) techniques were used to examine the corresponding fracture surfaces of tensile and compact tension samples in order to identify the relevant fracture.

Minjie Wu *et al.* (2020) has also investigated the effects of  $\text{Al}_2\text{O}_3$  nanoparticles on the mechanical properties of the composites by tensile and impact tests. For the prepared nanocomposite with 3.0 wt.% of  $\text{Al}_2\text{O}_3$  addition, the tensile strength, elongation at break and impact strength reached 74.83 MPa, 10.63% and 13.79  $\text{kJ/m}^2$ , and were improved by 82.60%, 33.38% and 63.58%, respectively, compared with those of pure epoxy resin.

Raouf Belgacemi *et al.* (2020) has prepared a unique hybrid material from various amounts of silane surface modified alumina nanoparticles, oxidized ultra-high molecular weight polyethylene (UHMWPE) fibers, and epoxy resin. The mechanical results, namely tensile and bending, confirmed the positive effects of increasing the nanofillers amounts up to 5 wt%. The thermochemical properties analyzed by dynamic mechanical analysis (DMA) revealed consequent improvements in the storage modulus and glass transition temperature upon the addition of the nanophase.

AHI Mourad *et al.* (2020) have reported the fabrication and characterization of high-strength Kevlar epoxy composite sheets for structural application. This process includes optimization of the curing conditions of composite preparation, such as curing time and temperature, and the incorporation of nanofillers, such as

aluminum oxide ( $\text{Al}_2\text{O}_3$ ), silicon carbide ( $\text{SiC}$ ), and multi-walled carbon nanotubes (MWCNT) in different weight percentages. In this study, the highest mechanical strength was obtained at 0.5% MWCNT incorporation.

SAB Hasan et al. (2014) investigated that Composites with the addition of alumina nanofillers show improvement in mechanical properties. The influence of the size and shape of the alumina fillers and the loading on the mechanical properties of the prepared composite were studied using Nanoindentation measurements and dynamic mechanical analysis. It was observed that both alumina whiskers and spherical alumina nanoparticles added to the matrix improved the mechanical properties of the composites, but the improvement was significantly higher with reinforcement by alumina whiskers.

P Vasanthkumar et al. (2019) studied and investigated a polymer in which Seashell particulates of size 75  $\mu\text{m}$  size are reinforced in the matrix of nylon 66, a thermoplastic polymer, to improve its properties by forming a polymer matrix composite. Sea Shells' great mechanical properties are due to both their nanoscale structure and their combination of inorganic and organic materials. EDX spectrum shows maximum peak values of calcium and oxygen and SEM micrograph shows mostly equalized seashell particles. Apart from this, uniform distribution of seashells is obtained by reinforcing them with the nylon 66 polymer matrix.

X Li et al. (2007) this article focus on the Seashells that have long been identified as natural armor materials. Seashells are composed of about 95% inorganic aragonite (a mineral form of  $\text{CaCO}_3$ ), with only 1% of organic biopolymer by volume. They exhibit superior structural robustness, despite the brittle nature of their ceramic constituents ( $\text{CaCO}_3$ ). The nanoparticle structured aragonite platelets are

not brittle in nature but somewhat ductile. The nanoparticle rotation and deformation are the two prominent mechanisms contributing to energy dissipation.

BV Ramnath et al. (2018) studied the mechanical and chemical properties of the shells were checked for their mechanical properties such as tensile strength, fineness, fracture property, crushing strength, abrasiveness, etc. At the end of the study, some suggestions have been made regarding where the potential of seashell composites to act as biomaterials as filler materials in concretes in civil engineering, as artistic composites with better mechanical properties, etc.

WASBW Mohammad et al. (2017) has investigated the properties of chemical and mechanical such as specific gravity, chemical composition, compressive strength, tensile strength and flexural strength of concrete produced using partial replacement of cement by seashells ash. Results show that the optimum percentage of seashells as cement replacement is between 4 – 5%.

R karthick et al. (2014) investigated the hardness and tribological characteristics of a PMMA-based denture composite reinforced with seashell nanopowder. The PMMA biocomposites contained 2%, 4%, 6%, 8%, 12%, 16%, and 20% by weight of seashell nanopowder. Scanning Electron Microscopy was used to investigate the wear mechanism and dispersion of seashell nanopowder in the specimen (SEM). It was concluded that PMMA biocomposite could be successfully reinforced by seashell nanopowder, with better properties at 12% seashell nanopowder content, followed by 8% filled composite.

Montazeri et al. (2010) has discussed the fabrication technique of MWCNT. The effect of MWNT addition and their surface modification on the mechanical properties were investigated. The fracture surfaces of MWNT/epoxy composite samples were analyzed by scanning electron microscope.

Sharma et al. (2018) investigated the interlaminar properties of the structural composite. The maximum flexural strength, tensile strength and storage modulus which reached 215 MPa, 356 MPa and 40 GPa, respectively for KE. SEM analysis confirmed the impregnation of Kevlar fabric with MWCNT webbed epoxy and transformation in the mode of failure due to impregnation

Gemi et al. (2017) Multi-walled CNT and three distinct ceramic nanoparticles (Ferrous oxide, Silicon dioxide and Alumina) reinforcements on epoxy were investigated in this study. In all testing, the weight percent of these additives was held constant at 0.5 wt percent. Tensile tests were used to characterize the mechanical properties. To ensure the reliability of the test results, statistical analysis was performed. A scanning electron microscope was used to investigate the fracture surfaces (SEM). Statistical analysis revealed that all additives increased tensile strength, with SiO<sub>2</sub> and providing ferrous oxide the greatest increase. It was also found that the highest reproducibility was obtained in the Alumina reinforced epoxy.

Lailesh Kumar et al. (2021) has proposed and investigated that the significant increment in mechanical and wear properties mainly originates from the fine-grain strengthening effects. A significant improvement was found in relative density, hardness and wear resistance of the nanostructured Al-MWCNT composites up to the addition of 2 wt% of the MWCNTs as compared with as-received Al and its composites. It was also investigated that the hardness of nanostructured



Al-2 wt% MWCNT composite (800 MPa), which is five times higher than as-received Al (170 MPa). Hardness and wear resistance were found to be inversely proportional to crystallite size and porosity.

B.G Demczyk *et al.* (2001) conducted pulling and bending tests on individual carbon nanotubes in-situ in a transition electron microscope. Based on the observation of the force required to break the tube, a tensile strength of 0.15 TPa was computed. The study suggests that these unique properties support the potential of nanotubes as reinforcement fibers in structural materials.

L. Sorrentino *et al.* (2014) has presented both the performance of composite armors made up of Kevlar 29 fabrics that were impregnated by thermosetting resin and the reliability of an analytical model to predict the ballistic limit velocity.

Albert Manero *et al.* (2015) showcases the influence of nano-particle additives on the energy absorption of the composite *via* the Kevlar® 29 fibers corresponding to residual Raman spectral shifts. It has indicated that different mechanisms employed by the two different nano-additives enhance  $V_{50}$  ballistic performance by 7.3% and 8% respectively over baseline panels with a 1% weight addition of nano and micro-sized particles by matrix toughening, cavitation, and strengthening of the fiber-matrix interface.

S. Rajesh *et al.* (2018) investigated the tensile property of a Kevlar composite prepared by hand layup method which has four layers of Kevlar laminate. Morphological analysis was performed using Scanning Electron Microscope to observe the internal structure of composite fibres after testing. The result showed that Kevlar has good tensile strength and hence can be a good alternative conventional material for many applications in engineering industries.

J.A.Bencomo-Cisneros et *al.* (2012) has presented results from tensile tests on single Kevlar-29 filaments, to characterize their intrinsic behavior under quasi-static loading, and nanoindentation tests, to evaluate their cross-section mechanical properties. The findings reveal that the elastic modulus measured in the fiber cross-section is lower than that obtained in the longitudinal direction due to the high anisotropy of the fibers.

Sushmita Naik et *al.* (2020) has done a systematic review on Kevlar, an aramid fibre used on a large scale in defense, aerospace, biomedical and automobile industries. Discussion on research pertaining to Kevlar fibre reinforced composites has been carried out with a focus on structural features and characterization, development, application in various engineering and allied sectors, failure mechanisms after ballistic impact and methods used in the analysis.

M.H. Lafitte et *al.* (1982) A variety of tensile cyclic and steady loading conditions have been applied to single Kevlar-29 fibres. The dispersion in tensile strengths of the samples tested was correlated to the distribution of faults in the fibre rather than differences in diameter between samples. Cyclic loading was observed to cause both longer and shorter lifetimes than steady loads equal to the maximal cyclic load. Longer lifetimes indicated creep failure, but lower lifetimes, found with larger load amplitudes, indicated fatigue failure. Because of the complicated splitting that happens in all cases, there was no difference in the fracture morphologies of Kevlar-29 fibres broken under simple tensile, fatigue, and creep conditions.

R Gokuldass et *al.* (2019) has investigated the mechanical properties and fracture toughness of woven fabric Glass/Kevlar-based hybrid composite tailored using modified epoxy with micro rubber and nano silica. The epoxy was modified with

the addition of 9% micro rubber and 11% of nano silica by weight fraction. At the accumulate layer stacking sequence, the composite with nano silica as reinforcement had the highest tensile and flexural strength of 275 and 162 MPa, respectively. The fractographic results revealed the dispersion of nano additions as well as hybrid composite fracture characteristics. These mechanically toughened epoxy composites could be used in mechanical applications requiring high damping.

TJ Singh *et al.* (2015) has studied the mechanical and thermal characterization of Kevlar fibre and its composites. Mechanical properties such as shear strength, flexural strength, and compressive strength of the aramid fibre composite is been studied.

Suhad D *et al.* (2016) at a 35% weight fraction, has evaluated the tension, compression, and tensile-compression fatigue behaviour of six layers of Kevlar hybridized with one layer of woven kenaf reinforced epoxy. Fatigue tests were performed, and they were loaded cyclically at 60%, 70%, 80%, and 90% of their ultimate compressive stress. The findings provide a comprehensive description of tensile and compressive properties and could be utilized to forecast fatigue-induced failure causes.

JAM Ferreira *et al.* (2012) has studied the fatigue strength of a Kevlar/epoxy laminate composite as well as the advantages of using a nanoclay-filled epoxy matrix. The filler was an organoclay Cloisite 30B that had been treated with an appropriate silane and other unique compounds to increase dispersion and interface adherence. Hand lay-up of twelve ply laminates of woven bidirectional Kevlar 292 in the same direction was performed using an SR 1500 epoxy resin. A vacuum moulding procedure was used to create the composite sheets. The inclusion of

nanoclays decreased static strength while increasing stiffness under tension and bend loading. Filled composites had tensile fatigue strengths that were 13% greater than unfilled matrices, but their fatigue strength in three-point bending was lower.

(Ahmet Erklig) et al. (2017) has evaluated the charpy impact and tensile properties effect of hybridizing Kevlar and glass fibers by impacting each side of the hybrid composite samples, a series of Charpy impact tests were performed to determine the amount of impact strength and absorbed energy. When the hybrid samples were impacted on the surface of the Kevlar side, they demonstrated greater impact resistance than the glass side impact. The degree of hybridization effects revealed that the insertion of Kevlar layers rather than glass layers contributed significantly to the total composite laminate's impact strength and absorbed energy.

## **2.2 RESEARCH GAP**

Through the extensive literature review done in this chapter, it is seen that experimentation with mixing MWCNT with nano additives like seashell and nano alumina with a Kevlar matrix-based composite material is not performed. It is also seen that material properties like mechanical, impact and fatigue are not investigated on the combination which we have proposed in this project work.

## **2.3 SUMMARY**

- This Chapter includes a systematic literature review on the research topics which are relevant to the project. Various articles on Composite materials with nano additives, fabrication process, material properties, mechanics, etc. were studied.
- Through the literature review, the research gap is identified.

## **CHAPTER 3**

### **METHODOLOGY**

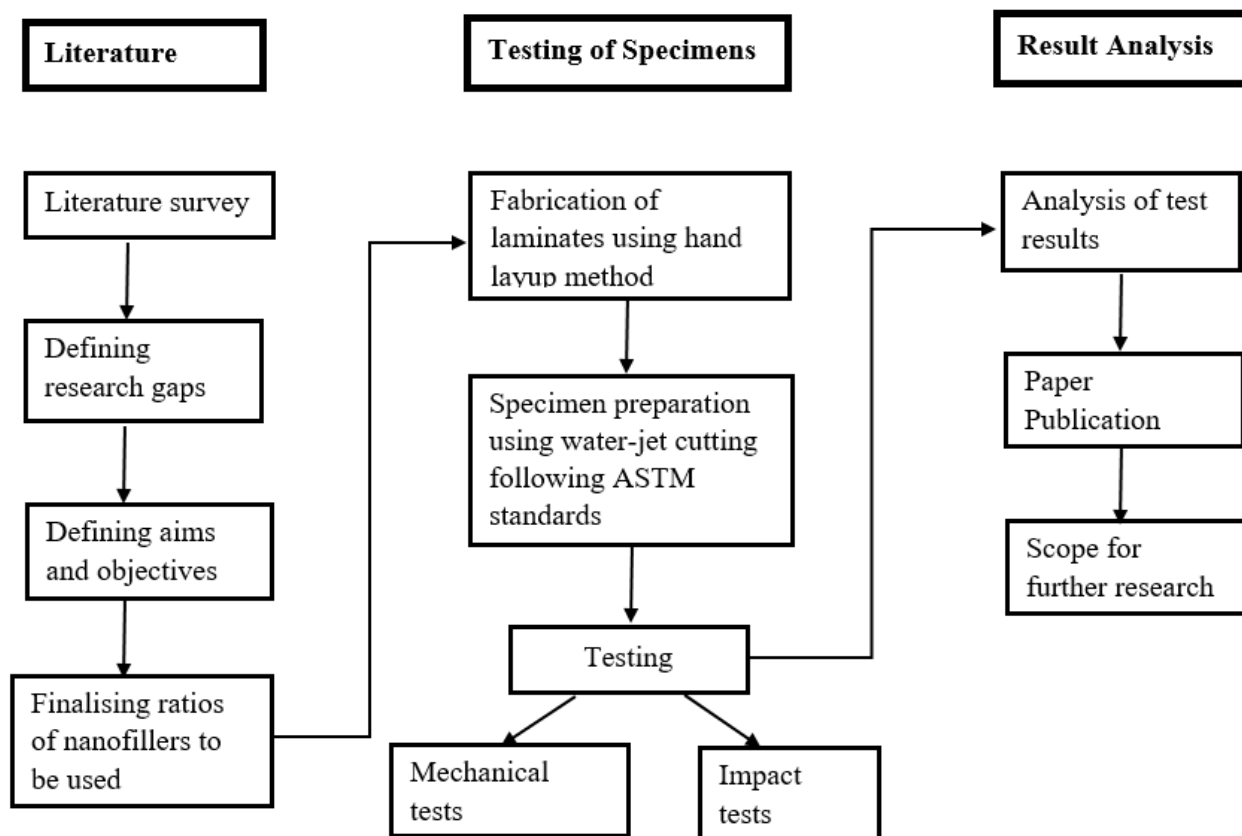
This research paper explains An Experimental Study of Mechanical and Impact behaviour of Nanofiller Infused Kevlar based Composites. It involved extended and individualized Primary Research with Understanding fundamental theories and concepts, performing literature review, conceptualizing the research gap and identifying current problems faced by the industry. Robust planning was done on how to develop, fabricate, test and analyse the composite plates. Work flow chart was prepared to maintain the project time frame discipline. Understanding of expected loads and conditions, such as strain rate and service temperature was considered. It was important to understand the design window for the geometry of design of composites.

An extensive literature review was performed on mechanical and impact behaviour of various nanofiller infused Kevlar composites. The most widely used nanofillers that affected the mechanical and impact behaviour of nanofillers include Carbon Nanotubes (CNTs), graphite, nano alumina, nano seashell, Nanoclay, nano silica, etc. The mechanical and impact properties were significantly seen to improve on addition of nano alumina, CNT individually. The literature review was done by following PRISMA analysis method where we initially found all the journal papers related to nanofiller infused Kevlar composites which we then shortlisted by searching specific key words like mechanical properties, impact properties, nano alumina, nano seashell, CNTs, etc. The abstracts of the papers were read and the most relevant papers to our study were taken into consideration for the literature review. After reviewing about 30 papers extensively, basic choices of filler percentages to be taken for experimentation were decided. For

an article to be included in the study, the following criteria were followed to scrutinize and shortlist the same: the articles were original studies that provided novel contributions to the field of nano filler incorporated composites, not a review article by itself and are in English. The articles that were not included in the study were literature review papers, incomplete experimental or theoretical studies, abstracts, case report studies and articles that did not have nano filler reinforcement for the composites.

Initially, the research aimed on finding out the optimum ratio of nano alumina and nano seashell to be used to get the best mechanical and impact properties by keeping the ratio of CNTs constant as 0.25% wt. After critical analysis of the property enhancement provided by the three nano fillers individually, for nano alumina the ratios were chosen as 1%, 3% and 6% wt. and for nano seashell they were chosen as 1%, 3% and 7% wt. An extensive study had to be performed to find the most viable method of mixing the nano fillers into the resin in a homogenous way. Various researchers previously used the method of ultra-sonication to do the same. An Ultrasonicator does the job of homogenously mixing the fillers into the resin so the property of the mixture doesn't vary throughout its composition. The timing for ultra-sonication of each filler depends on the individual filler property which ranged between 2 hours for nano seashell + MWCNT mixture to 4 hours for the alumina + MWCNT mixture at a frequency of 33 kHz. After the ultra-sonication was done, the method of preparation of the composite plates came into action. Hand lay-up method was chosen to fabricate the plates for its various advantages like it is a very cost effective method, the process being very simple and need of minimum equipment, less sophistication required and allowing a freedom of a wide range of sizes and shapes of composite plates.

After extensive literature survey, the resin that was weighed was taken for fabrication of the plate was equal to the weight of all the layers of Kevlar combined. After the fabrication was done, specimens required for various tests were cut out of the plate by water-jet cutting method by following the ASTM standards like ASTM 3039 for tensile test, ASTM D790 for flexural test, ASTM D256 for Charpy Impact test and ASTM D2433 for inter-laminar test. The tests were performed on the respective machines like tensile test, flexural test and inter-laminar test on the universal testing machine and impact test on the Charpy Impact Test equipment. The standard procedure for performing each test as prescribed by the respective standards was followed to perform each test and results were obtained. After acquiring the data sets from the computerised UTM and manually noting down values for the Charpy Impact test, calculations of required quantities for each test were performed. The formulae required for the same were obtained from the literature survey and various parameters like stress, strain, flexural modulus, flexural stress, impact energy, impact strength etc. All these values were calculated for all the given ratios of nanofillers and the graphs were plotted as to observe how the mechanical and impact properties changed with change in filler percentage. The consolidated trends gave a clear idea on the appropriate ratio of alumina and sea shell nanofiller to be used in order to have a positive and desirable effect on the mechanical and impact properties of Kevlar based composites.





# **CHAPTER 4**

## **SEASHELL + MWCNT**

### **4.1 INTRODUCTION**

Composites are a macroscopic combination of two or more different materials with separate recognizable interfaces that separate them. Composites are combinations of high performance resin matrices and various combinations of fibers that change the traditional engineer's approach and enable matrix alloys for specific structural implementations. Improved materials, analysis and manufacturing methods have pushed traditional composite structures to new performance limits. The main aim of composites is to achieve better results compared to traditional metal parts.

Advanced composites usually made from high performance fibers and / or resins have historically been popular in the aerospace and defense sectors, and in many sporting goods. Engineering composites have been manufactured over decades primarily from materials such as E-glass fiber reinforced plastics and polyesters, some low temperature performance epoxy, or various engineering thermoplastics commonly referred to as fiber reinforced plastics or FRP.

Fillers have the ability to improve mechanical characteristics. In modern composites, fibers and particles are embedded in a matrix of other materials. With increasing global recognition, the use of natural fibers in composites is steadily increasing. Similarly, the ability of seashells as fillers in the modern world is being investigated. The seashell is a natural nanocomposite with excellent mechanical strength and toughness. The most important properties such as hardness, toughness, water absorption, compressive strength and tensile strength are satisfied by various seashells. Composites made from seashells are tested for a variety of me-

chanical properties such as toughness, tensile strength, impact strength and bending strength. Carbon nanotubes are extremely suitable as fillers for polymer composites due to their unique properties such as high electrical and thermal conductivity, ultra-high mechanical strength, and high length / diameter ratio ( $\sim 1000$ ) at nano scale diameter values. It's interesting.

Limitations to advanced composites are focused on cost of raw materials and fabrication. Its transverse properties may be weak and with low toughness as matrix is weak. Analysis is difficult as it is subject to matrix environmental degradation. Composite fabrication process is labor-intensive. Advanced composites allow very less margin of error and could put whole design system into loop for slight deviation from targeted results.

## **4.2 PREPARATION OF NANO SEASHELL**

Seashells of different sizes are collected from sea shore and hammered down to lowest possible size. They are then processed in Planetary Ball Milling machine for 6-8 hours until seashell was broken down to nano size. This nano seashell powder prepared is known as Seashell Nanofiller which was further used to investigate the mechanical property enhancement when infused with Kevlar fibre at different filler ratios by % wt. Preparation process is shown in **Figure 4.1** to **Figure 4.4** as a flow sheet.



**Figure 4.1** Seashells



**Figure 4.2** Hammered Seashells



**Figure 4.3** Ball Milling Machine



**Figure 4.4** Nano Seashell Powder

### 4.3 MORPHOLOGICAL STUDIES OF NANO SEASHELL

Morphology, or the study of form, which includes shape, size, and structure, is critical for materials research in general. Morphology is very important for nanostructured materials, also known as nano materials, since shape determines physical and chemical characteristics of the material itself.

The scanning electron microscope (SEM) is a powerful and frequently used instrument. The SEM has an extremely large depth of focus and is therefore well suited for topographic imaging. The specimen is bombarded by a convergent electron beam, which is scanned across the surface. This electron beam generates a number of different 52 types of signals, which are emitted from the area of the specimen where the electron beam is impinging, SEM was employed to monitor the surface morphologies as shown in **Figure 4.5** and **Figure 4.6**.

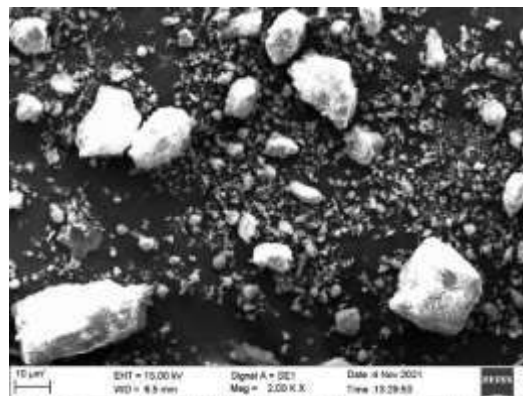


**Figure 4.5** SEM Image of Nano Seashell

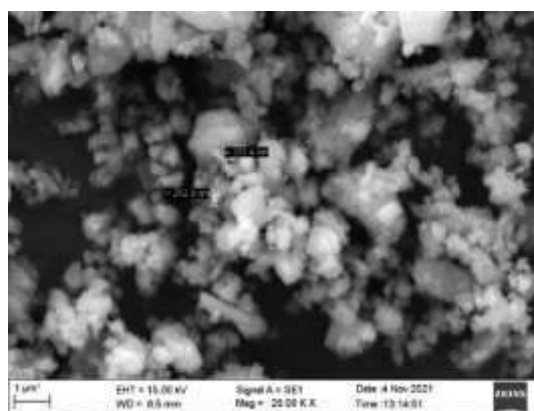


**Figure 4.6** SEM Image of Nano Seashell

X-ray diffraction (XRD) is a rapid analytical technique primarily used for phase identification of a crystalline material and can provide information on unit cell dimensions. The analysed material is fine, homogenized and average bulk composition is determined as shown in **Figure 4.7**.

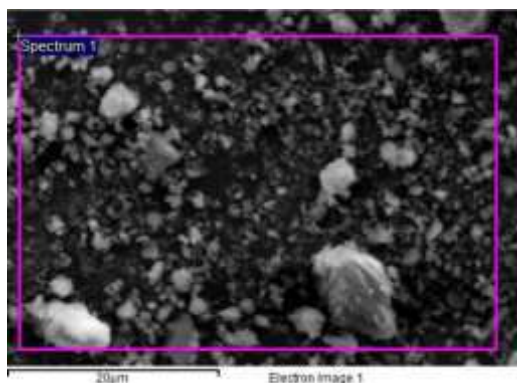


**Figure 4.7** XRD of Nano Seashell

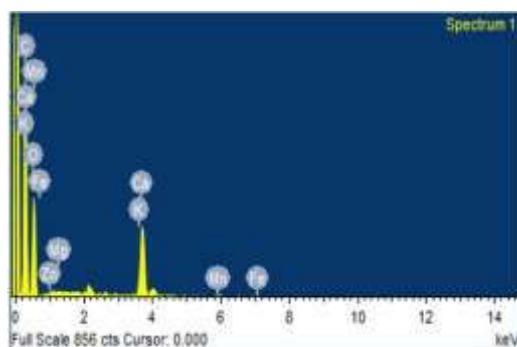


**Figure 4.8** EDS of Nano Seashell

**Table 4.1** Elemental Concentration of Nano Seashell

Element	Weight%	Atomic%
C	49.10	60.10
O	38.56	35.43
Mg	0.07	0.04
K	0.05	0.02
Ca	11.67	4.28
Mn	0.18	0.05
Fe	0.01	0.00
Zn	0.35	0.08
Totals	100.00	

## 4.4 FABRICATION OF PLATES

### 4.4.1 Plates with Neat Kevlar

Dimensions: 320 mm × 320 mm

Thickness of Plate: 2.4-2.7 mm

No of Kevlar Layers: 7 -8 (0.3 mm thickness each)

Total Mass of Kevlar = 140 g – 160 g

Mass of Resin LY556 = 140 g – 160 g

Mass of Hardener = 15 g

Hand Lay-up Method of Fabrication of composites

First Kevlar material is cut into plate dimensions of 320 mm × 320 mm layers and then according to the thickness of fabricated plate required no of layers of Kevlar to be stacked was decided. The weight of all layers of Kevlar to be stacked together is measured using the weighing balance. Weight of Kevlar layers is noted down and equal mass of Epoxy LY556 is measured in a clean glass beaker after tearing glass beaker weight on weighing balance.



**Figure 4.9** Kevlar Fabric of 320 mm × 320 mm



**Figure 4.10** Epoxy LY556 measured

Two ceramic plates for Hand Lay-up were cleaned by applying Acetone and properly cleaning each corner neatly. Mylar sheets were cut exactly to the dimensions of the ceramic plates. Wax was applied on ceramic plates and on both sides of Mylar Sheet properly.

The weight of glass beaker filled with epoxy was torn to zero on weighing balance and then Hardener HY951 was poured into the resin with 1:10 ratio weight of epoxy and then the epoxy-hardener mixture was thoroughly mixed. A brush was taken and the mixture is initially applied on one of the Mylar layers and the first layer of the stack of Kevlar is put on top of it. After that again another layer of the resin + hardener mixture is spread on the layer and next layer is put on top. The process is repeated for all the layers of Kevlar. It is important to make sure that proper wetting is occurring while applying the resin at each layer. After the top most layer of Kevlar is coated with resin, the Mylar sheet is put on top. With the help of rollers, excess resin which might be present in between the layers of Kevlar is extracted by simply rolling the roller in the Mylar sheet. After this is done, the second ceramic plate was put on top the set up that was later topped by dead weights to help make the plates firm. The set up was left undisturbed for 24 hours to give the time for the composite plate to cure. Next day, the fabricated composite plate could be removed out of the set up.



**Figure 4.11** Applying Epoxy-Hardener Mixture



**Figure 4.12** Dead weights for curing of composite plates

Specimen sizing according to ASTM Standards of tests to be performed was marked on Fabricated Kevlar Plate for Water Jet Cutting. Specimens for various mechanical and impact properties were tested and then analysis of the data was done for detailed report.



**Figure 4.13** Fabricated Kevlar Composite Plate



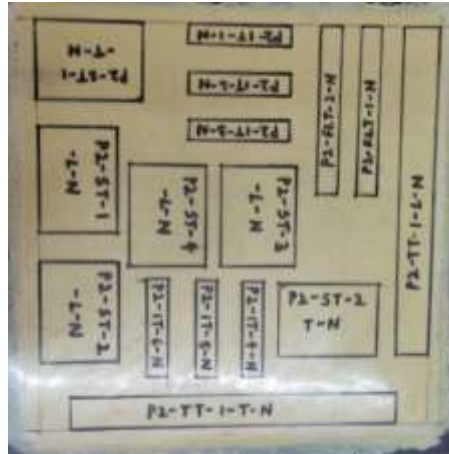


**Figure 4.1** Specimen sizing according to ASTM Standards of tests to be performed marked on Fabricated Kevlar Plate for Water Jet Cutting

#### 4.4.2 Plates with Seashell + CNT

Dimensions: 320 mm × 320 mm

Thickness of Plate: 2.4 mm

No of Kevlar Layers: 8 (0.3 mm thickness each)

Total Mass of Kevlar = 160 g

Mass of Resin LY556 = 160 g

Mass of Hardener = 15 g

Weight of MWCNT= 0.25 g

Weight of 1% Seashell nanofiller by weight of epoxy = 1.4 g

Weight of 3% Seashell nanofiller by weight of epoxy = 4.8 g

Weight of 7% Seashell nanofiller by weight of epoxy = 11.2 g

Hand Lay-up Method of Fabrication of composites

First Kevlar material is cut into plate dimensions of 320 mm × 320 mm layers and then according to the thickness of fabricated plate required no of layers of Kevlar to be stacked was decided. The weight of all layers of Kevlar to be stacked

together is measured using the weighing balance. Weight of Kevlar layers is noted down and equal mass of Epoxy LY556 is measured in a clean glass beaker after tearing glass beaker weight on weighing balance.



**Figure 4.2** Kevlar Fabric of 320 mm × 320 mm



**Figure 4.3** Epoxy LY556 measured

On digital weighing balance MWCNT of 0.25 g is measured and kept aside. Similarly weight of 1% Seashell nanofiller, 3% Seashell nanofiller and 7% Seashell nanofiller by weight of epoxy is measured and kept aside.



**Figure 4.4** MWCNT OF 0.25 g



**Figure 4.5** Seashell Nanofiller

In the glass beaker with epoxy, MWCNT and Seashell nanofiller measured according to the ratio of plate to be fabricated were added. The mixture was mixed well with a stirrer. Conventionally hand stirring is done for 1 hour on the epoxy-nanofiller mixture and later it is kept for Ultra sonification in the 33 KHz frequency Ultrasonicator for 1 hour and 30 min to make uniform mixture of epoxy-nanofiller and to avoid agglomeration of nanofiller and MWCNT particles in the mixture.



**Figure 4.6** Sonification of Epoxy-nanofiller mixture

Two ceramic plates for Hand Lay-up were cleaned by applying Acetone and properly cleaning each corner neatly. Mylar sheets were cut exactly to the dimensions of the ceramic plates. Wax was applied on ceramic plates and on both sides of Mylar Sheet properly.

The weight of glass beaker filled with epoxy was torn to zero on weighing balance and then Hardener HY951 was poured into the resin with 1:10 ratio weight of epoxy and then the epoxy-hardener mixture was thoroughly mixed. A brush was

taken and the mixture is initially applied on one of the Mylar layers and the first layer of the stack of Kevlar is put on top of it. After that again another layer of the resin + hardener mixture is spread on the layer and next layer is put on top. The process is repeated for all the layers of Kevlar. It is important to make sure that proper wetting is occurring while applying the resin at each layer. After the top most layer of Kevlar is coated with resin, the Mylar sheet is put on top. With the help of rollers, excess resin which might be present in between the layers of Kevlar is extracted by simply rolling the roller in the Mylar sheet. After this is done, the second ceramic plate was put on top the set up that was later topped by dead weights to help make the plates firm. The set up was left undisturbed for 24 hours to give the time for the composite plate to cure. Next day, the fabricated composite plate could be removed out of the set up.



**Figure 4.7** Applying Resin + Seashell nanofiller+ MWCNT Mixture on Kevlar plates



**Figure 4.8** Dead weights for curing of composite plates

Specimen sizing according to ASTM Standards of tests to be performed was marked on Fabricated Kevlar Plate for Water Jet Cutting. Specimens for various mechanical and impact properties were tested and then analysis of the data was done for detailed report.

## **4.5 MECHANICAL & IMPACT TESTS ANALYSIS FOR PREPARED SPECIMENS**

Tensile, flexural, tension shear, and inter-laminar shear tests were carried out at room temperature (25°C) on an INSTRON universal testing machine a capacity of 100 KN. Load-displacement data were obtained from the DAQ system connected to a computer unit and machine used for testing. Five to six samples were tested for each test, and the average value was calculated and reported along with standard deviation in the report.

### **4.5.1 TENSILE TEST – ASTM D3039**

The tensile tests and their properties, i.e., ultimate tensile strength, Elastic modulus, Strain to failure of the fabricated Kevlar plates, were conducted and evaluated according to the ASTM D3039 at a constant cross-head speed of 2 mm/min. The tests specimens were cut from the fabricated plates using an abrasive water jet cutting method with 250 mm length and 25 mm width. The load-elongation curves obtained from the tensile tests were used to calculate engineering stress and strain measurements.



**Figure 4.9** INSTRON Universal Testing Machine



**Figure 4.10** Tensile Test Specimen fixed in UTM Fixture

The test process involves placing the test specimen in the testing machine and slowly extending it until it fractures. During this process, the elongation of the gauge section is recorded against the applied force. The data is manipulated so that it is not specific to the geometry of the test sample. The elongation measurement is used to calculate the engineering strain,  $\epsilon$ , using the following equation:

$$\epsilon = \frac{\Delta L}{L_0} = \frac{L - L_0}{L_0}$$

Where  $\Delta L$  is the change in gauge length,  $L_0$  is the initial gauge length, and  $L$  is the final length. The force measurement is used to calculate the engineering stress,  $\sigma$ , using the following equation:

$$\sigma = \frac{F_n}{A}$$

Where F is the tensile force and A is the nominal cross-section of the specimen. The machine does these calculations as the force increases, so that the data points can be graphed into a stress–strain curve.

#### 4.5.1.1 Plain Neat Kevlar

From the Stress-Strain Curve obtained from the tensile test, maximum stress point is observed and marked on graph as Ultimate Tensile Strength (UTS) for Neat Kevlar specimens as shown in Figure 4.24.

Mean Ultimate Tensile Strength is calculated for the set of specimens of Neat Kevlar tested and Standard Deviation is marked.

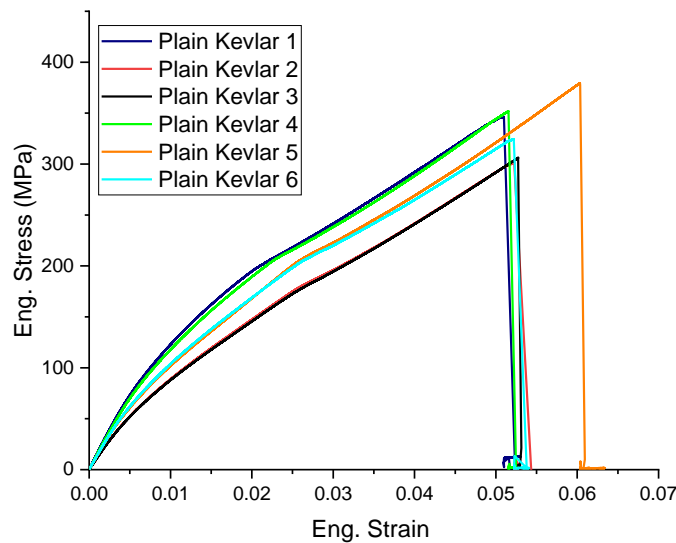


**Figure 4.11** Engineering Stress - Strain Graph for Neat Kevlar Specimens

Later graph is selected till UTS Point and Linear slope is calculated for the initial linear curve of the graph from 0 to UTS point. The slope m, obtained is the Young's Modulus of the Neat Kevlar tested specimen. Mean Young's Modulus is calculated for the set of specimens tested of Neat Kevlar and Standard Deviation is marked.

#### 4.5.1.2 Seashell 1 % + 0.25 % MWCNT

From the Stress-Strain Curve obtained from the tensile test, maximum stress point is observed and marked on graph as Ultimate Tensile Strength (UTS) for Kevlar infused with 1% Seashell nanofiller and 0.25% MWCNT specimen as shown in Figure 4.25.

Mean Ultimate Tensile Strength is calculated for the set of specimens tested and Standard Deviation is marked.

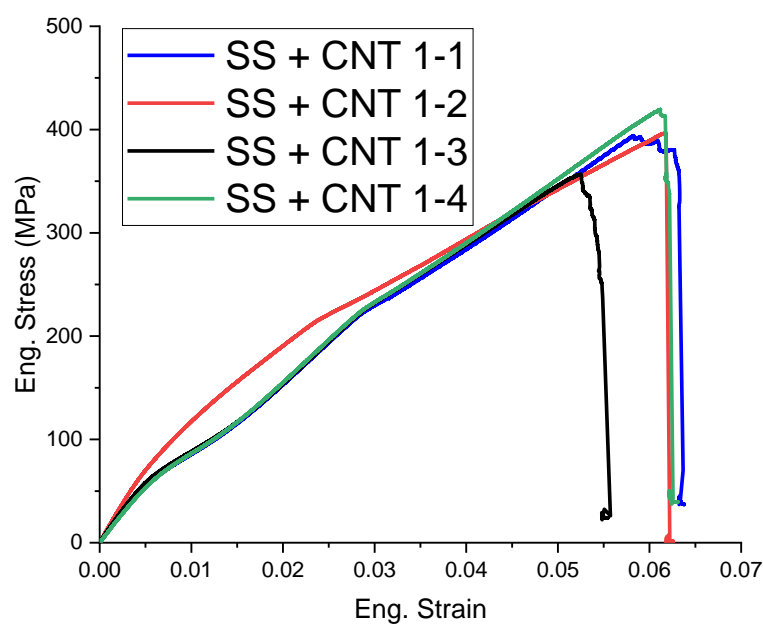


**Figure 4.12** Engineering Stress - Strain Graph for Seashell 1% + 0.25% MWCNT Specimens

Later graph is selected till Ultimate Tensile Strength Point and Linear slope is calculated for the initial linear curve of the graph from 0 to UTS point. The slope  $m$ , obtained is the Young's Modulus of the Kevlar infused with 1% Seashell nanofiller and 0.25% MWCNT specimen.

Mean Young's Modulus is calculated for the set of specimens tested and Standard Deviation is marked.



#### 4.5.1.3 Seashell 3 % + 0.25 % MWCNT

From the Stress-Strain Curve obtained from the tensile test, maximum stress point is observed and marked on graph as Ultimate Tensile Strength (UTS) for Kevlar infused with 3% Seashell nanofiller and 0.25% MWCNT specimen as shown in Figure 4.26.

Mean Ultimate Tensile Strength is calculated for the set of specimens tested and Standard Deviation is marked.

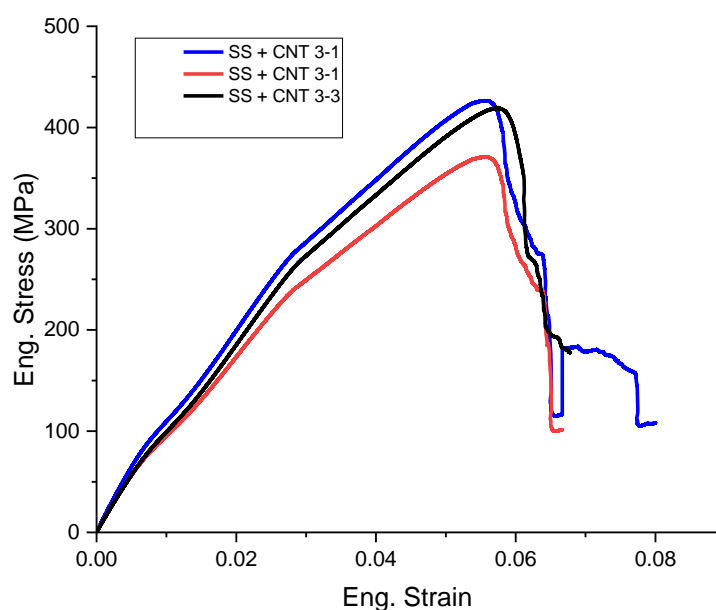


**Figure 4.13** Engineering Stress - Strain Graph for Seashell 3% + 0.25% MWCNT Specimens

Later graph is selected till Ultimate Tensile Strength Point and Linear slope is calculated for the initial linear curve of the graph from 0 to UTS point. The slope  $m$ , obtained is the Young's Modulus of the Kevlar infused with 3% Seashell nanofiller and 0.25% MWCNT specimen.

Mean Young's Modulus is calculated for the set of specimens tested and Standard Deviation is marked.

#### 4.5.1.4 Seashell 7 % + 0.25 % MWCNT

From the Stress-Strain Curve obtained from the tensile test, maximum stress point is observed and marked on graph as Ultimate Tensile Strength (UTS) for Kevlar infused with 7% Seashell Nanofiller and 0.25% MWCNT specimen as shown in Figure 4.27.

Mean Ultimate Tensile Strength is calculated for the set of specimens tested and Standard Deviation is marked.

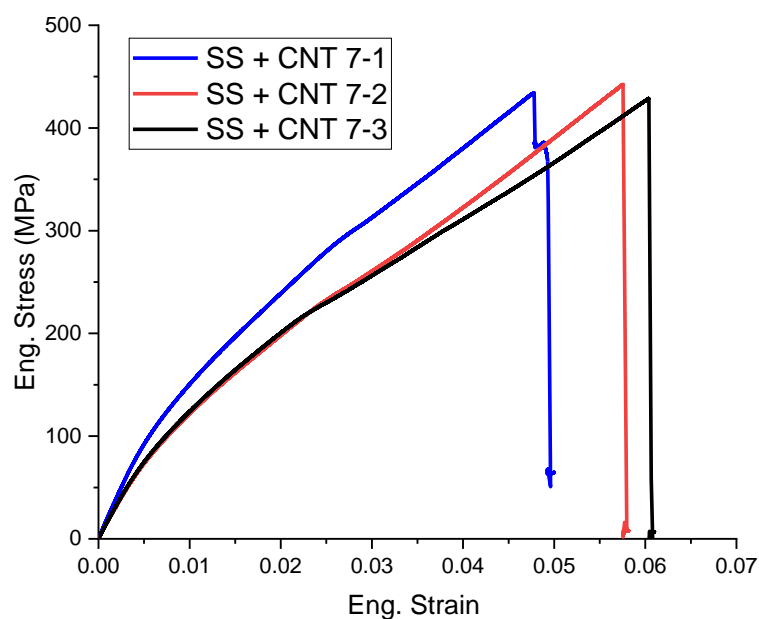


**Figure 4.14** Engineering Stress - Strain Graph for Seashell 7% + 0.25% MWCNT Specimens  
Later graph is selected till Ultimate Tensile Strength Point and Linear slope is calculated for the initial linear curve of the graph from 0 to UTS point. The slope  $m$ , obtained is the Young's Modulus of the Kevlar infused with 3% Seashell nanofiller and 0.25% MWCNT specimen.

Mean Young's Modulus is calculated for the set of specimens tested and Standard Deviation is marked.

**Table 4.2** Comparative Analysis of UTM and Young's Modulus for different Seashell Nano-filler content

S. No	Nanofiller Content	Ultimate Tensile Strength (MPa)	Young's Modulus (MPa)
1	Neat Kevlar	$334.17 \pm 27.11$	$6890.47 \pm 632.44$
2	Seashell 1 % + 0.25 % MWCNT	$387.50 \pm 22.64$	$7195.13 \pm 87.15$
3	Seashell 3 % + 0.25 % MWCNT	$404.33 \pm 24.44$	$8110.7 \pm 570.91$
4	Seashell 7 % + 0.25 % MWCNT	$433.67 \pm 5.44$	$8680.7 \pm 1255.15$

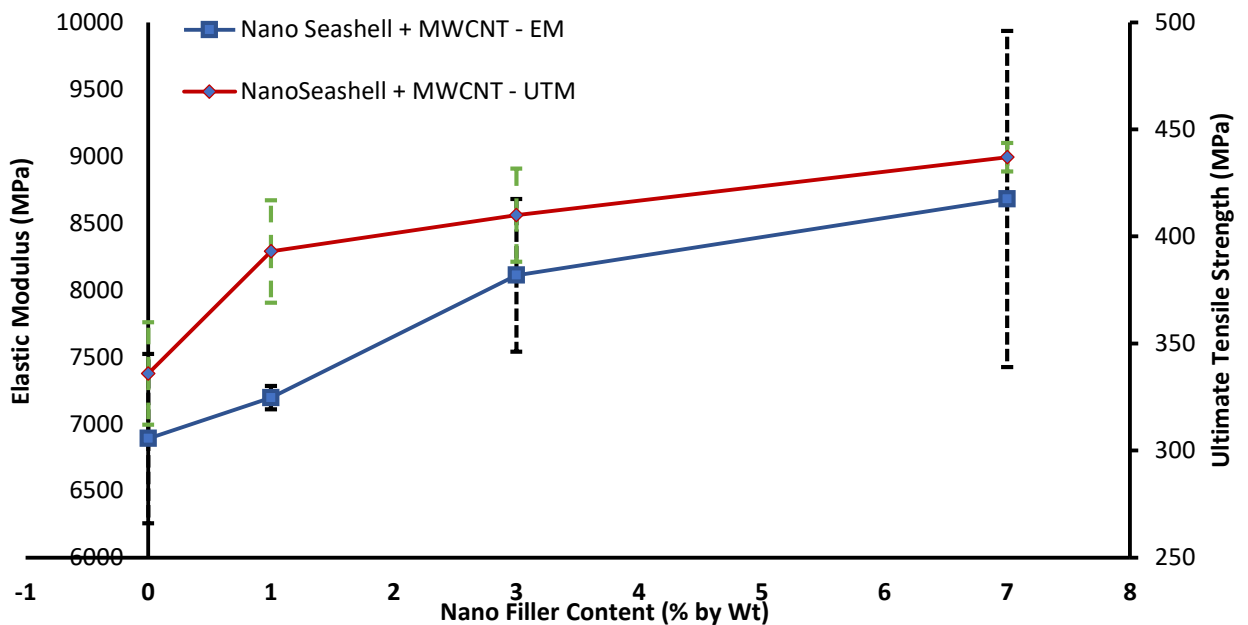


**Figure 4.15** Comparative Analysis of UTM and Young's Modulus for different Seashell Nanofiller content

Based on the comparative study for Tensile test done for various Neat Kevlar specimens and Kevlar infused with different percentage of Seashell nanofiller and 0.25% MWCNT specimens, it is concluded that there is gradual increment in values of Ultimate Tensile Strength and Young's Modulus as we increase the Seashell nanofiller percentage up to 7%. We can see increment of around 23% in Ultimate Tensile Strength and increment of around 21% in Young's Modulus for

Kevlar infused Seashell nanofiller with MWCNT at 7% nano seashell filler content w.r.t Neat Kevlar.

#### 4.5.1.5 Failed Specimens

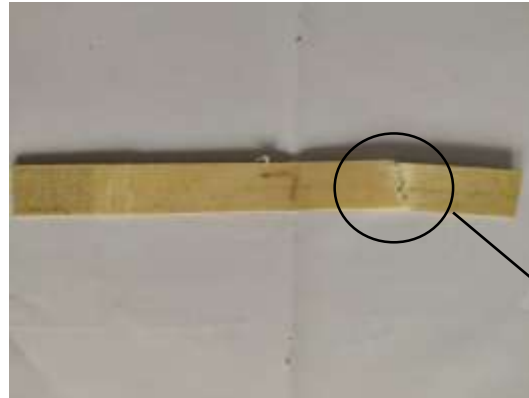


**Figure 4.16** Failed Tensile Test Specimens



**Figure 4.17** Failed Tensile Test Specimen

Crack formation  
after Tensile Test

As the load is applied ahead of Ultimate Tensile Stress the fibre pull out begins and matrix interface is sheared and specimen crack initiation begins. Later on continuous load application we can see brittle failure and specimen crack is formed as it can be seen in figure 4.29 and figure 4.30.

#### 4.5.1.5.1 SEM Images of Failed Tensile Test Specimens

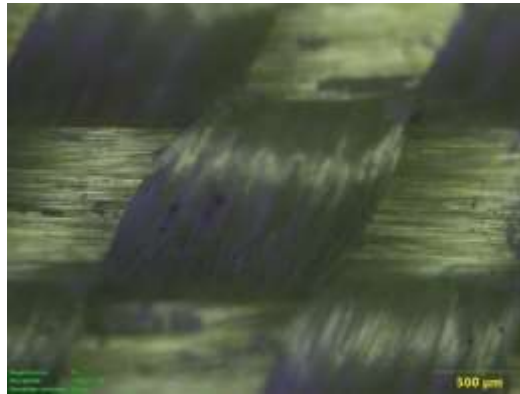


**Figure 4.18** SEM Image of Failed Tensile Test Specimen

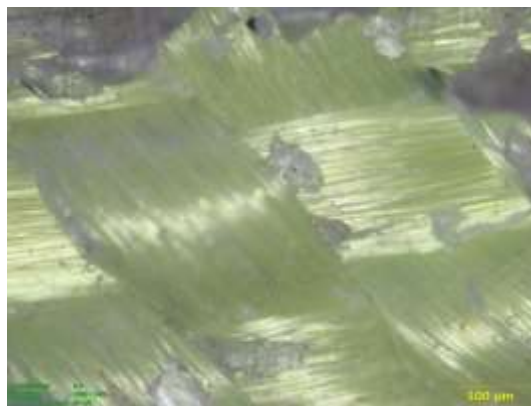


**Figure 4.19** SEM Image of Failed Tensile Test Specimen

#### 4.5.2 3 POINT BENDING TEST – ASTM D790

The effect of seashell nanoparticles on the flexural properties of specimens was characterized at the crosshead speed of 2 mm/min by applying a point at the centre of the specimen using the INSTRON universal testing machine. The length and width of the Kevlar specimens used for this test as per ASTM D790 were 12.7 mm and 125 mm, respectively, with a span length of 40 mm. One of the typical setup arrangements is shown in the figure below. Flexural stress and flexural Strain were calculated by using the load and displacement values in the following equations given below respectively for the known width, thickness and span length:

$$\sigma_f = 1.5 Lu / W t^2$$

$$\epsilon_f = \frac{6t\delta}{Z^2}$$

Where,  $\sigma_f$  &  $\epsilon_f$  are the flexural strength and Strain, respectively;  $L$  and  $u$  are the flexural load and displacement, respectively;  $w$  and  $t$  are the width and thickness of the specimen, respectively;  $Z$  is the span length of the specimen.

$$E_{fl} = L^3 m / 4bh^3$$

Where,  $E_{fl}$  is Flexural Modulus,  $L$  represents the support span length,  $P_f$  is the maximum flexural load and  $m$  denotes the slope of the initial linear portion of the load v/s deflection curve.



**Figure 4.20** 3 Point Bending Test Setup



**Figure 4.21** 3 Point Bending Test of Specimen

### 4.5.2.1 PLAIN NEAT KEVLAR

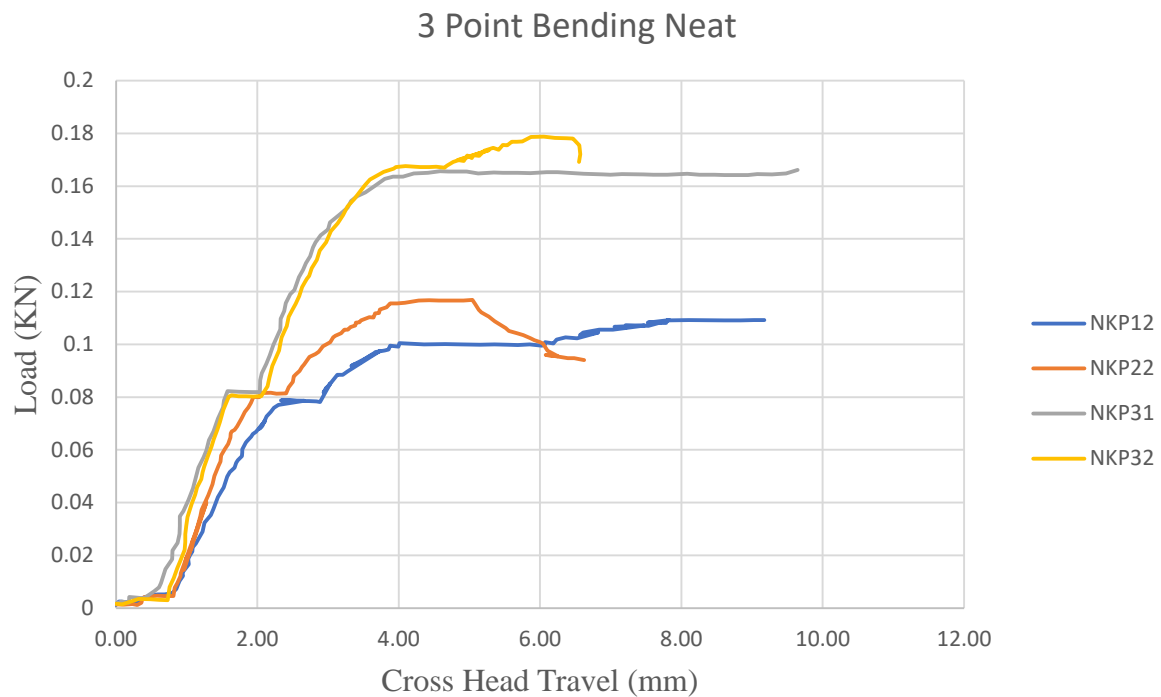


**Figure 4.22** Load v/s Cross Head Travel for Neat Kevlar Specimens

### 4.5.2.2 SEASHELL 1% + 0.25% MWCNT

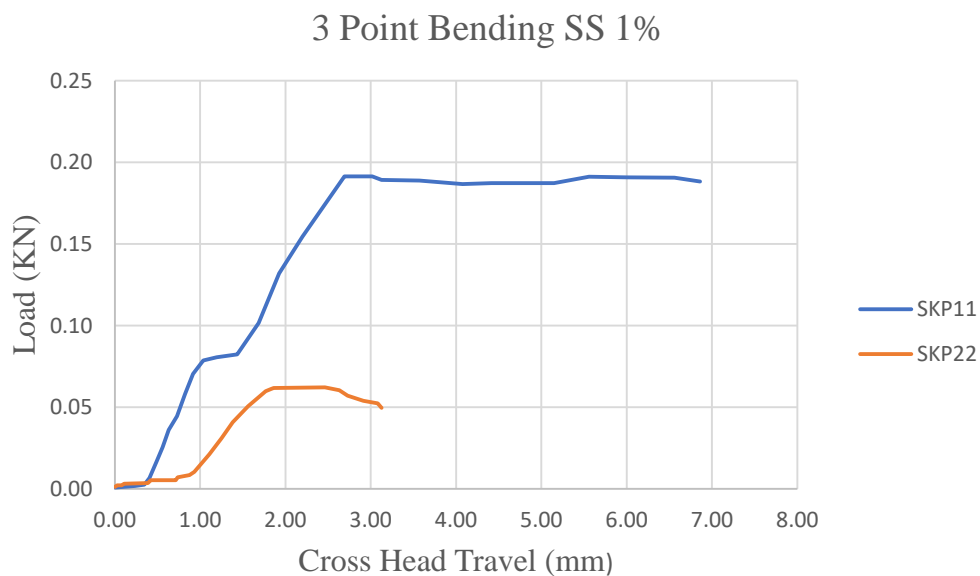


**Figure 4.23** Load v/s Cross Head Travel for 1% Seashell + 0.25% MWCNT infused Kevlar Specimens

### 4.5.2.3 SEASHELL 3% + 0.25% MWCNT

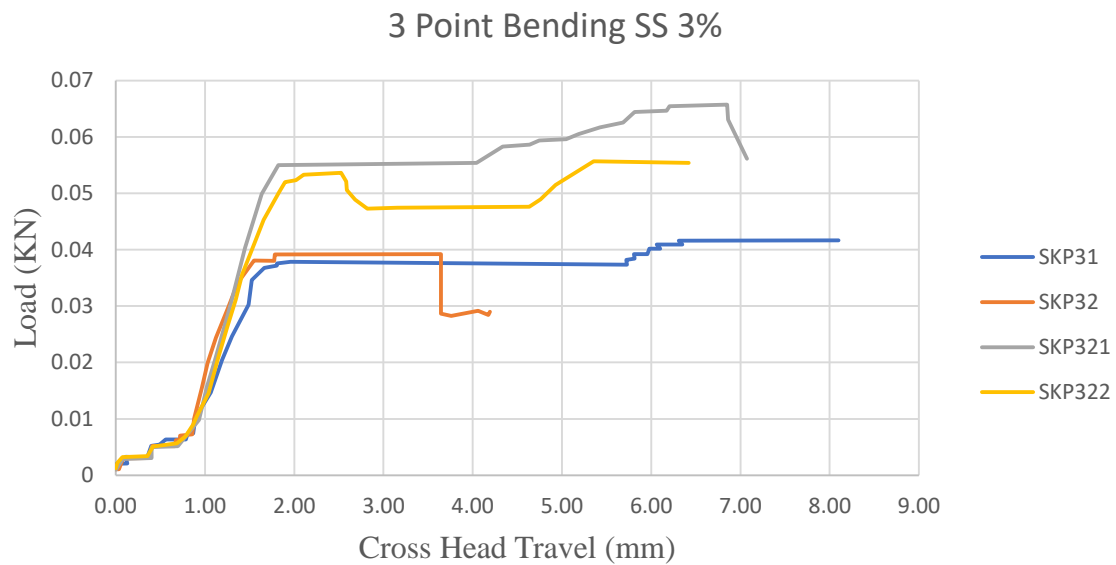


**Figure 4.24** Load v/s Cross Head Travel for 3% Seashell + 0.25% MWCNT infused Kevlar Specimens

### 4.5.2.4 SEASHELL 7% + 0.25% MWCNT

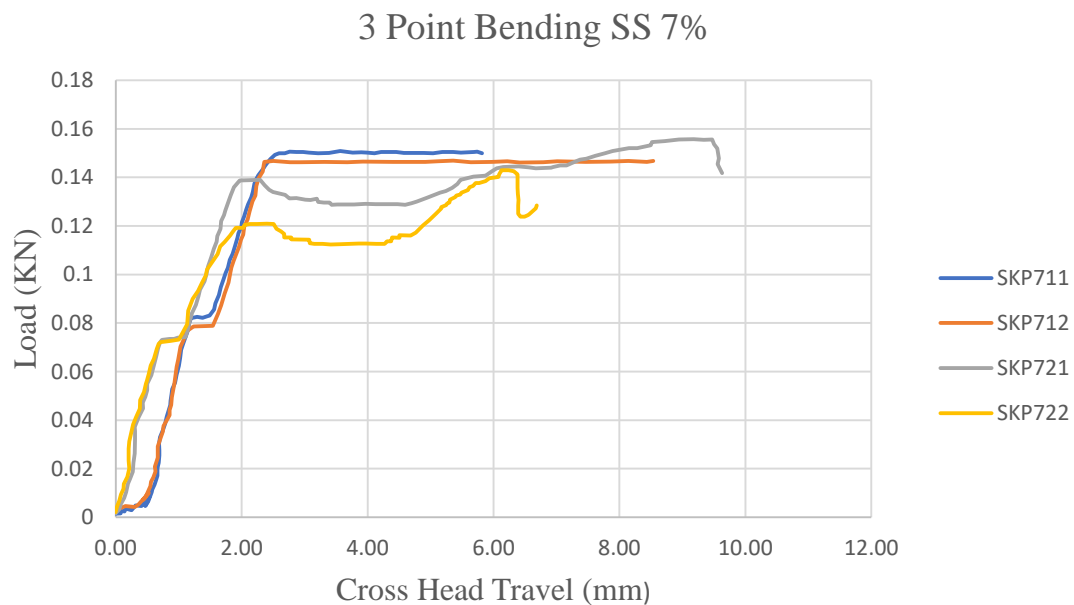


**Figure 4.25** Load v/s Cross Head Travel for 7% Seashell + 0.25% MWCNT infused Kevlar Specimens



**Table 4.3** Flexural Stress Variation in different Seashell filler content

Flexural Stress Variation in Seashell	
FILLER %	Flexural Stress (N/mm <sup>2</sup> )
0	121.15 ± 35.38
1	98.44 ± 70.71
3	39.45 ± 9.23
7	115.63 ± 4.90

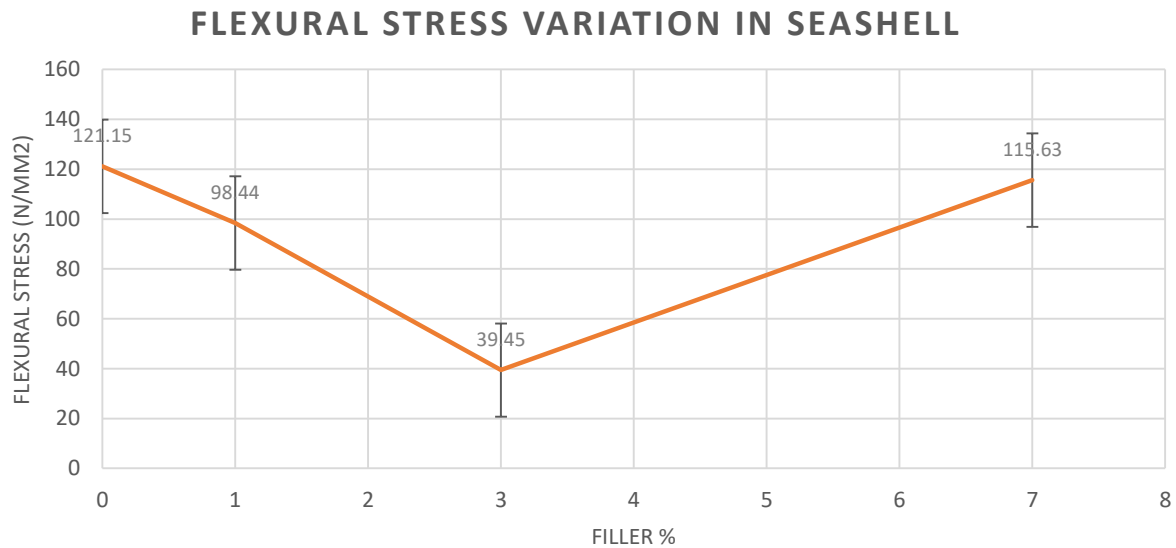


**Figure 4.26** Flexural Stress Variation in different Seashell filler content

**Table 4.4** Flexural Strain Variation in different Seashell filler content

SEASHELL Flexural Strain Variation	
Filler %	Flexural Strain
0	0.08 ± 0.02
1	0.04 ± 0.01
3	0.06 ± 0.02
7	0.07 ± 0.01

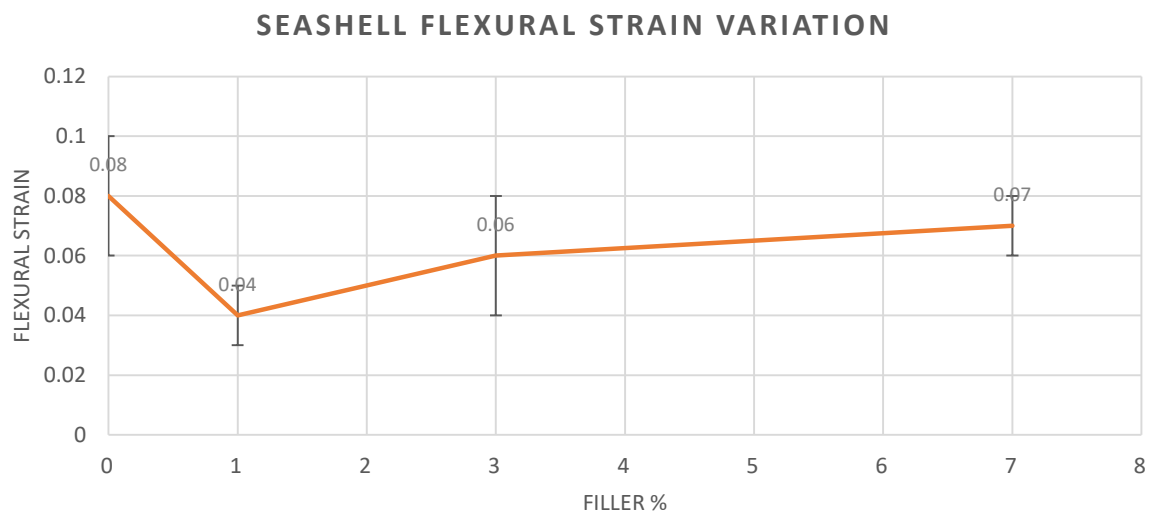


**Figure 4.27** Flexural Strain Variation in different Seashell filler content

**Table 4.5** Flexural Strength Variation in different Seashell filler content

SEASHELL Flexural Strength Variation	
Filler %	Flexural Strength (N/mm <sup>2</sup> )
0	20.27 ± 7.99
1	9.75 ± 2.53
3	6.92 ± 2.41
7	24.04 ± 4.52

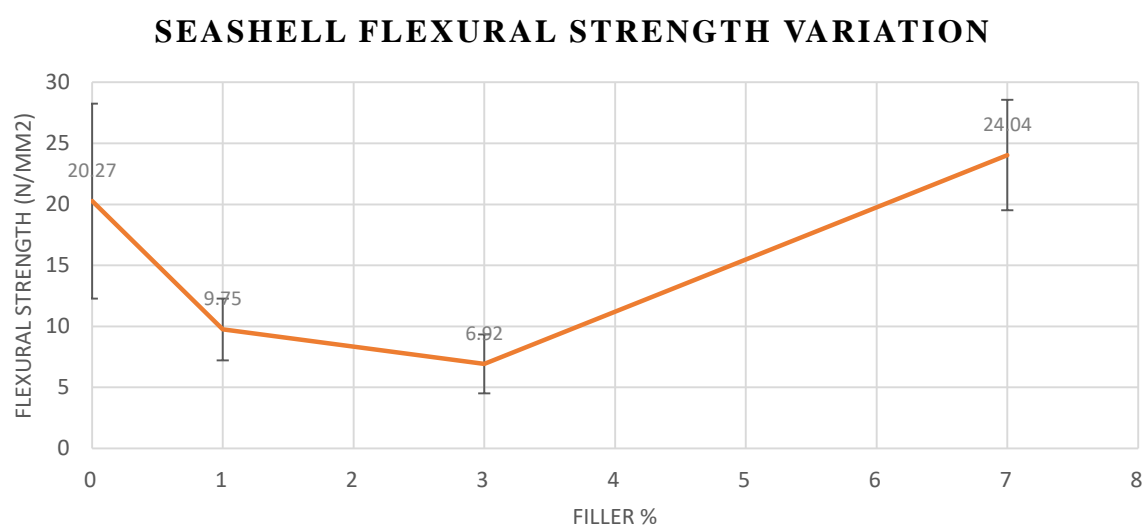


**Figure 4.28** Flexural Strength Variation in different Seashell filler content

Using the Flexural Modulus Formula, put necessary parameters into the formula and calculate it for each set of specimens and further calculate Mean and Standard Deviation and tabulate it. Later compare the Flexural Modulus for Plain Neat Kevlar specimens and Seashell nanofiller with MWCNT infused Kevlar at different ratios.

**Table 4.6** Comparative Analysis of Results obtained by 3 point bending test

S. No	Nanofiller Content	Flexural Stress (N/mm <sup>2</sup> )	Flexural Strain	Flexural Modulus (N/mm <sup>2</sup> )
1	Neat Kevlar	121.15 ± 35.38	0.08 ± 0.02	5990.196 ± 1299.967
2	Seashell 1 % + 0.25 % MWCNT	98.44 ± 70.71	0.04 ± 0.01	7328.908 ± 2488.292
3	Seashell 3 % + 0.25 % MWCNT	39.45 ± 9.23	0.06 ± 0.02	3690.573 ± 621.2975
4	Seashell 7 % + 0.25 % MWCNT	115.63 ± 4.90	0.07 ± 0.01	9151.841 ± 476.9786

Based on the comparative study for 3 Point Bending test done for various Neat Kevlar specimens and Kevlar infused with different percentage of Seashell nanofiller and 0.25% MWCNT specimens, it is concluded that there is gradual decrement in values of Flexural Stress till 3% Seashell filler and then an increment in Flexural stress till 7% seashell filler content. There is not much appreciable change in Flexural Strain values with addition of seashell nanofiller content with neat Kevlar. We can see variation in Flexural Modulus as we increase the Seashell nanofiller percentage up to 7%.

#### 4.5.2.5 Failed Specimens

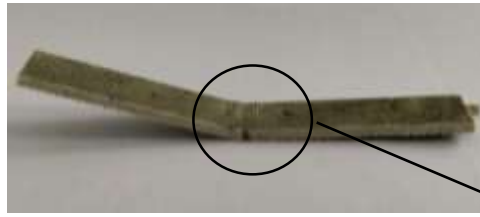


**Figure 4.29** Failed 3 Point Bending Test Specimens

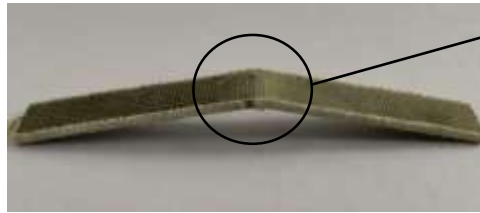


**Figure 4.30** Failed 3 Point Bending Test Specimens

Failure of Specimen after 3 Point Bending Test

As point load is applied on simply supported beam, it bends in the sagging manner and maximum deflection is at centre of beam. Load is transferred layer by layer and matrix supports the fibers from breaking. Top layers are in compression and bottom layers are in tension. When maximum load bearing point is attained the fiber layers break and matrix interface is sheared and specimen attains U shape as it can be seen in figure 4.42 and figure 4.43.

#### 4.5.3 INTERLAMINAR SHEAR TEST (ILSS) – ASTM D2344

The short beam shear test (ILSS) was conducted in accordance with ASTM D2344 at a cross-head rate of 1 mm/min and the results were reported using the INSTRON universal testing machine. In order to allow for lateral movement, each FMLs specimen was placed on two roller supports, with the load being placed directly in the centre of the FMLs specimen. In this experiment, the beam was loaded until failure occurred, and the failure load was used to calculate the apparent interlaminar shear strength (ILSS) of the specimen.

The length and width of the specimens used for this test as per ASTM D2344 were 40 mm and 15 mm, respectively, with a span length of 24 mm.

After test is performed Load v/s Cross Head Travel graph is plotted for each specimen and Flexural Modulus is calculated for every specimen. Mean and Standard Deviation is calculated and the data is tabulated.

#### 4.5.3.1 PLAIN NEAT KEVLAR

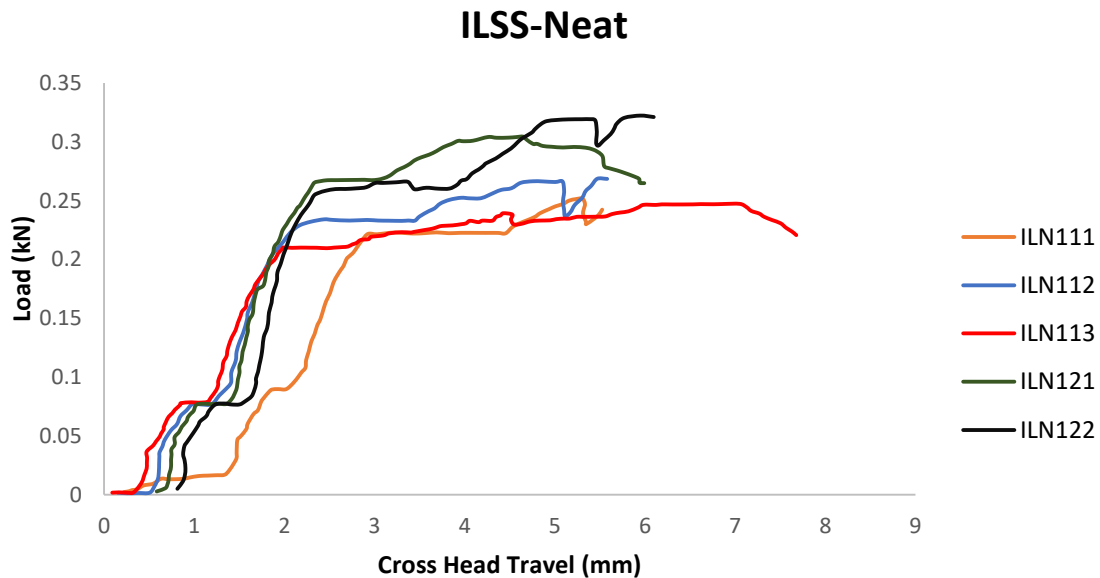


**Figure 4.31** Load v/s Cross Head Travel for Neat Kevlar Specimens of ILSS

#### 4.5.3.2 SEASHELL 1% + 0.25% MWCNT

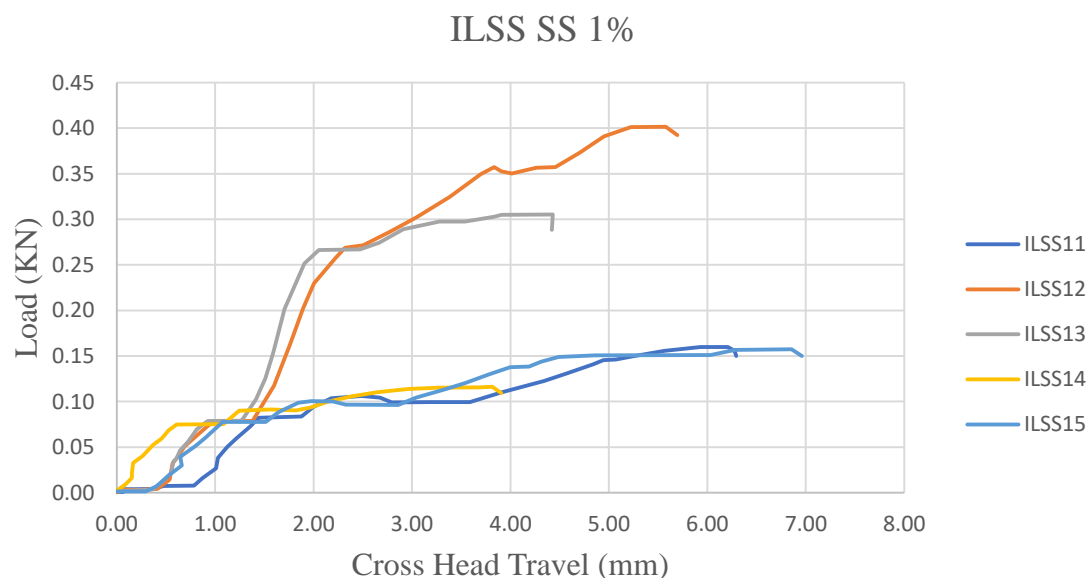


**Figure 4.32** Load v/s Cross Head Travel for Neat Kevlar Specimens of ILSS

### 4.5.3.3 SEASHELL 3% + 0.25% MWCNT

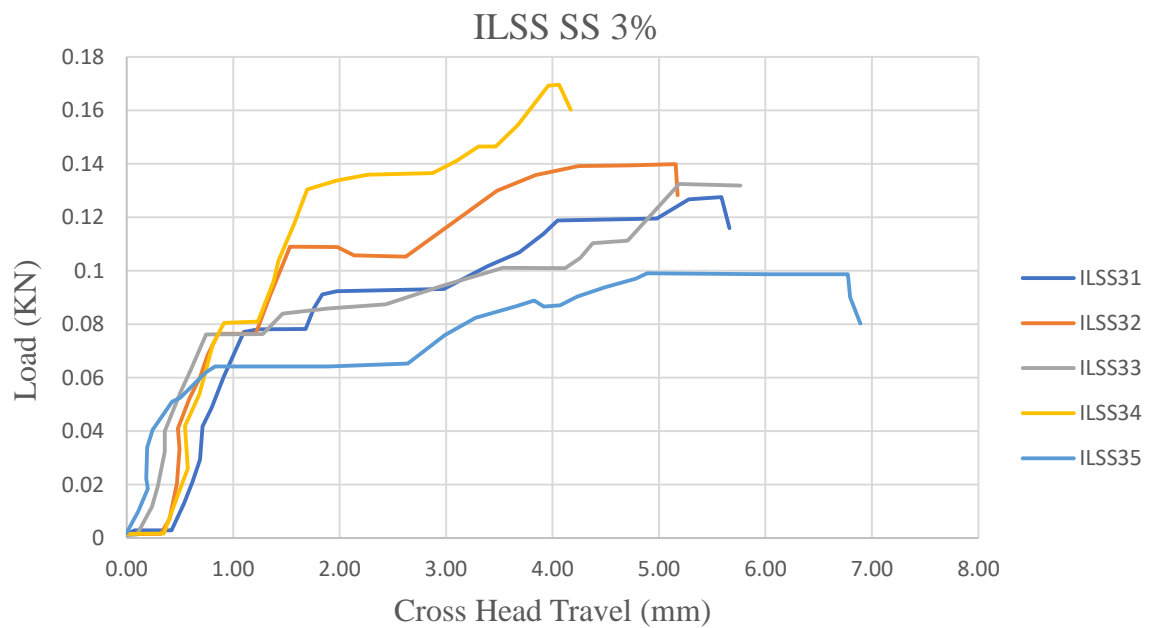


**Figure 4.33** Load v/s Cross Head Travel for 3% Seashell + 0.25% MWCNT infused Kevlar Specimens of ILSS

### 4.5.3.4 SEASHELL 7% + 0.25% MWCNT

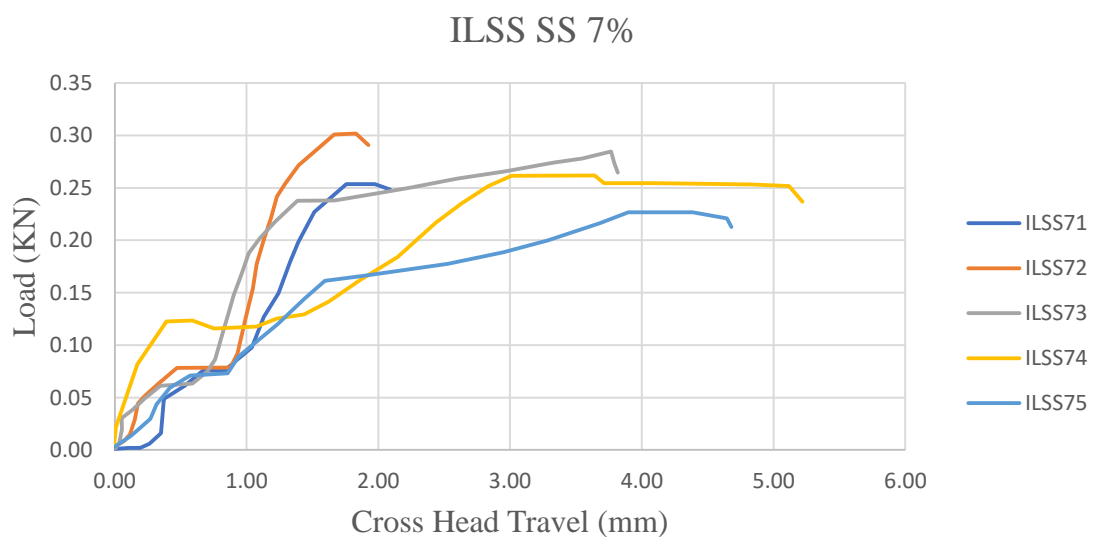


**Figure 4.34** Load v/s Cross Head Travel for 7% Seashell + 0.25% MWCNT infused Kevlar Specimens of ILSS

**Table 4.7** Variation of Flexural Modulus for different Seashell Fillers content

Seashell Filler %	Interlaminar Shear Strength (MPa)
0	$5.78 \pm 0.63$
1	$4.76 \pm 2.53$
3	$2.80 \pm 0.51$
7	$5.59 \pm 0.60$

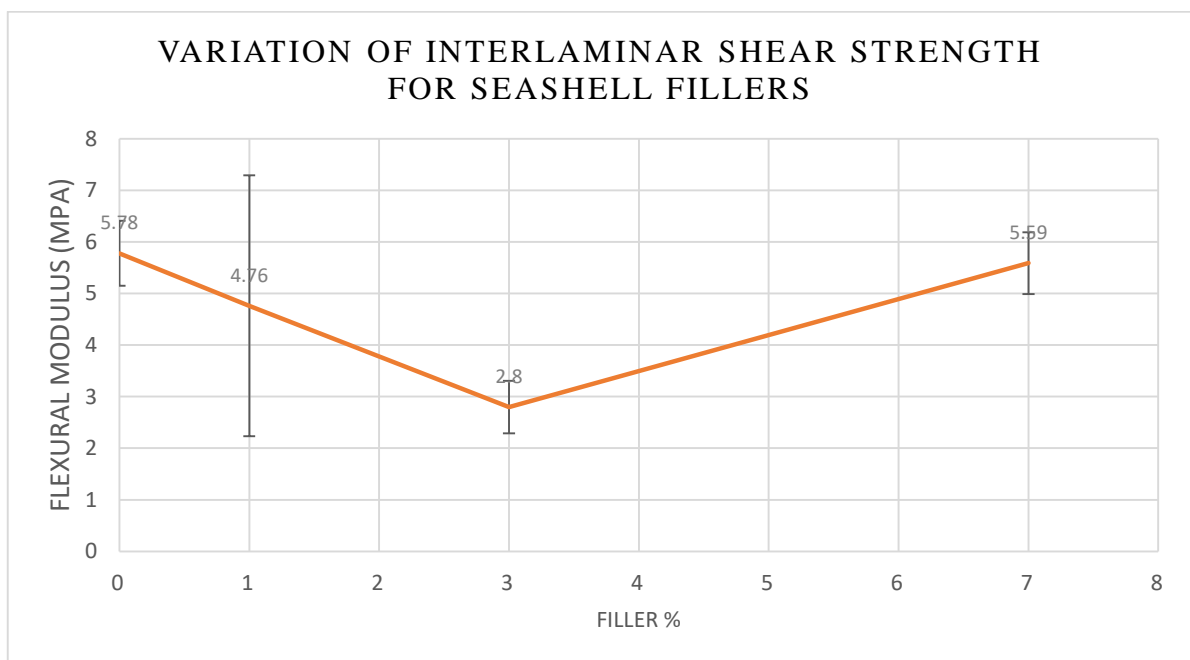


**Figure 4.35** Variation of Flexural Modulus for different Seashell Fillers content

#### 4.5.3.5 Failed Specimens

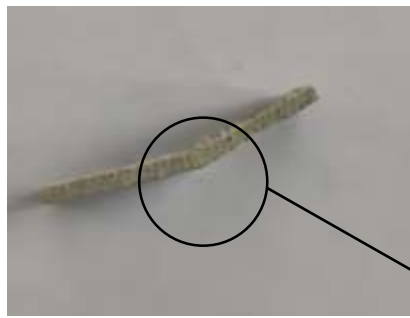


**Figure 4.36** Failed ILSS Test Specimen

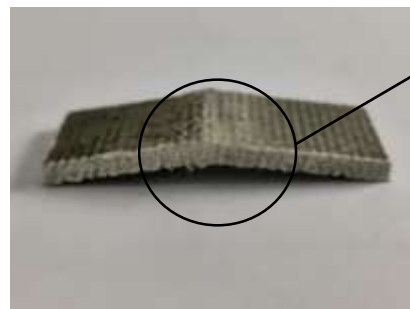


**Figure 4.37** Failed ILSS Test Specimen

Failure of Specimen after ILSS Test

As point load is applied on simply supported beam, it bends in the sagging manner and maximum deflection is at centre of beam. Load is transferred layer by layer and matrix supports the fibers from breaking. Top layers are in compression and bottom layers are in tension. When maximum load bearing point is attained the fiber layers break and matrix interface is sheared and specimen attains U shape as shown in figure 4.49 and figure 4.50.

#### 4.5.4 CHARPY IMPACT TEST – ASTM D256

The Charpy impact test, also known as the Charpy U-notch test, is a standardized high strain-rate test which determines the amount of energy absorbed by a material during fracture. Absorbed energy is a measure of the material's notch toughness. It is widely used in industry, since it is easy to prepare and conduct and results can be obtained quickly and cheaply.



The apparatus consists of a pendulum of known mass and length that is dropped from a known height to impact a notched specimen of material. The energy transferred to the material can be inferred by comparing the difference in the height of the hammer before and after the fracture (energy absorbed by the fracture event).

The notch in the sample affects the results of the impact test, thus it is necessary for the notch to be of regular dimensions and geometry. For this test we have referred ASTM D256 with specimen dimensions of 75 mm x 13 mm having a U-notch at centre of 5 mm depth.

Test hammer is raised up to top position and locked. Specimen is kept at exact centre position with U-notch facing opposite to the impact of hammer. Position of arrow reader is kept at 0. Hammer lock is released and hammer is allowed to impact the specimen freely. Specimen breaks at notch position and Energy absorbed is noted.

Test is repeated for every sample and later mean and Standard Deviation is calculated for each set of specimens to tabulate the results.



**Figure 4.38** Charpy Impact Testing Setup



**Figure 4.39** Absorbed Energy Reader

**Table 4.8** Variation of Impact Strength with different Seashell filler content

Seashell Filler %	Energy Absorbed (J)	Impact Strength (MPa)
0	$2.35 \pm 0.55$	31.25
1	$2.65 \pm 0.98$	35
3	$3.52 \pm 0.48$	47
7	$2.58 \pm 0.47$	34.45

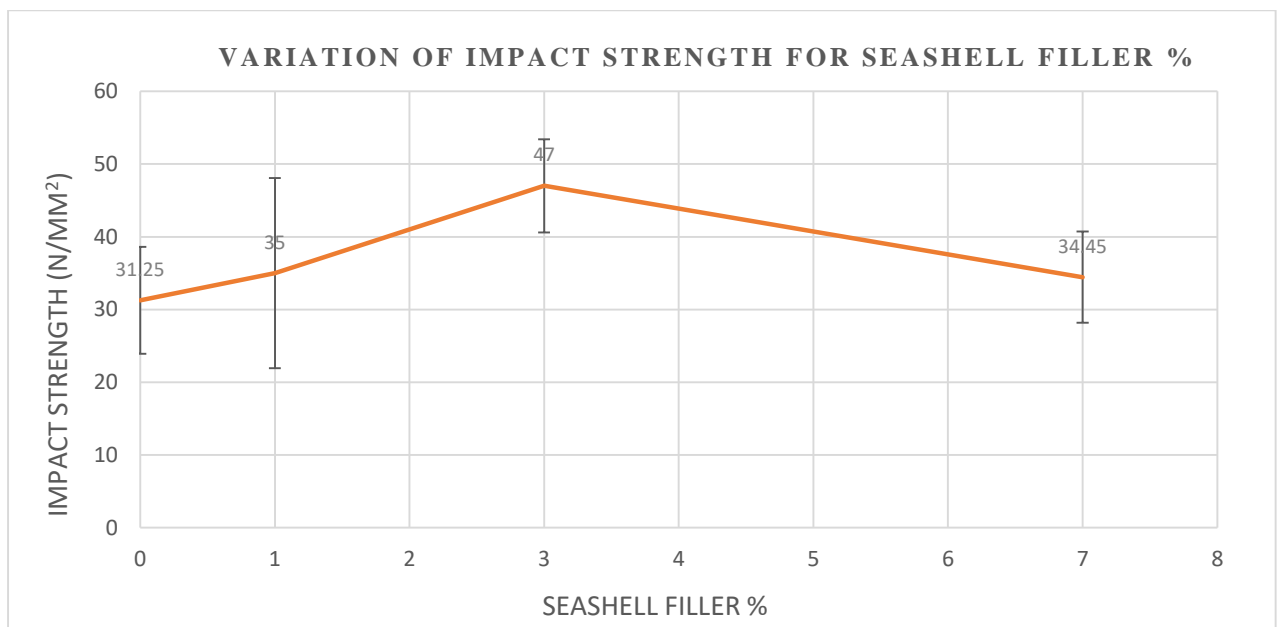


**Figure 4.40** Variation of Impact Strength for different Seashell Filler content

Based on the comparative study of Impact Strength of Plain Neat Kevlar with Kevlar infused Seashell Nanofiller with MWCNT specimens it is concluded that

with increment in Seashell Nanofiller content till 3% by wt. we can see gradual increasing trend with around 33.51 % and then again starts to dip when it comes to 7% seashell nanofiller content but still showing greater Impact strength than plain neat Kevlar specimens.

#### 4.5.5 Failed Specimens



**Figure 4.41** Failed Charpy Impact Test Specimen

Failure of Specimen  
after Charpy Impact  
Test



**Figure 4.42** Failed Charpy Impact Test Specimen

V- Notch Specimen is allowed to get Impact from the machine rod, Strain Energy is absorbed and fracture is attained at notch area and specimen is cracked into two halves as shown in figure 4.54 and figure 4.55.

#### 4.5.6 SHEAR TEST- ASTM D7078

The effect of seashell nanoparticles on the shear properties of specimens was characterized at the crosshead speed of 2 mm/min by applying a shearing force of the specimen using the SHIMADZU Universal Testing Machine. The length and width of the Kevlar specimens used for this test as per ASTM D7078 were 76 mm and 56 mm, respectively, with a span length of 31 mm. One of the typical setup arrangements is shown in the figure below.

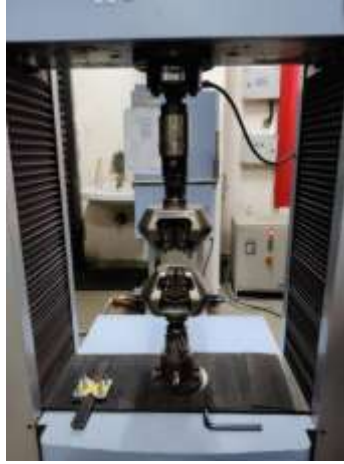


**Figure 4.43** Universal Testing Machine for Shear Test



**Figure 4.44** Shear testing fixture attached in UTM

Shear stress and Shear Strain were calculated by using the force and stroke values in the following equations given below respectively for the known width, thickness and span length:

$$\sigma_s = F / w t$$

$$\epsilon_f = \tan \left( \left( \frac{s}{31} \right) * 0.0174 \right)$$

Where,  $\sigma_s$  &  $\epsilon_f$  are the shear stress and Strain, respectively; **F** and **s** are the shear load and stroke, respectively; **w** and **t** are the width and thickness of the specimen, respectively; 31 is the shearing length of the specimen.

ASTM D7078 is a V-notched rail shear testing method that is widely used to determine the in-plane shear characteristics of composite materials.



**Figure 4.45.** Shear Test Specimen fixed in the testing fixture

#### 4.5.6.1 PLAIN NEAT KEVLAR

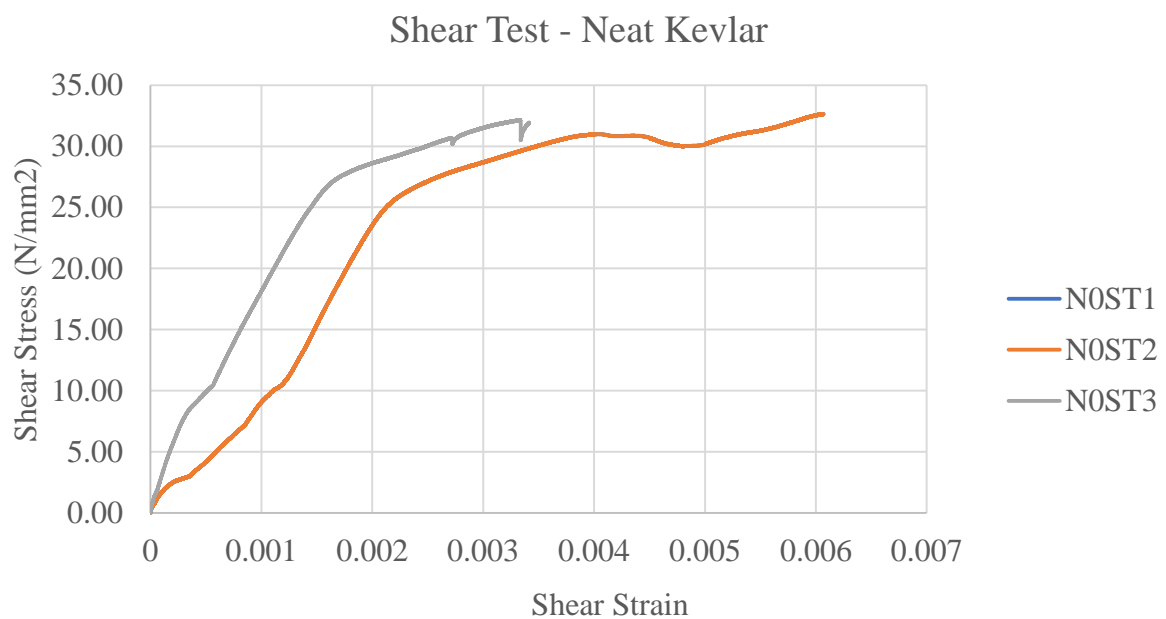


**Figure 4.46** Shear Stress vs Shear Strain Graph for Neat Kevlar Specimens

#### 4.5.6.2 SEASHELL 1% + 0.25% MWCNT

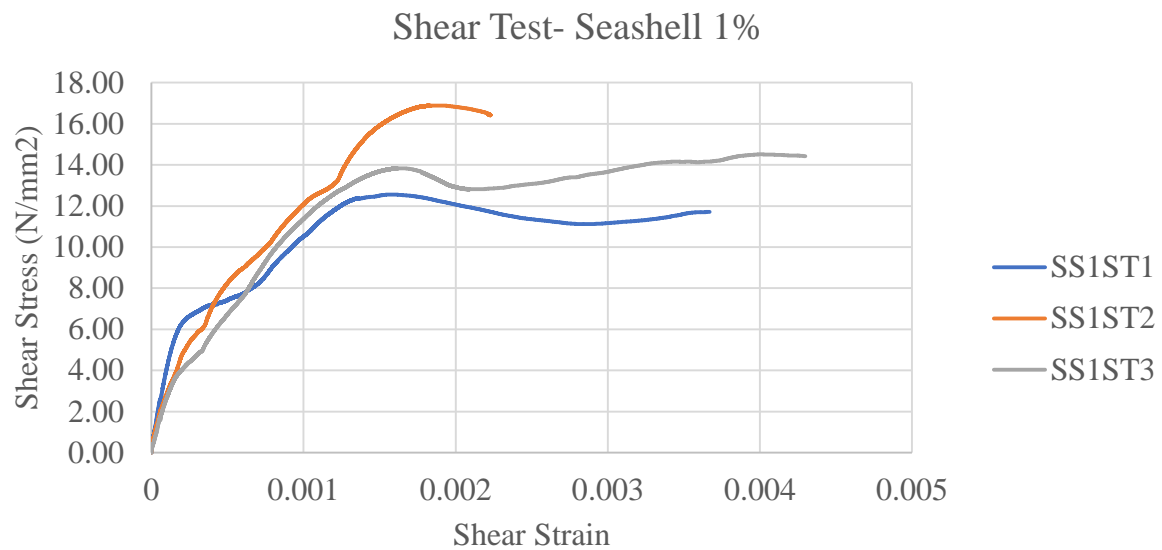


**Figure 4.47** Shear Stress vs Shear Strain Graph for 1% Seashell + 0.25% MWCNT infused Kevlar Specimen

#### 4.5.6.3 SEASHELL 3% + 0.25% MWCNT

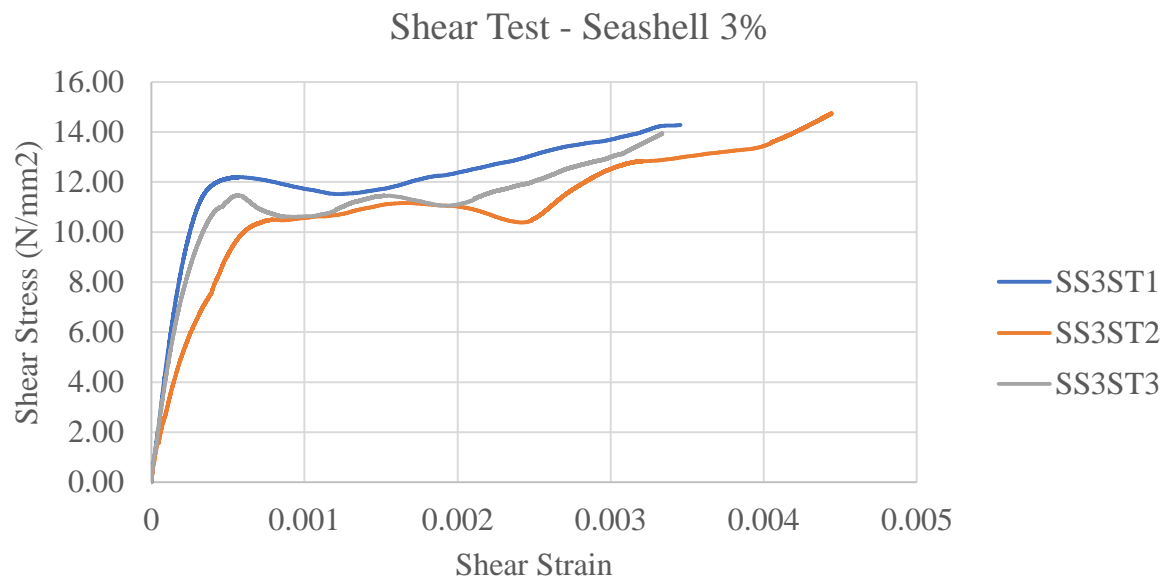


**Figure 4.48** Shear Stress vs Shear Strain Graph for 3% Seashell + 0.25% MWCNT infused Kevlar Specimens

#### 4.5.6.4 SEASHELL 7% + 0.25% MWCNT

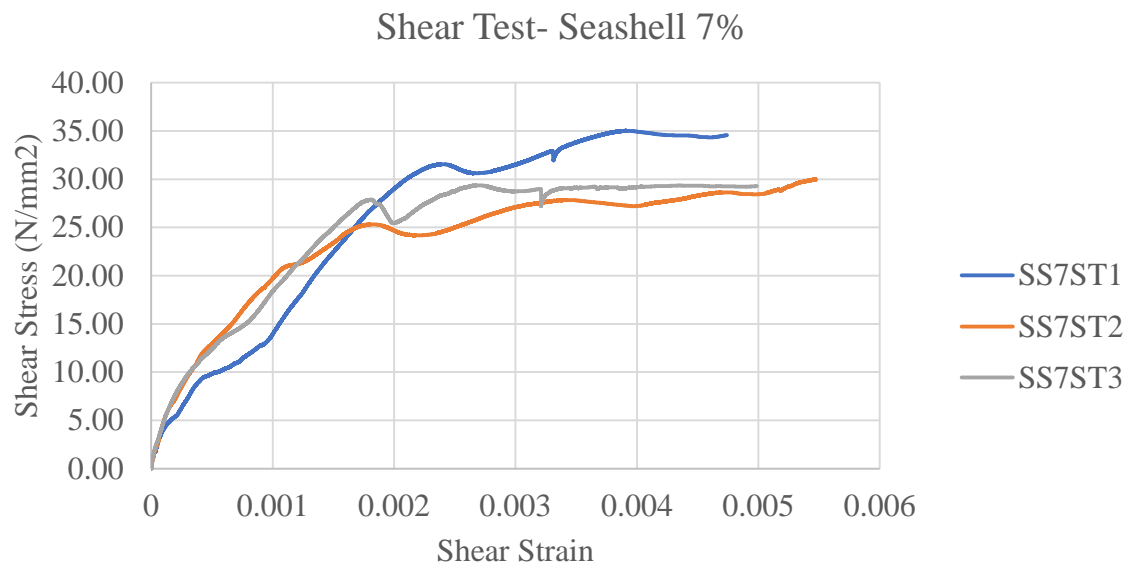


**Figure 4.49** Shear Stress vs Shear Strain Graph for 7% Seashell + 0.25% MWCNT infused Kevlar Specimens

Based on the comparative study of Maximum Shear Stress of Plain Neat Kevlar with Kevlar infused Seashell Nanofiller with MWCNT specimens it is concluded that with increment in Seashell Nanofiller content till 3% by wt. we can see gradual decreasing trend and then again starts to increase when it comes to 7% seashell nanofiller content with values close to that of Neat Kevlar showing greater Maximum Shear Stress in plain neat Kevlar specimens that seashell nanofiller infused Kevlar specimens.

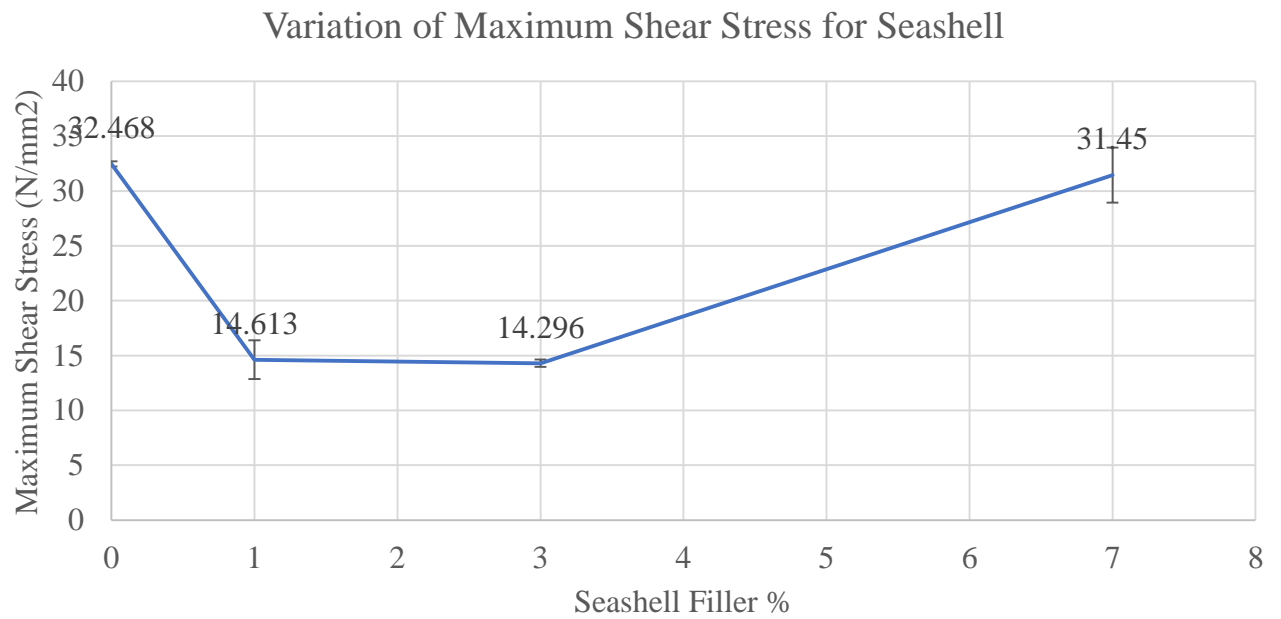


**Figure 4.50** Variation of Maximum Shear Stress for different Seashell filler content

#### 4.5.6.5 Failed Specimens

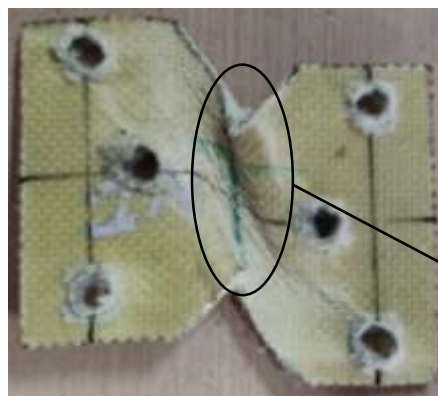


**Figure 4.51** Failed Shear Test Specimen

Failure of Specimen after Shear Test

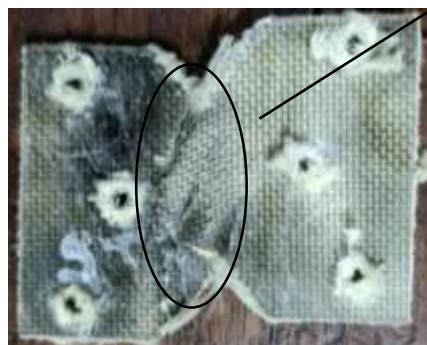


**Figure 4.52** Failed Shear Test Specimen



As the fixture with shear test specimen is allowed to pull, inter laminar fibres shear with matrix interface. Shearing occurs at central axis of Shearing length. After maximum shear load bearing capacity of the fibre-matrix, complete deformation of the sample is seen in Figure 4.64 and Figure 4.65.

## **4.6 SUMMARY**

In this chapter we have discussed about

- General Introduction to Seashell and Preparation of nano seashell with morphological study of nano seashell involving XRD & SEM Imaging and EDS of nano seashell.
- Fabrication of neat Kevlar and nano seashell infused Kevlar composites plates is been explained in great detail.
- Mechanical and Impact test analysis for the specimens is done which includes namely Tensile Test, 3 Point Bending Test, ILSS Test, Charpy Test and Shear Test to study the mechanical and impact property variation after adding seashell nanofiller to neat Kevlar.

# CHAPTER 5

## ALUMINA + MWCNT

### 5.1 GENERAL INTRODUCTION

The addition of different nanofillers enhances the properties of polymer composites in which Alumina nanofillers are considered as one of the well-established nanofiller due to their excellent mechanical, thermal and Tribological properties.  $\text{Al}_2\text{O}_3$  nanoparticles and  $\text{Al}_2\text{O}_3$  Nano fibres increase the mechanical strength of the composites, due to their reinforcing effect on the epoxy matrices.  $\text{Al}_2\text{O}_3$  nanoparticles have a porous morphology (Vinay SS, 2020).  $\text{Al}_2\text{O}_3$  is a ceramic material, which is used as a reinforcing filler component in both micro and nano sizes. The micro and nanofiller are in the size range of 20–70  $\mu\text{m}$  and 120–40 nm, respectively. Nano-  $\text{Al}_2\text{O}_3$  is prepared by using aluminium nitrate monohydrate ( $\text{Al}(\text{NO}_3)_3 \cdot 9\text{H}_2\text{O}$ ) and citric acid in the auto combustion process. (Raghavendra, 2015). The alpha aluminium oxide nanoparticles from the United States are coated with the aluminic ester ( $\text{Al}_2\text{O}_3$ : aluminic ester = 98.1:1.2, alpha, 60 nm, super hydrophobic higher lipophilic). According to the MSDS, the aluminium acid ester coating's composition is  $\text{Al}_2\text{O}_3$ : aluminic ester 98.1 wt. percent: 1.2 wt. percent. Because of their phase stability, high hardness, and dimensional stability, these nanoparticles are widely employed (Omar M. Yousri, 2017). To improve the qualities of epoxy resins, several nanoparticles such as graphite nano fibre, carbon nanotubes, Nanoclay, cellulose nano fibre, and nano alumina have been used. It is widely acknowledged that the enormous surface-to-volume ratio of nano scale incorporations plays an important role in mechanical property enhancement. The increased need for nanomaterial's is due to the fact that novel chemical and

physical properties can be obtained when nano sized fillers are added to polymer matrixes, but a single molecule or the identical material without a nano-filler does not display such advantages (Abdollah Omrani, 2009). Alumina nano powder has a surface area of 300–700 square meters per gram. Individual fibres are manufactured using electro-explosion of metal wire, and they appear linear and co-mingled in a bundle under a TEM microscope. The fibres feature unique sorption capabilities, as well as cationic and anionic chemisorption properties, such as the ability to scavenge precious and heavy metals from water. They are agglomerated along the length of the axis. The alumina nano fibres also exhibit aspect ratios greater than 20, and several of the fibres appear to be hundreds of nano meters long (S.A. Meguid, 2003).

**Table 5.1** Properties of Alumina Nano powder

Properties	Alumina Nan powder
Size	2–4 nm in diameter
Young's Modulus	300 GPA
Tensile Strength	2000 MPa
Aspect Ratio	20–80
Surface Area	300–700 m <sup>2</sup> /g

One of the most cost-effective and commercially feasible materials is alumina. It has a melting point of ~2071 ° C. and a density of 3.75-3.95 gm/cc. Aside from these characteristics, its bulk modulus is ~324 GPA, its compressive strength is in the 2000-4000 MPa range. Alumina has a fracture toughness of ~5 MPa and a coefficient of thermal expansion of  $10.9 \times 10^{-6}/K$ . Despite its outstanding functional qualities, alumina's uses are limited due to its low fracture toughness. Significant attempts have been made to increase the fracture toughness of alumina by the use of nanofillers or novel sintering methods such as spark plasma sintering (SPS) (Nidhi Sharma, 2019).

## 5.2 MORPHOLOGICAL IMAGES OF NANO ALUMINA

Morphology, or the study of form, which includes shape, size, and structure, is critical for materials research in general. Morphology is very important for nanostructured materials, also known as nano materials, since shape determines physical and chemical characteristics.

The scanning electron microscope (SEM) is a powerful and frequently used instrument. The SEM has an extremely large depth of focus and is therefore well suited for topographic imaging. The specimen is bombarded by a convergent electron beam, which is scanned across the surface. This electron beam generates a number of different 52 types of signals, which are emitted from the area of the specimen where the electron beam is impinging, SEM was employed to monitor the surface morphologies as shown in the Figure 5.1 to Figure 5.2.

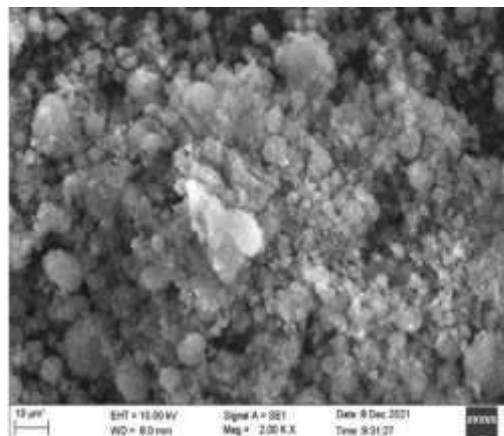


**Figure 5.1** SEM Image of Nano Alumina

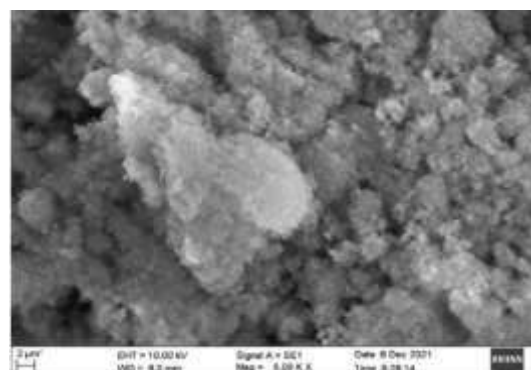


**Figure 5.2** SEM Image of Nano Alumina

X-ray diffraction (XRD) is a rapid analytical technique primarily used for phase identification of a crystalline material and can provide information on unit cell dimensions. The analysed material is fine, homogenized and average bulk composition is determined as shown in the figure 5.3.

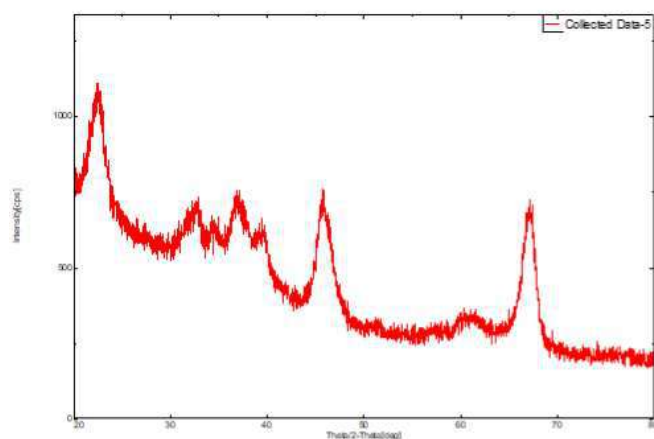


**Figure 5.3** XRD Image of Nano Alumina

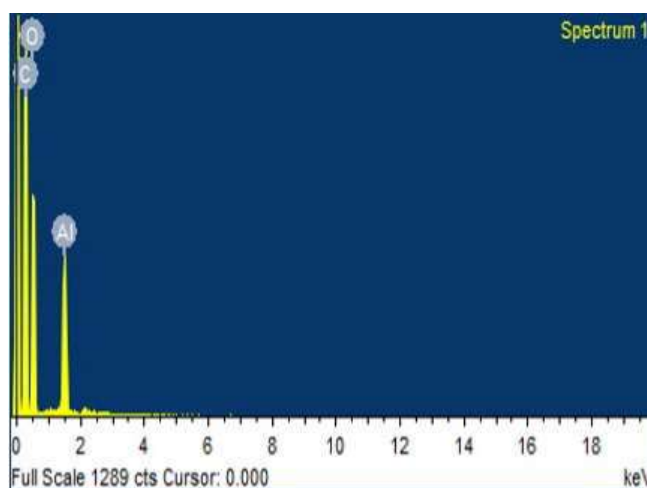


**Figure 5.4** EDS of Nano Alumina

**Table 5.2** Elemental Concentration of Nano Alumina

Element	Weight%	Atomic%
C	50.95	59.51
O	41.97	36.81
Al	7.08	3.68
Totals	100.00	

## **5.3 FABRICATION OF PLATES**

### **5.3.1 Plates with Alumina + CNT**

Dimensions: 320 mm × 320 mm

Thickness of Plate: 2.4 mm

No of Kevlar Layers: 8 (0.3 mm thickness each)

Total Mass of Kevlar = 160 g

Mass of Resin LY556 = 160 g

Mass of Hardener = 15 g

Weight of MWCNT= 0.25 g

Weight of 1% Alumina nanofiller by weight of epoxy = 1.6 g

Weight of 3% Alumina nanofiller by weight of epoxy = 5 g

Weight of 7% Alumina nanofiller by weight of epoxy = 9.5 g

Hand Lay-up Method of Fabrication of composites for Alumina + MWCNT Plates is same as mentioned above in **Section 4.4** of this report.

## **5.4 MECHANICAL & IMPACT TESTS ANALYSIS FOR PREPARED SPECIMENS**

Tensile, flexural, tension shear, and inter-laminar shear tests were carried out at room temperature (25°C) on an INSTRON universal testing machine with a capacity of 100 KN. Load-displacement data were obtained from the DAQ system connected to a computer unit and machine used for testing. Five to six samples were tested for each test, and the average value was calculated and reported along with standard deviation in the report.

### 5.4.1 TENSILE TEST – ASTM D3039

The tensile tests and their properties, i.e., ultimate tensile strength, Elastic modulus, Strain to failure of the fabricated Kevlar plates, were conducted and evaluated according to the ASTM D3039 at a constant cross-head speed of 2 mm/min. The load-elongation curves obtained from the tensile tests were used to calculate engineering stress and strain measurements.



**Figure 5.5** INSTRON Universal Testing Machine

The test process involves placing the test specimen in the testing machine and slowly extending it until it fractures. During this process, the elongation of the gauge section is recorded against the applied force. The data is manipulated so that it is not specific to the geometry of the test sample. The elongation measurement is used to calculate the engineering strain,  $\epsilon$ , using the following equation:

$$\epsilon = \frac{\Delta L}{L_0} = \frac{L - L_0}{L_0}$$

Where  $\Delta L$  is the change in gauge length,  $L_0$  is the initial gauge length, and  $L$  is the final length. The force measurement is used to calculate the engineering stress,  $\sigma$ , using the following equation:

$$\sigma = \frac{F_n}{A}$$

Where F is the tensile force and A is the nominal cross-section of the specimen. The machine does these calculations as the force increases, so that the data points can be graphed into a stress–strain curve.

#### 5.4.1.1 Plain Neat Kevlar

From the Stress-Strain Curve obtained from the tensile test, maximum stress point is observed and marked on graph as Ultimate Tensile Strength (UTS) for Neat Kevlar specimens.

Mean Ultimate Tensile Strength is calculated for the set of specimens of Neat Kevlar tested and Standard Deviation is marked as shown in the Table 0.3

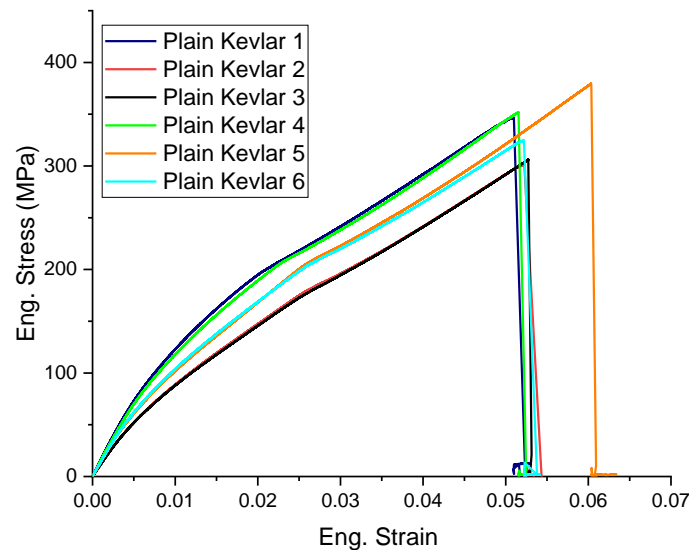


**Figure 5.6** Engineering Stress - Strain Graph for Neat Kevlar Specimens

Later graph is selected till UTS Point and Linear slope is calculated for the initial linear curve of the graph from 0 to UTS point. The slope m, obtained is the Young's Modulus of the Neat Kevlar tested specimen. Mean Young's Modulus is calculated for the set of specimens tested of Neat Kevlar and Standard Deviation is marked.



### 5.4.1.2 ALUMINA 1% + 0.25% MWCNT

From the Stress-Strain Curve obtained from the tensile test, maximum stress point is observed and marked on graph as Ultimate Tensile Strength (UTS) for Kevlar infused with 1% Alumina nanofiller and 0.25% MWCNT specimen.

Mean Ultimate Tensile Strength is calculated for the set of specimens tested and Standard Deviation is marked.

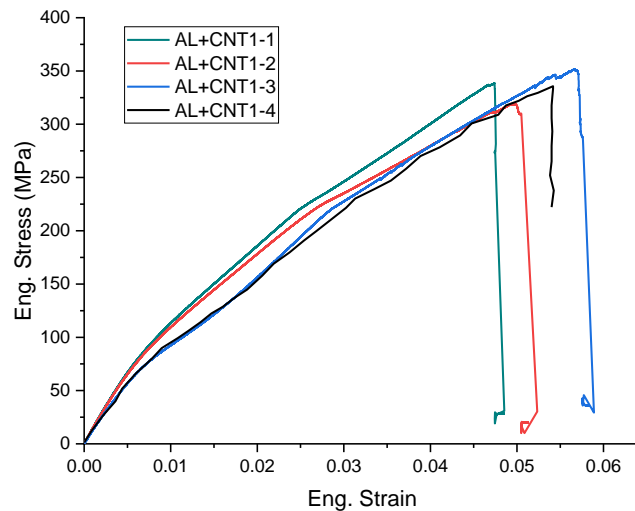


**Figure 5.7** Engineering Stress - Strain Graph for Alumina 1% + 0.25% MWCNT Specimens

Later graph is selected till Ultimate Tensile Strength Point and Linear slope is calculated for the initial linear curve of the graph from 0 to UTS point. The slope  $m$ , obtained is the Young's Modulus of the Kevlar infused with 1% Alumina nanofiller and 0.25% MWCNT specimen.

Mean Young's Modulus is calculated for the set of specimens tested and Standard Deviation is marked.

### 5.4.1.3 ALUMINA 3% + 0.25% MWCNT

From the Stress-Strain Curve obtained from the tensile test, maximum stress point is observed and marked on graph as Ultimate Tensile Strength (UTS) for Kevlar infused with 3% Alumina nanofiller and 0.25% MWCNT specimen.

Mean Ultimate Tensile Strength is calculated for the set of specimens tested and Standard Deviation is marked.

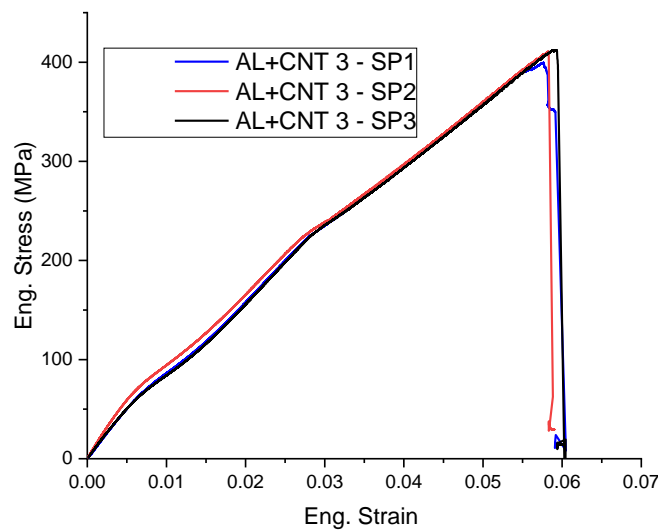


**Figure 5.8** Engineering Stress - Strain Graph for Alumina 3% + 0.25% MWCNT Specimens  
Later graph is selected till Ultimate Tensile Strength Point and Linear slope is calculated for the initial linear curve of the graph from 0 to UTS point. The slope  $m$ , obtained is the Young's Modulus of the Kevlar infused with 3% Alumina nanofiller and 0.25% MWCNT specimen.

Mean Young's Modulus is calculated for the set of specimens tested and Standard Deviation is marked.

#### 5.4.1.4 ALUMINA 6% + 0.25% MWCNT

From the Stress-Strain Curve obtained from the tensile test, maximum stress point is observed and marked on graph as Ultimate Tensile Strength (UTS) for Kevlar infused with 6% Alumina nanofiller and 0.25% MWCNT specimen.

Mean Ultimate Tensile Strength is calculated for the set of specimens tested and Standard Deviation is marked.

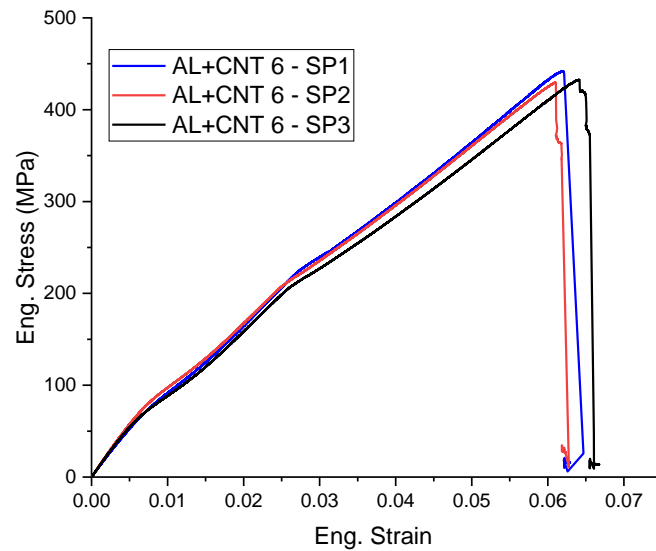


**Figure 5.9** Engineering Stress - Strain Graph for Alumina 6% + 0.25% MWCNT Specimens  
Later graph is selected till Ultimate Tensile Strength Point and Linear slope is calculated for the initial linear curve of the graph from 0 to UTS point. The slope  $m$ , obtained is the Young's Modulus of the Kevlar infused with 6% Alumina nanofiller and 0.25% MWCNT specimen.

Mean Young's Modulus is calculated for the set of specimens tested and Standard Deviation is marked.

**Table 5.4** Comparative Analysis of UTM and Young's Modulus for different Alumina Nanofiller content

S. No	Nanofiller Content	Ultimate Tensile Strength (MPa)	Young's Modulus (MPa)
1	Neat Kevlar	$334.17 \pm 27.11$	$6890.47 \pm 632.44$
2	Alumina 1 % + 0.25 % MWCNT	$335.25 \pm 11.43$	$7244.7 \pm 542.79$
3	Alumina 3 % + 0.25 % MWCNT	$404.33 \pm 5.91$	$7370.87 \pm 63.81$
4	Alumina 6 % + 0.25 % MWCNT	$430.67 \pm 4.50$	$7311.37 \pm 210.97$

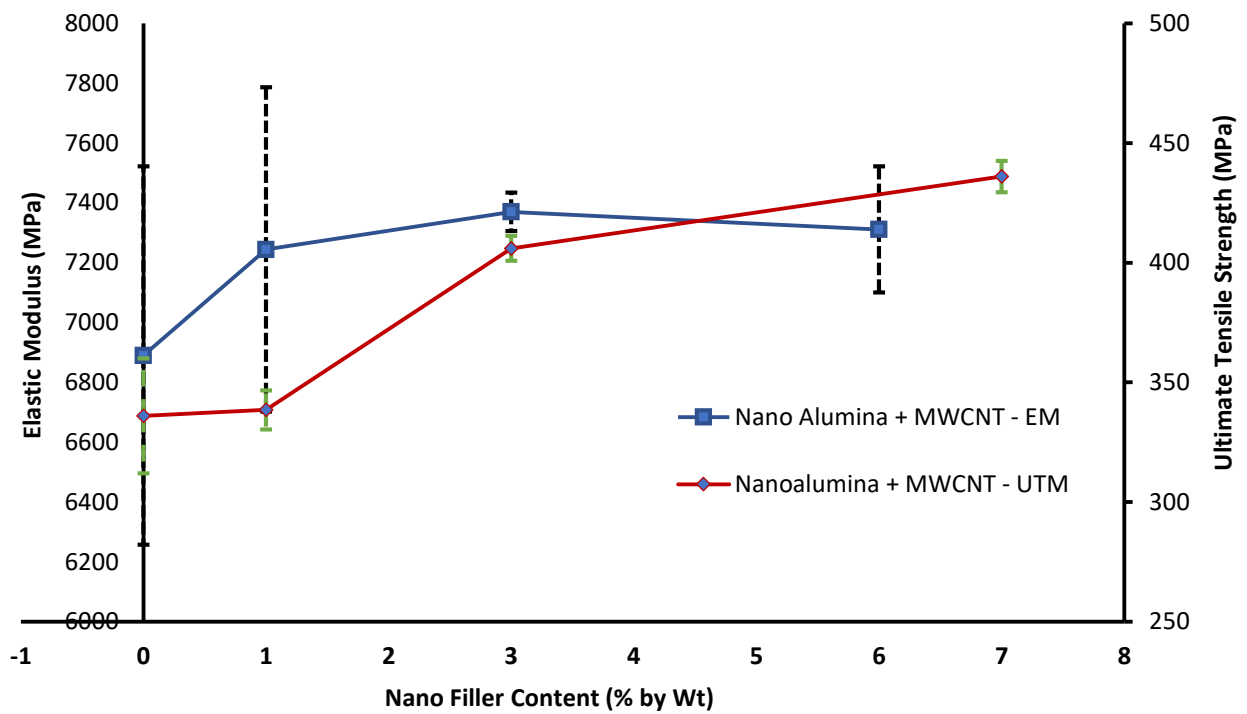


**Figure 5.10** Comparative Analysis of UTM and Young's Modulus for different Alumina Nanofiller content

Based on the comparative study for Tensile test done for various Neat Kevlar specimens and Kevlar infused with different percentage of Alumina nanofiller and 0.25% MWCNT specimens, it is concluded that there is gradual increment in values of Ultimate Tensile Strength and Young's Modulus as we increase the Alumina nanofiller percentage up to 6%. We can see increment of around 22% in Ultimate Tensile Strength and increment of around 6% in Young's Modulus for Kevlar infused Alumina nanofiller with MWCNT at 6% nano Alumina filler content w.r.t Neat Kevlar.

#### 5.4.1.5 Failed Specimens

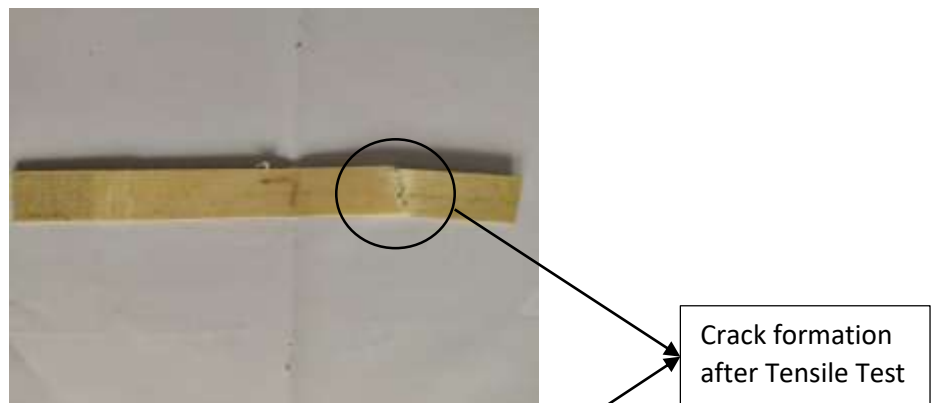


**Figure 5.11** Failed Tensile Test Specimen



**Figure 5.12** Failed Tensile Test Specimen

As the load is applied ahead of Ultimate Tensile Stress the fibre pull out begins and matrix interface is sheared and specimen crack initiation begins. Later on continuous load application we can see brittle failure and specimen crack is formed as shown in Figure 5.11 and Figure 5.12.

#### 5.4.1.5.1 SEM Images of Failed Tensile Test Specimens

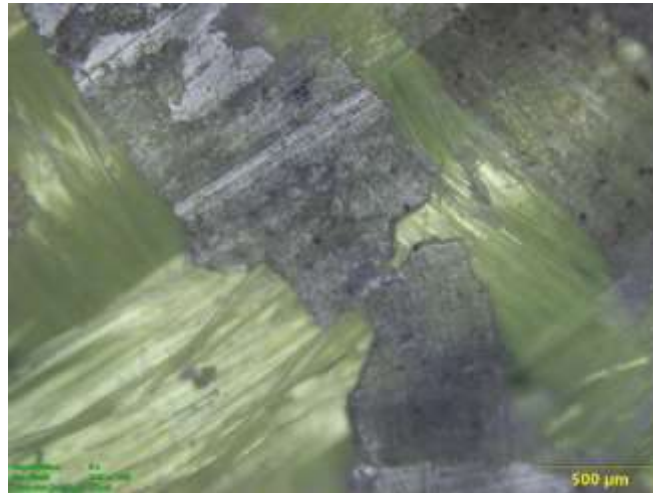


**Figure 5.113** SEM Image of Failed Tensile Test Specimen

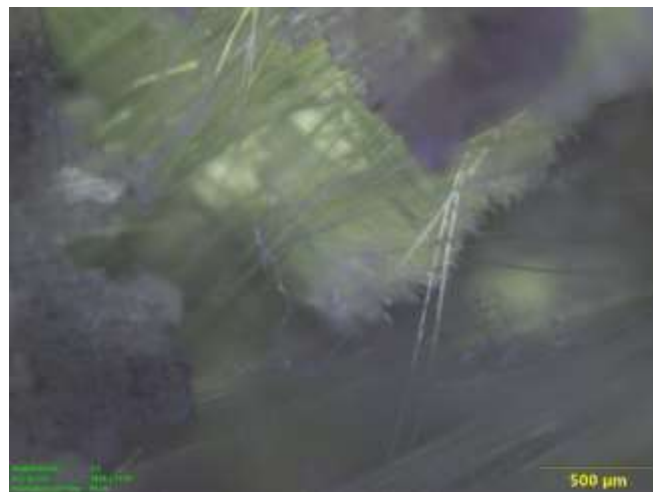


**Figure 5.14** SEM Image of Failed Tensile Test Specimen

#### 5.4.2 3 POINT BENDING TEST – ASTM D790

The effect of alumina nanoparticles on the flexural properties of specimens was characterized at the crosshead speed of 2 mm/min by applying a point at the centre of the specimen using the INSTRON universal testing machine. The length and width of the Kevlar specimens used for this test as per ASTM D790 were 12.7 mm and 125 mm, respectively, with a span length of 40 mm. One of the typical setup arrangements is shown in the figure below. Flexural stress and flex-

ural Strain were calculated by using the load and displacement values in the following equations given below respectively for the known width, thickness and span length:

$$\sigma_f = 1.5 Lu / W t^2$$

$$\epsilon_f = \frac{6t\delta}{Z^2}$$

Where,  $\sigma_f$  &  $\epsilon_f$  are the flexural strength and Strain, respectively;  $L$  and  $u$  are the flexural load and displacement, respectively;  $w$  and  $t$  are the width and thickness of the specimen, respectively;  $Z$  is the span length of the specimen.

$$E_{fl} = L^3 m / 4bh^3$$

Where,  $E_{fl}$  is Flexural Modulus,  $L$  represents the support span length,  $P_f$  is the maximum flexural load and  $m$  denotes the slope of the initial linear portion of the load v/s deflection curve.

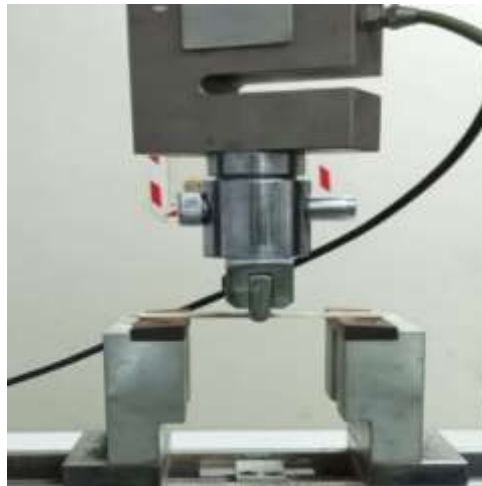


**Figure 5.15** 3 Point Bending Test Setup

### 5.4.2.1 PLAIN NEAT KEVLAR

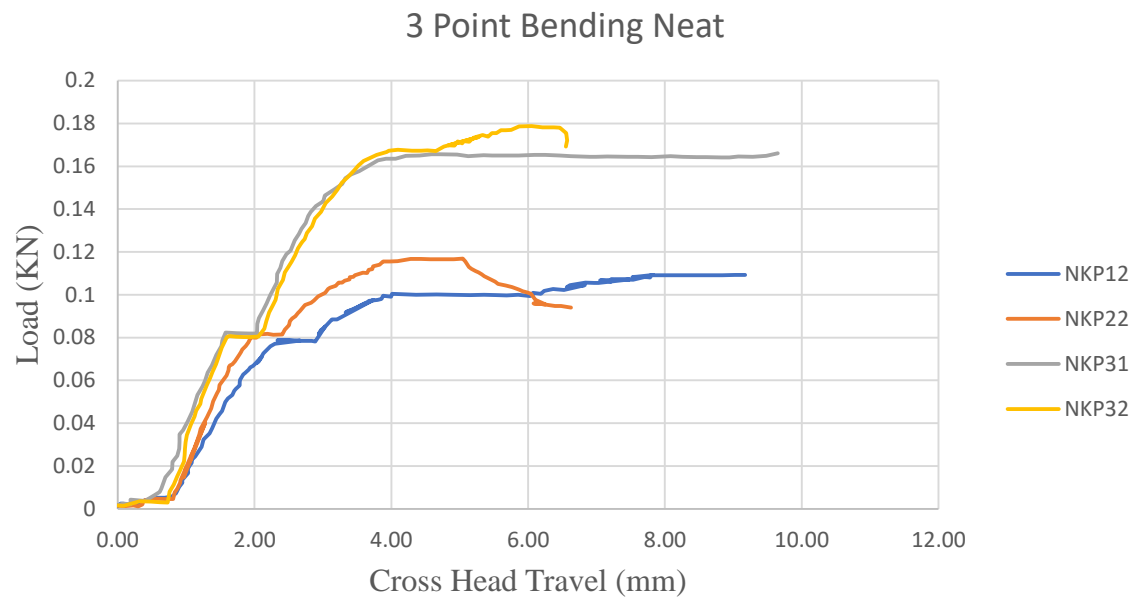


**Figure 5.16** Load v/s Cross Head Travel for Neat Kevlar Specimens

### 5.4.2.3 ALUMINA 1% + 0.25% MWCNT

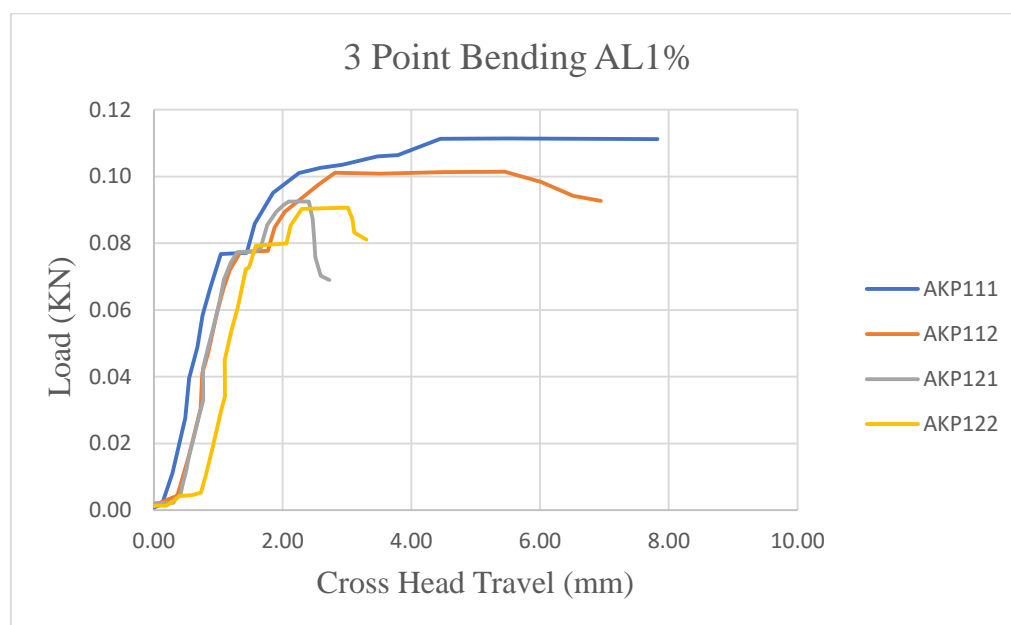


**Figure 5.17** Load v/s Cross Head Travel for 1% Alumina + 0.25% MWCNT infused Kevlar Specimens



#### 5.4.2.4 ALUMINA 3% + 0.25% MWCNT

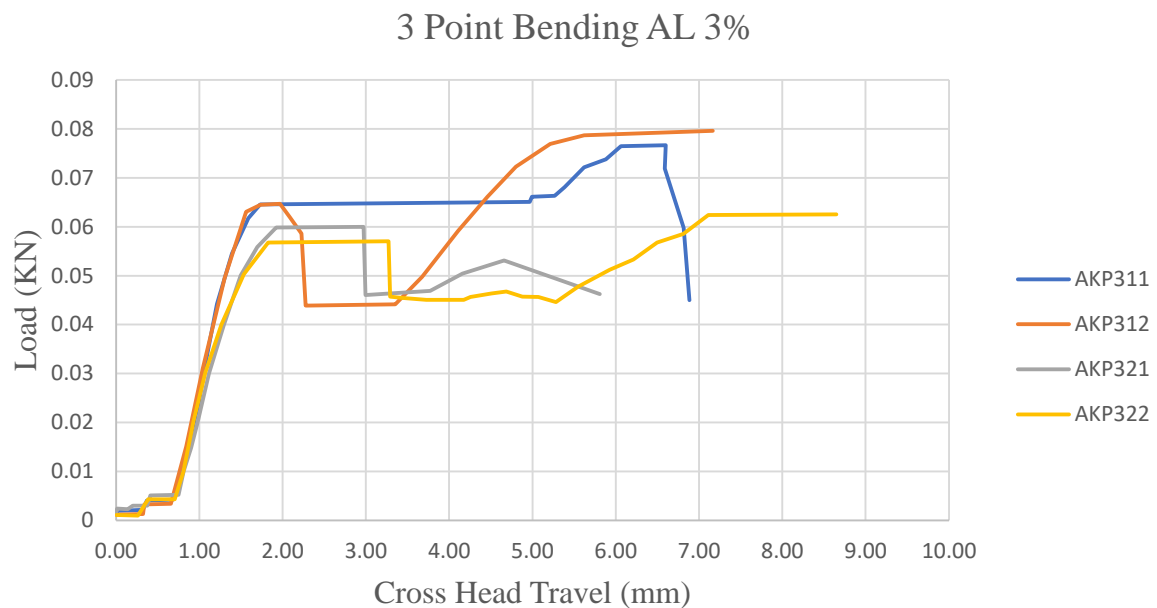


**Figure 5.18** Load v/s Cross Head Travel for 3% Alumina + 0.25% MWCNT infused Kevlar Specimens

#### 5.4.2.5 ALUMINA 6% + 0.25% MWCNT

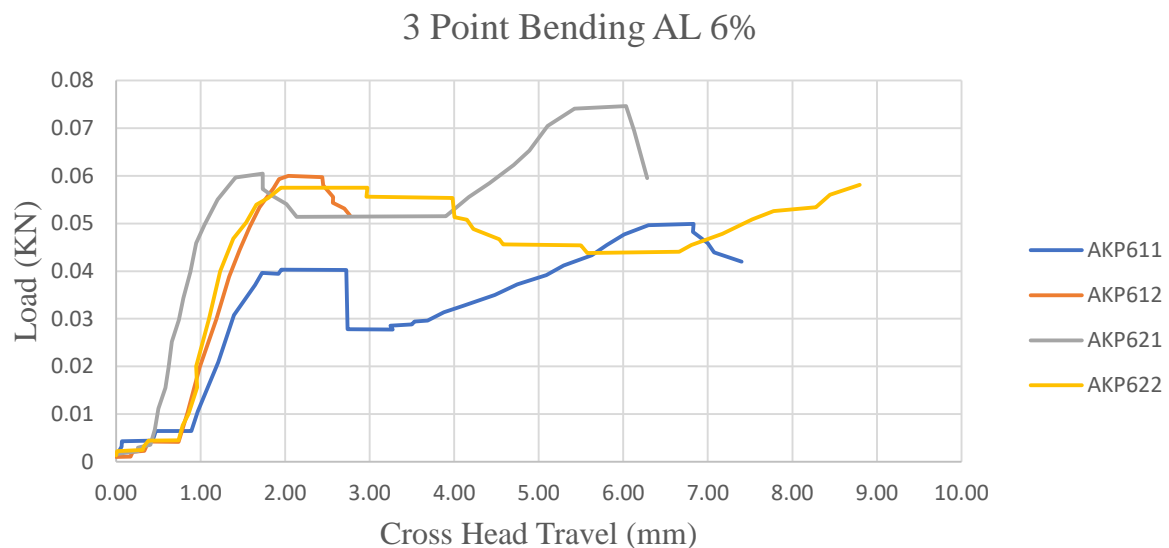


**Figure 5.19** Load v/s Cross Head Travel for 3% Alumina + 0.25% MWCNT infused Kevlar Specimens

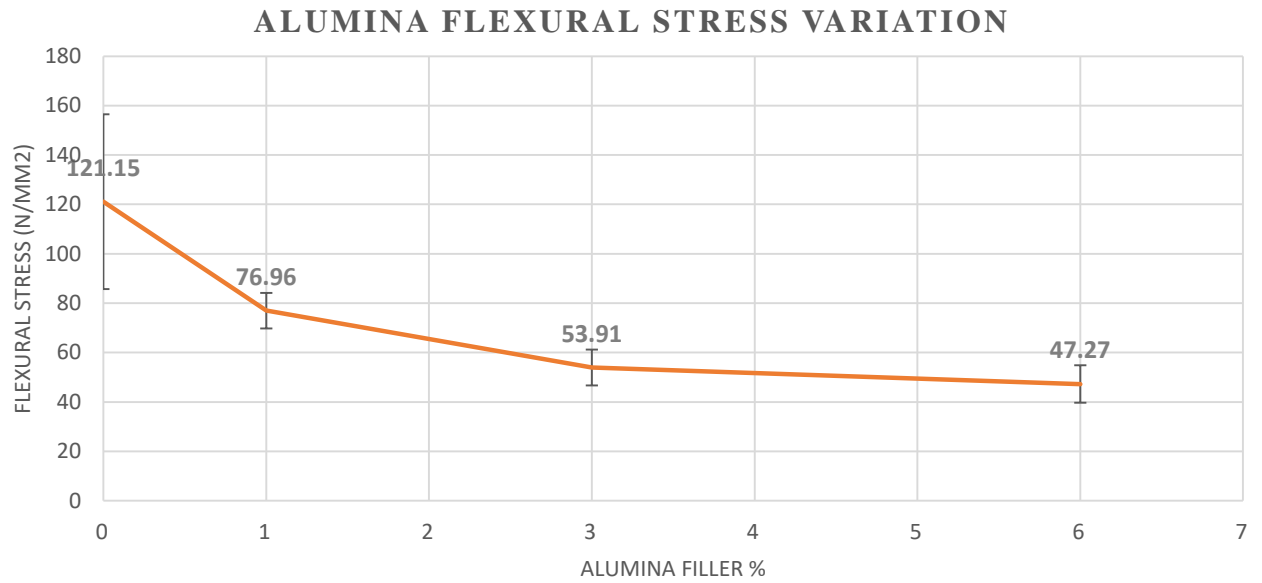


**Figure 5.20** Flexural Stress Variation in different Alumina filler content

**Table 5.5** Flexural Strain Variation in different Alumina filler content

ALUMINA Flexural Strain Variation	
Filler %	Flexural Strain
0	0.08 ± 0.02
1	0.05 ± 0.02
3	0.06 ± 0.02
6	0.06 ± 0.02

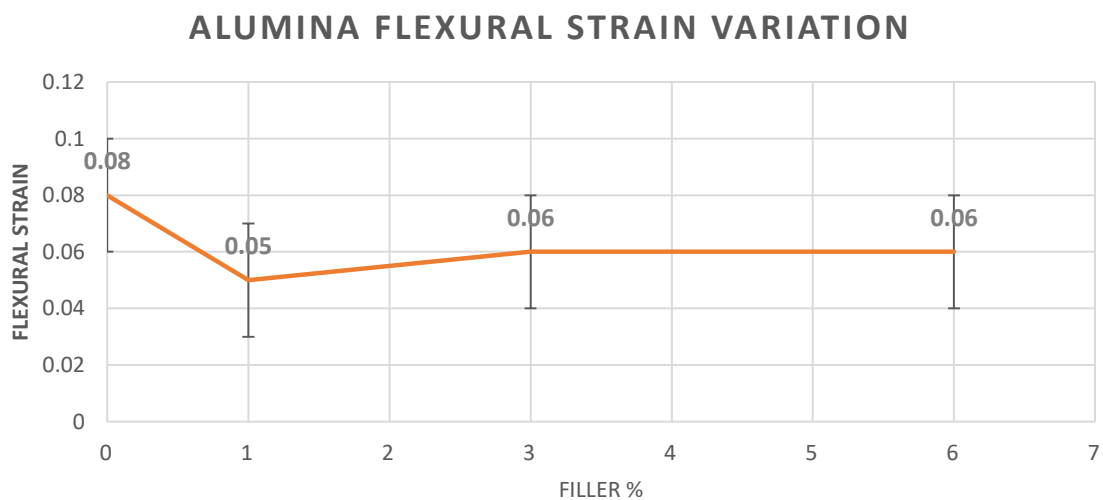


**Figure 5.21** Flexural Strain Variation in different Alumina filler content

**Table 5.6** Flexural Strength Variation in different Alumina filler content

ALUMINA Flexural Strength Variation	
Filler %	Flexural Strength (N/mm <sup>2</sup> )
0	20.27 ± 7.99
1	10.31 ± 5.16
3	9.59 ± 3.28
6	8.07 ± 2.76

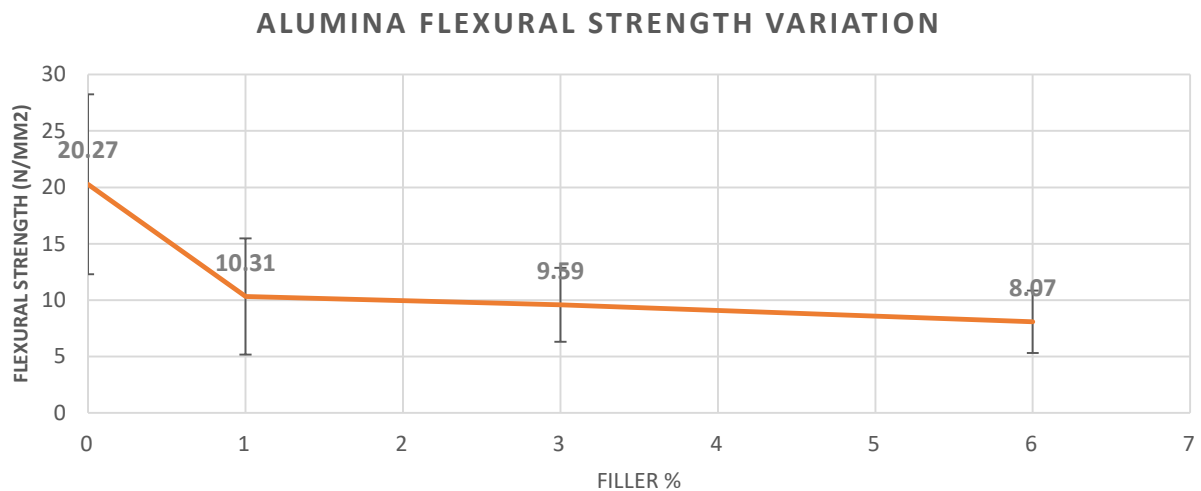


**Figure 5.22** Flexural Strength Variation in different Alumina filler content

Using the Flexural Modulus Formula, put necessary parameters into the formula and calculate it for each set of specimens and further calculate Mean and Standard Deviation and tabulate it. Later compare the Flexural Modulus for Plain Neat Kevlar specimens and Alumina nanofiller with MWCNT infused Kevlar at different ratios.

**Table 5.7** Comparative Analysis of Results obtained by 3 point bending test

S. No	Nanofiller Content	Flexural Stress (N/mm <sup>2</sup> )	Flexural Strain	Flexural Modulus (N/mm <sup>2</sup> )
1	Neat Kevlar	121.15 ± 35.38	0.08 ± 0.02	5990.196 ± 1299.967
2	Alumina 1 % + 0.25 % MWCNT	76.96 ± 7.23	0.05 ± 0.02	6951.904 ± 250.262
3	Alumina 3 % + 0.25 % MWCNT	53.91 ± 7.27	0.06 ± 0.02	4838.277 ± 740.628
4	Alumina 6 % + 0.25 % MWCNT	47.27 ± 7.56	0.06 ± 0.02	4133.626 ± 542.207

Based on the comparative study for 3 Point Bending test done for various Neat Kevlar specimens and Kevlar infused with different percentage of Alumina nanofiller and 0.25% MWCNT specimens, it is concluded that there is gradual decrement in values of Flexural Stress till 6% Alumina filler content. There is not much applicable change in Flexural Strain values with addition of seashell nanofiller content with neat Kevlar. We can see variation in Flexural Modulus as we increase the Alumina nanofiller percentage up to 6% as it increases firstly and then again dips down.

#### 5.4.2.6 Failed Specimens



**Figure 5.23** Failed 3 Point Bending Test Specimens

Failure of Specimen after 3 Point Bending Test

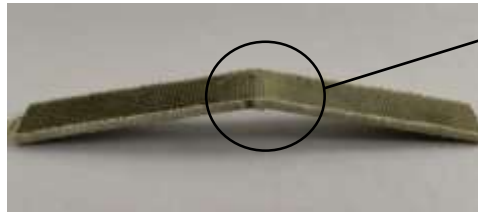


**Figure 5.24** Failed 3 Point Bending Test Specimens

As point load is applied on simply supported beam, it bends in the sagging manner and maximum deflection is at centre of beam. Load is transferred layer by layer and matrix supports the fibers from breaking. Top layers are in compression and bottom layers are in tension. When maximum load bearing point is attained the fiber layers break and matrix interface is sheared and specimen attains U shape.

#### 5.4.3 INTERLAMINAR SHEAR TEST (ILSS) – ASTM D2344

The short beam shear test (ILSS) was conducted in accordance with ASTM D2344 at a cross-head rate of 1 mm/min and the results were reported using the INSTRON universal testing machine. In order to allow for lateral movement, each FMLs specimen was placed on two roller supports, with the load being placed directly in the centre of the FMLs specimen. In this experiment, the beam was loaded until failure occurred, and the failure load was used to calculate the apparent interlaminar shear strength (ILSS) of the specimen.

The length and width of the specimens used for this test as per ASTM D2344 were 40 mm and 15 mm, respectively, with a span length of 24 mm.

After test is performed Load v/s Cross Head Travel graph is plotted for each specimen and Flexural Modulus is calculated for every specimen. Mean and Standard Deviation is calculated and the data is tabulated.

### 5.4.3.1 PLAIN NEAT KEVLAR

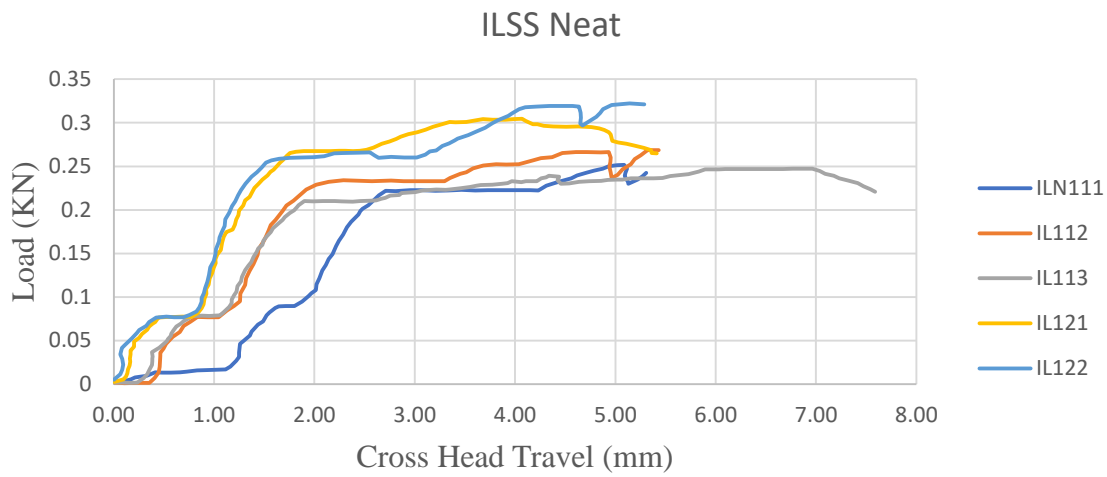


**Figure 5.25** Load v/s Cross Head Travel for Neat Kevlar Specimens of ILSS

### 5.4.3.2 ALUMINA 1% + 0.25% MWCNT

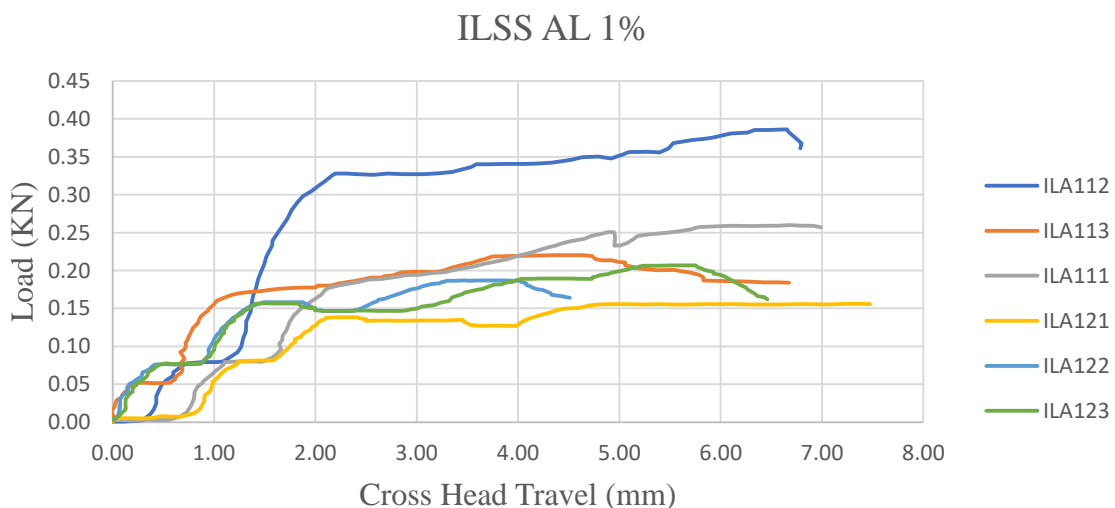


**Figure 5.26** Load v/s Cross Head Travel for 1% Alumina + 0.25% MWCNT infused Kevlar Specimens of ILSS

### 5.4.3.3 ALUMINA 3% + 0.25% MWCNT

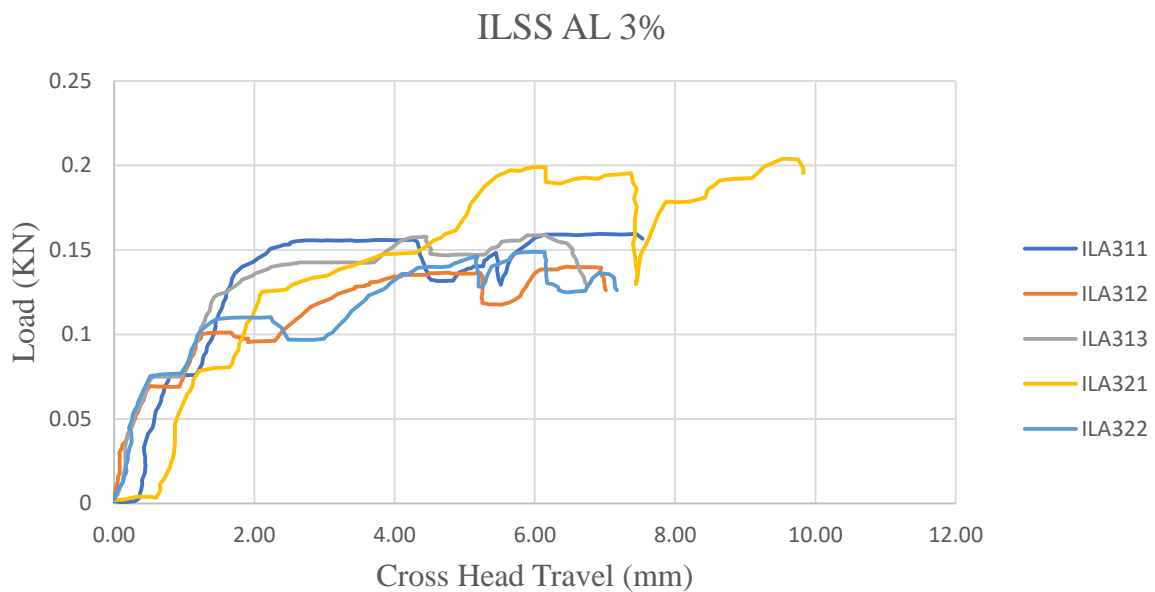


**Figure 5.27** Load v/s Cross Head Travel for 3% Alumina + 0.25% MWCNT infused Kevlar Specimens of ILSS

### 5.4.3.4 ALUMINA 6% + 0.25% MWCNT

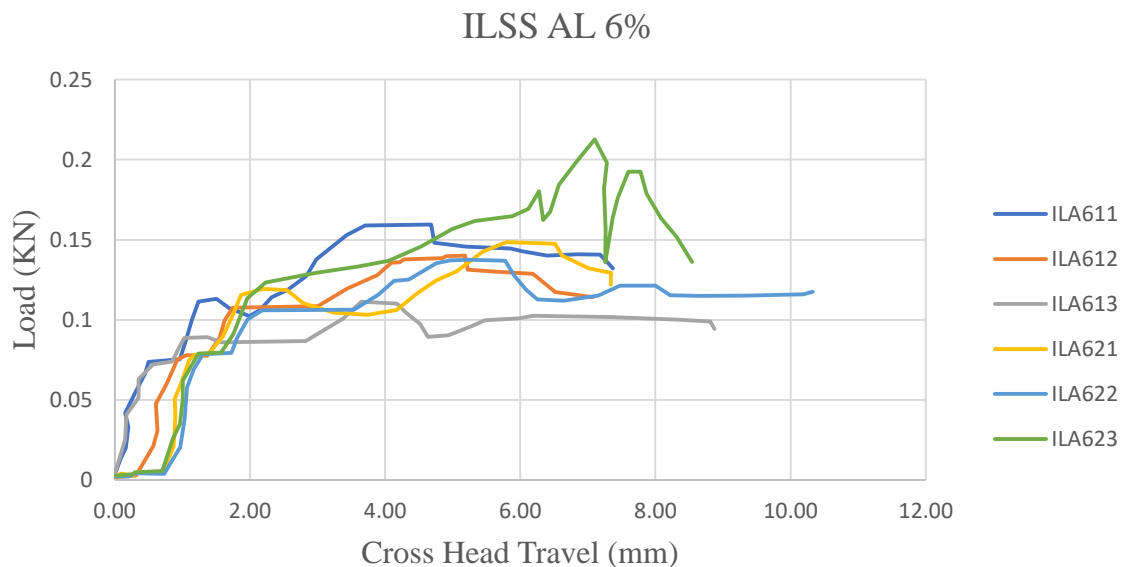


**Figure 5.28** Load v/s Cross Head Travel for 6% Alumina + 0.25% MWCNT infused Kevlar Specimens of ILSS

**Table 5.8** Variation of Interlaminar Shear Strength for different Alumina Fillers content

Variation of Interlaminar Shear Strength for Alumina Fillers	
Filler %	Interlaminar Shear Strength (MPa)
0	$5.78 \pm 0.63$
1	$4.85 \pm 1.71$
3	$3.34 \pm 0.51$
6	$3.15 \pm 0.71$

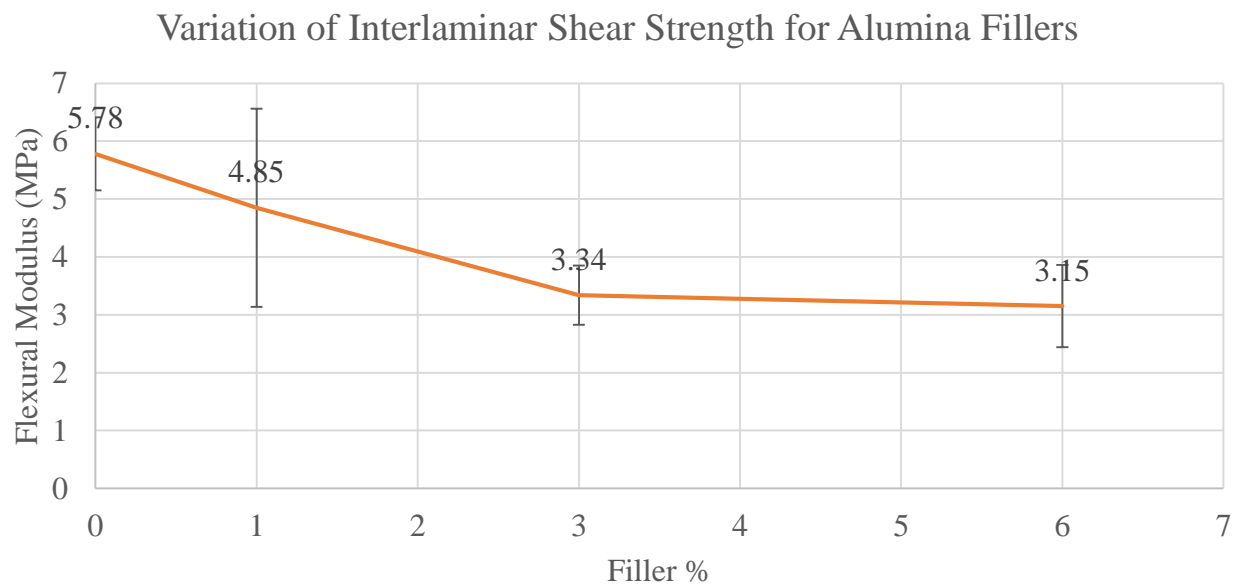


**Figure 5.29** Variation of Flexural Modulus for different Alumina Fillers content



#### 5.4.3.5 Failed Specimens

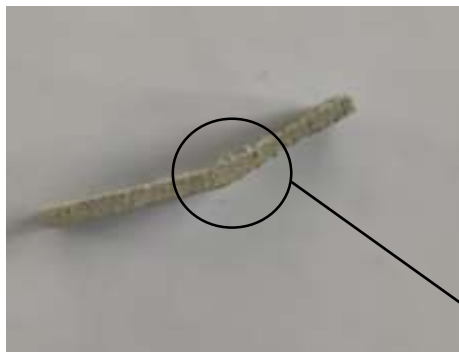


**Figure 5.30** Failed ILSS Test Specimen

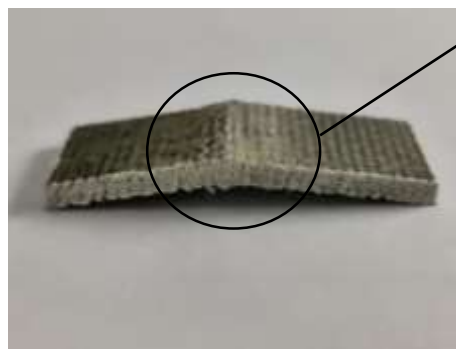


**Figure 5.31** Failed ILSS Test Specimen

Failure of Specimen after ILSS Test

As point load is applied on simply supported beam, it bends in the sagging manner and maximum deflection is at centre of beam. Load is transferred layer by layer and matrix supports the fibers from breaking. Top layers are in compression and bottom layers are in tension. When maximum load bearing point is attained the fiber layers break and matrix interface is sheared and specimen attains U shape.

#### 5.4.4 CHARPY IMPACT TEST – ASTM D256

The Charpy impact test, also known as the Charpy U-notch test, is a standardized high strain-rate test which determines the amount of energy absorbed by a material during fracture. Absorbed energy is a measure of the material's notch toughness. It is widely used in industry, since it is easy to prepare and conduct and results can be obtained quickly and cheaply.

Test procedure and details are already discussed in detail in the **Section 4.5.4** of this report.



**Figure 5.32** Charpy Impact Testing Setup

**Table 5.9** Variation of Impact Strength of different Alumina nano filler content

Alumina Filler %	Energy Absorbed (J)	Impact Strength (MPa)
0	$2.35 \pm 0.55$	31.25
1	$2.88 \pm 0.93$	38.46
3	$3.67 \pm 0.59$	49.01
7	$2.65 \pm 0.45$	35.39

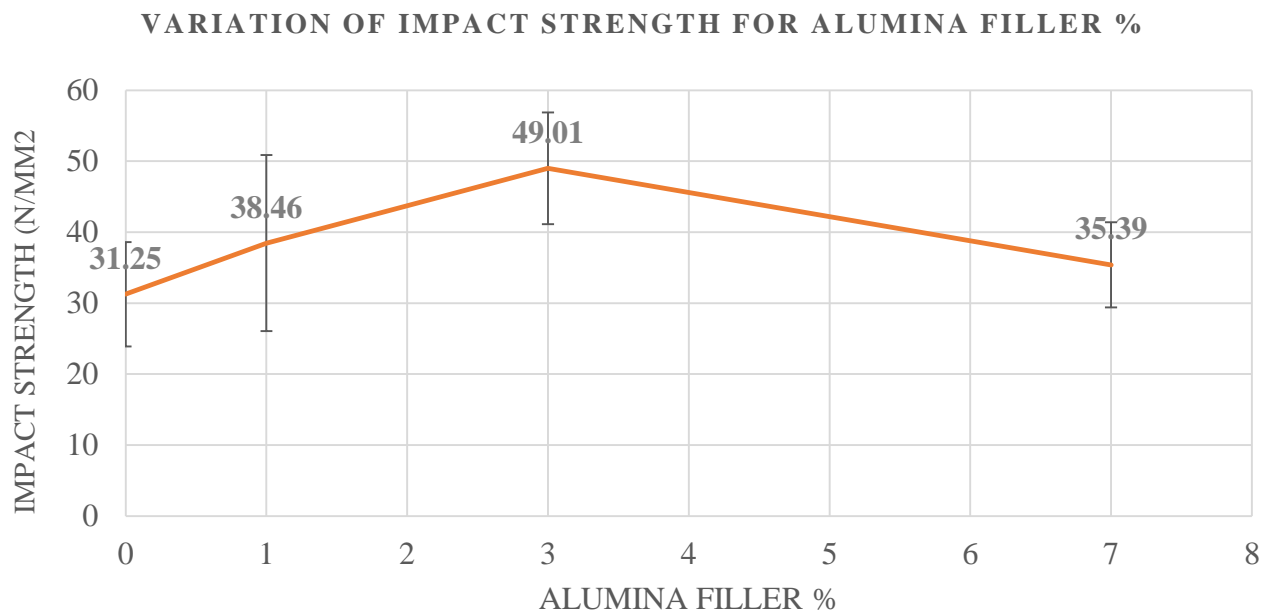


**Figure 5.33** Variation of Impact Strength for different Alumina filler content

Based on the comparative study of Impact Strength of Plain Neat Kevlar with Kevlar infused Alumina Nanofiller with MWCNT specimens it is concluded that with increment in Alumina Nanofiller content till 3% by wt. we can see gradual increasing trend with around 36 % and then again starts to dip up to 7% seashell nanofiller content but still showing greater Impact strength than plain neat Kevlar specimens.

#### 5.4.5 Failed Specimens



**Figure 5.34** Failed Charpy Impact Test Specimen



**Figure 5.35** Failed Charpy Impact Test Specimen

Failure of Specimen  
after Charpy Impact  
Test

V- Notch Specimen is allowed to get Impact from the machine rod, Strain Energy is absorbed and fracture is attained at notch area and specimen is cracked into two halves as shown in Figure 5.34 and Figure 5.35.

#### 5.4.6 SHEAR TEST- ASTM D7078

The effect of seashell nanoparticles on the shear properties of specimens was characterized at the crosshead speed of 2 mm/min by applying a shearing force of the specimen using the SHIMADZU Universal Testing Machine. The length and width of the Kevlar specimens used for this test as per ASTM D7078 were 76 mm and 56 mm, respectively, with a span length of 31 mm. One of the typical setup arrangements is shown in the figure below.



**Figure 5.36** Universal Testing Machine for Shear Test

Test procedure and details are already discussed in detail in the **Section 4.5.6** of this report.



**Figure 5.37** Shear Test Specimen fixed in the testing fixture

### 5.4.6.1 PLAIN NEAT KEVLAR

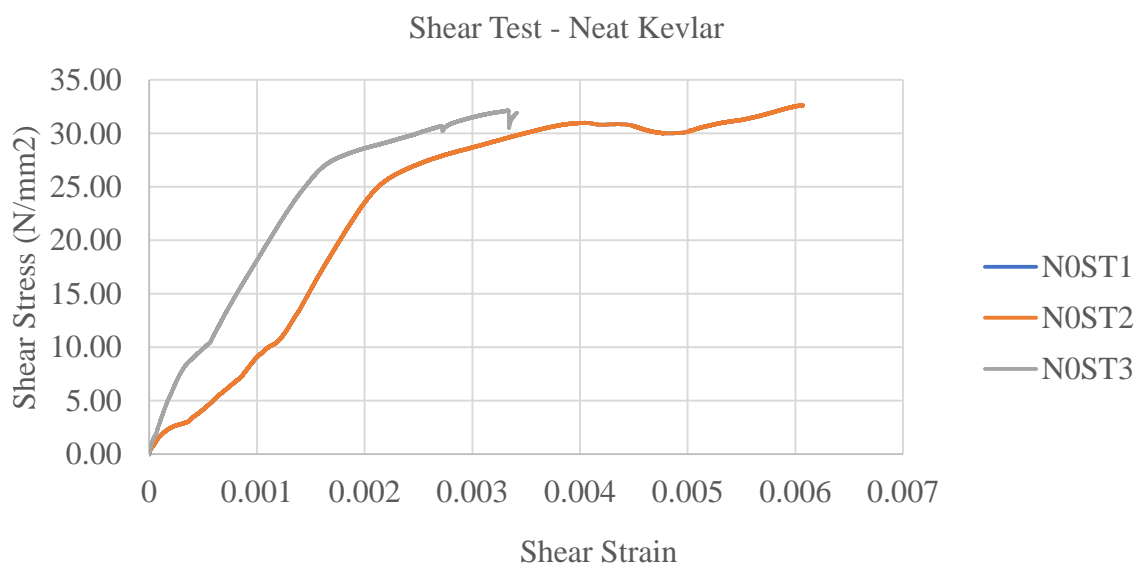


**Figure 5.38** Shear Stress vs Shear Strain Graph for Neat Kevlar Specimens

### 5.4.6.2 ALUMINA 1% + 0.25% MWCNT

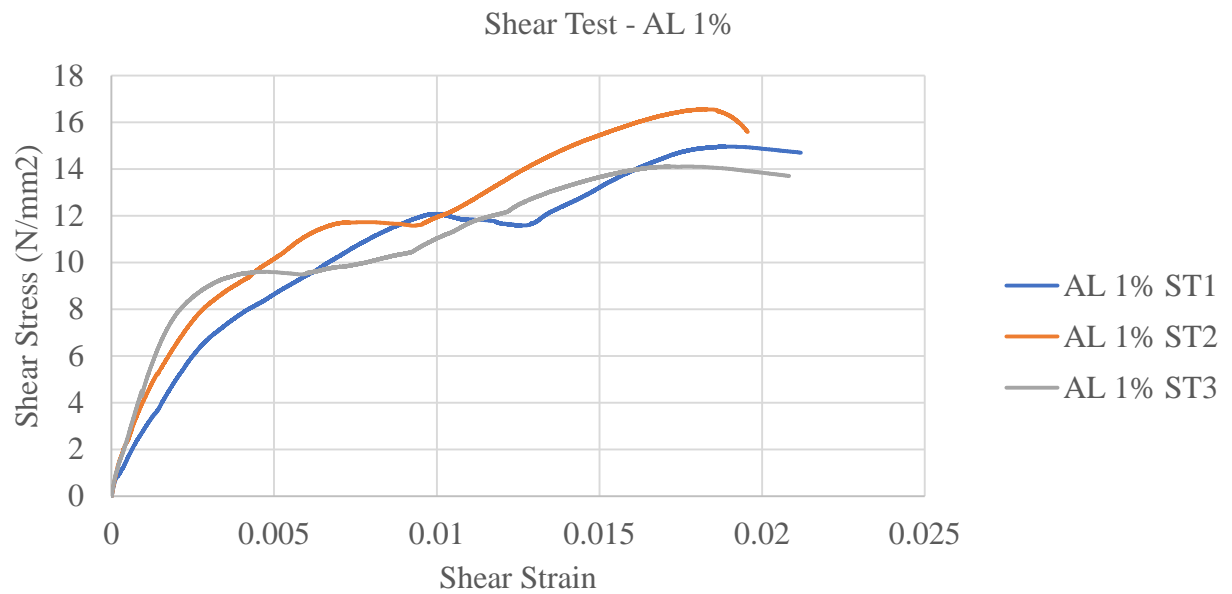


**Figure 5.39** Shear Stress vs Shear Strain Graph for 1% Alumina + 0.25% MWCNT infused Kevlar Specimens

### 5.4.6.3 ALUMINA 3% + 0.25% MWCNT

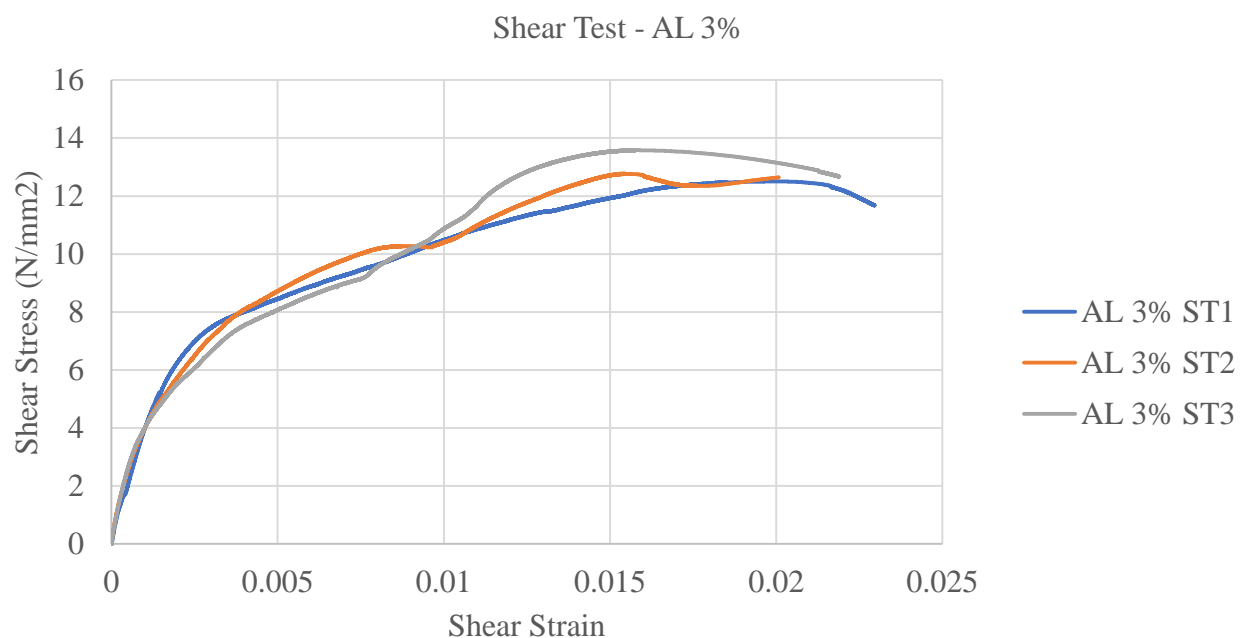


**Figure 5.40** Shear Stress vs Shear Strain Graph for 3% Alumina + 0.25% MWCNT infused Kevlar Specimens

#### 5.4.6.4 ALUMINA 6% + 0.25% MWCNT

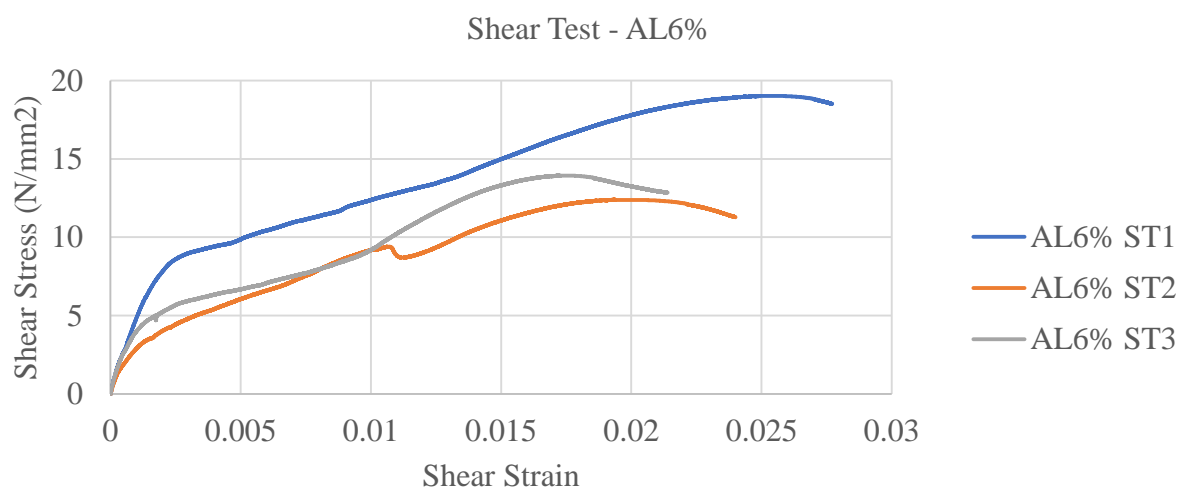


**Figure 5.41** Shear Stress vs Shear Strain Graph for 6% Alumina + 0.25% MWCNT infused Kevlar Specimens

**Table 5.10** Maximum Shear Stress for different nanofiller content

S.No	Nanofiller Content	Mean $\pm$ SD
1	Neat Kevlar	32.468 $\pm$ 0.242
2	Alumina 1 % + 0.25 % MWCNT	15.211 $\pm$ 1.013
3	Alumina 3 % + 0.25 % MWCNT	12.954 $\pm$ 0.461
4	Alumina 6 % + 0.25 % MWCNT	15.118 $\pm$ 2.833

Based on the comparative study of Maximum Shear Stress of Plain Neat Kevlar with Kevlar infused Alumina Nanofiller with MWCNT specimens it is concluded that with increment in Alumina Nanofiller content till 3% by wt. we can see gradual decreasing trend and then again starts to increase when it comes to 6% Alumina nanofiller content with values close to that of Alumina 1% nanofiller infused Kevlar specimens.

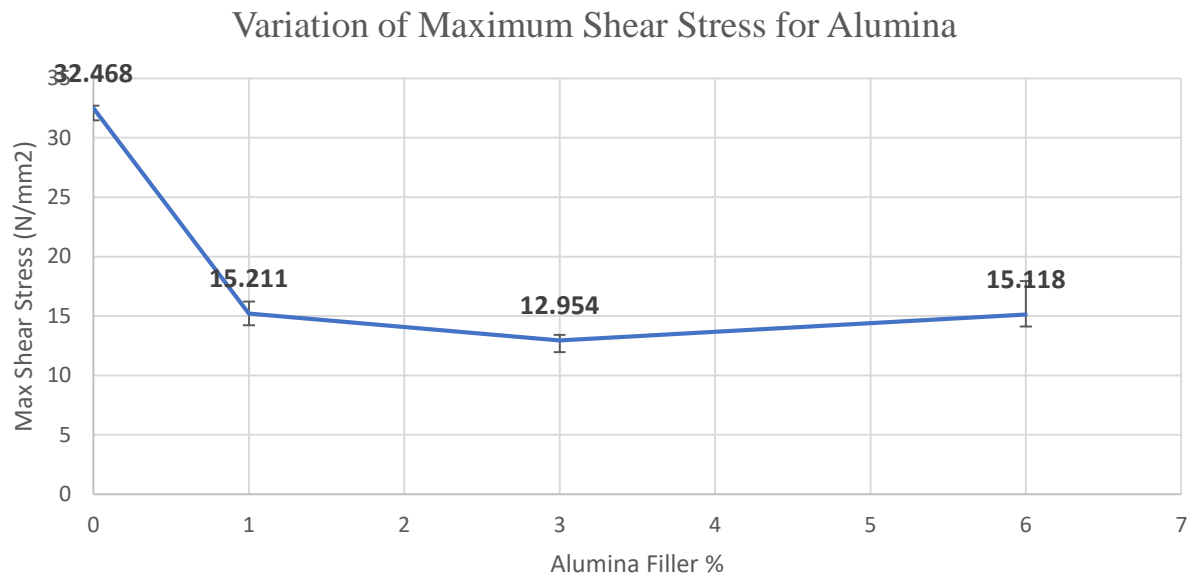


**Figure 5.42** Variation of Maximum Shear Stress for different Alumina filler content

#### 5.4.6.4 Failed Specimens

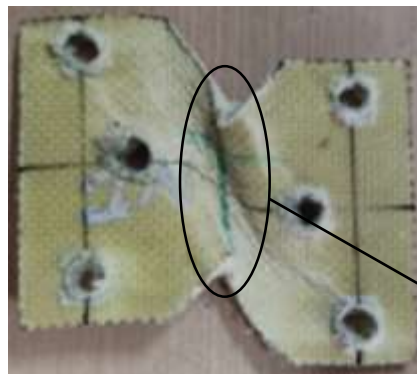


**Figure 5.43** Failed Shear Test Specimen

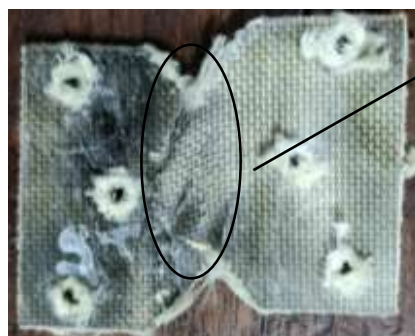


**Figure 5.44** Failed Shear Test Specimen

Failure of Specimen after Shear Test

As the fixture with shear test specimen is allowed to pull, inter laminar fibres shear with matrix interface. Shearing occurs at central axis of Shearing length. After maximum shear load bearing capacity of the fibre-matrix, complete deformation of the sample is seen.

## **5.5 SUMMARY**

In this chapter we have discussed about

- General Introduction to Alumina with morphological study of nano alumina involving XRD & SEM Imaging and EDS of nano alumina.
- Fabrication of neat Kevlar and nano alumina infused Kevlar composites plates is been explained in great detail.
- Mechanical and Impact test analysis for the specimens is done which includes namely Tensile Test, 3 Point Bending Test, ILSS Test, Charpy Test and Shear Test to study the mechanical and impact property variation after adding alumina nanofiller to neat Kevlar.



# CHAPTER 6

## CONCLUSION & FUTURE WORKS

### 6.1 SUMMARY

It has been observed that symmetric laminates produce better results. Composites containing 0.25 percent wt. MWCNT demonstrated the best flexural performance and absorbed the most impact energy. Because of the presence of stiff filler material, the inclusion of nanofillers changed the material failure behaviour from ductile to brittle. Agglomeration occurs when the concentration of nanofiller increases. To understand the performance of composite material, it is very significant to investigate its mechanical, Impact, fatigue behaviour, and morphological properties. In this work, an attempt has been made in studying the material behaviour of neat Kevlar along with the infusion of nano additives like alumina, seashell, and MWCNT in varying proportions. Based on the obtained experimental values, graphs were plotted to demonstrate the variation of properties when these infusions were made. There is a significant improvement in the Modulus values of the material, Ultimate tensile strength and Impact strength after the incorporation of the nano additives.

### 6.2 CONCLUSION

The Conclusions are as follows:

- For the combination of Seashell + MWCNT, it is also found that Ultimate Tensile Strength is considerably improved. It was observed that, that there is a 15.96% improvement in Seashell 1% + 0.25% wt. MWCN, 21% improvement in Seashell 3% + 0.25% wt. MWCNT and 29.78% improvement in Seashell 7% + 0.25% wt. MWCNT compared to neat aramid fibre composite specimen.

- The Ultimate Tensile Strength was improved by 0.32% in Alumina 1% + 0.25% wt. MWCNT, 21% improvement was found in Alumina 3% + 0.25% wt. MWCNT and 28.86% improvement in alumina 6 % + 0.25% wt. MWCNT compared to neat aramid fibre composite specimen.
- The Young's Modulus was improved by 4.42% in Seashell 1% + 0.25% wt. MWCNT, 17.7% improvement is seashell 3% + 0.25% wt. MWCNT and 26% improvement in Seashell 7% + 0.25% wt. MWCNT compared to neat aramid fibre composite specimen.
- The Young's Modulus was improved by 5.14% in Alumina 1% ASTMD 256 6.97% improvement in Alumina 3% + 0.25% wt. MWCNT and 6.1% improvement in Alumina 6% + 0.25% wt. MWCNT compared to the neat aramid fibre composite specimen.
- The Impact strength was evaluated by performing Charpy Impact Test (ASTMD 256). It was found that there is a 12% improvement in Seashell 1% + 0.25% wt. MWCNT, for Seashell 3% + 0.25% wt. MWCNT, there is a 50% increment in the Impact Strength value.
- It is also seen that impact properties have significantly improved when the combination of Alumina + MWCNT was added. There is a 23.072% rise in Alumina 1% + 0.25% wt. MWCNT and 56.83% improvement in Alumina 3% + + 0.25% wt. MWCNT compared to its neat aramid fibre composite specimen.

### **6.3 FUTURE WORKS**

- Experimentation and study of bullet Penetration Test for investigation of ballistic performance in defence and aerospace applications.

## **CHAPTER 8**

### **REFERENCES**

1. S Ilangovan, S Senthil Kumaran, A Vasudevan, K Naresh. "Effect of silica nanoparticles on mechanical and thermal properties of neat epoxy and filament wounded E-glass/epoxy and basalt/epoxy composite tubes" , Materials Research Express, 2019
2. Sanmartín C, Font M, Palop JA. Molecular symmetry: a structural property frequently present in new cytotoxic and proapoptotic drugs. *Mini Rev Med Chem*. 2006 Jun; 6(6):639-50. doi: 10.2174/138955706777435652. PMID: 16787374.
3. Peters, S.T. (2006). Ten common mistakes in composite design and manufacture and how to avoid them. *Sampe Journal*. 42. 53-59.
4. Dametew AW (2017) Design and Empirical Analysis of Selected Machine Elements from Composite Materials is better to Use. *Int J Swarm Intel Evol Comput* 6: 157. doi: 10.4172/2090-4908.1000157.
5. Ferreira, J. A. M., Reis, P. N. B., Costa, J. D. M., & Richardson, M. O. W. (2013). Fatigue behaviour of Kevlar composites with nanoclay-filled epoxy resin. *Journal of composite materials*, 47(15), 1885-1895.
6. Erklığ, A., & Bulut, M. (2017). Experimental investigation on tensile and Charpy impact behavior of Kevlar/S-glass/epoxy hybrid composite laminates. *Journal of Polymer Engineering*, 37(2), 177-184.
7. Salman, S. D., Sharba, M. J., Leman, Z., Sultan, M. T., Ishak, M. R., & Cardona, F. (2016). Tension-compression fatigue behavior of plain woven kenaf/kevlar hybrid composites. *BioResources*, 11(2), 3575-3586.
8. Singh, T. J., & Samanta, S. (2015). Characterization of Kevlar fiber and its composites: a review. *Materials Today: Proceedings*, 2(4-5), 1381-1387.

9. Gokuldass, R., & Ramesh, R. (2019). Mechanical strength behavior of hybrid composites tailored by glass/Kevlar fibre-reinforced in nano-silica and micro-rubber blended epoxy. *Silicon*, 11(6), 2731-2739.
10. Lafitte, M. H., & Bunsell, A. R. (1982). The fatigue behaviour of Kevlar-29 fibres. *Journal of Materials Science*, 17(8), 2391-2397.
11. Naik, S., Dandagwhal, R. D., & Loharkar, P. K. (2020). A review on various aspects of Kevlar composites used in ballistic applications. *Materials Today: Proceedings*, 21, 1366-1374.
12. Bencomo-Cisneros, J. A., Tejeda-Ochoa, A., García-Estrada, J. A., Herrera-Ramírez, C. A., Hurtado-Macías, A., Martínez-Sánchez, R., & Herrera-Ramírez, J. M. (2012). Characterization of Kevlar-29 fibers by tensile tests and nanoindentation. *Journal of Alloys and Compounds*, 536, S456-S459.
13. Manero II, A., Gibson, J., Freihofer, G., Gou, J., & Raghavan, S. (2015). Evaluating the effect of nano-particle additives in Kevlar® 29 impact resistant composites. *Composites Science and Technology*, 116, 41-49.
14. Sorrentino, L., Bellini, C., Corrado, A., Polini, W., & Aricò, R. (2014). Ballistic performance evaluation of composite laminates in kevlar 29. *Procedia Engineering*, 88, 255-262.
15. Kumar, L., Alam, S. N., & Sahoo, S. K. (2021). Influence of nanostructured Al on the mechanical properties and sliding wear behavior of Al-MWCNT composites. *Materials Science and Engineering: B*, 269, 115162.
16. Gemi, L., Yazman, S., Uludağ, M., Dispinar, D., & Tiryakioğlu, M. (2017). The effect of 0.5 wt% additions of carbon nanotubes and ceramic nanoparticles on tensile properties of epoxy-matrix composites: a comparative study. *Mater. Sci Nanotechnol*.
17. Montazeri, A., Javadpour, J., Khavandi, A., Tcharkhtchi, A., & Mohajeri, A. (2010). Mechanical properties of multi-walled carbon nanotube/epoxy composites. *Materials & Design*, 31(9), 4202-4208.

- 18.Karthick, R., Sirisha, P., & Sankar, M. R. (2014). Mechanical and tribological properties of PMMA-sea shell based biocomposite for dental application. *Procedia materials science*, 6, 1989-2000.
- 19.Mohammad, W. A. S. B. W., Othman, N. H., Ibrahim, M. H. W., Rahim, M. A., Shahidan, S., & Abd Rahman, R. (2017, November). A review on seashells ash as partial cement replacement. In *IOP Conference Series: Materials Science and Engineering* (Vol. 271, No. 1, p. 012059). IOP Publishing.
- 20.Ramnath, B. V., Jeykrishnan, J., Ramakrishnan, G., Barath, B., & Ejoelavendhan, E. (2018). Sea shells and natural fibres composites: a review. *Materials Today: Proceedings*, 5(1), 1846-1851.
- 21.Li, X. (2007). Nanoscale structural and mechanical characterization of natural nanocomposites: Seashells. *Jom*, 59(3), 71-74.
- 22.Vasanthkumar, P., Senthilkumar, N., Palanikumar, K., & Rathinam, N. (2019). Influence of Seashell addition on thermo-mechanical properties of Nylon 66 polymer matrix composite. *J New Mater Electrochem Syst*, 22(1), 25.
- 23.Mourad, A. H. I., Cherupurakal, N., Hafeez, F., Barsoum, I., A Genena, F., S Al Mansoori, M., & A Al Marzooqi, L. (2020). Impact strengthening of laminated kevlar/epoxy composites by nanoparticle reinforcement. *Polymers*, 12(12), 2814.
- 24.Belgacemi, R., Derradji, M., Trache, D., Mouloud, A., Zegaoui, A., Mehelli, O., & Khiari, K. (2020). Effects of silane surface modified alumina nanoparticles on the mechanical, thermomechanical, and ballistic impact performances of epoxy/oxidized UHMWPE composites. *Polymer Composites*, 41(11), 4526-4537.
- 25.Zhang, H., Tang, L., Liu, G., Zhang, D., Zhou, L., & Zhang, Z. (2010). The effects of alumina nanofillers on mechanical properties of high-performance epoxy resin. *Journal of nanoscience and nanotechnology*, 10(11), 7526-7532.

26. Raghavendra, G., Ojha, S., Acharya, S. K., & Pal, S. K. (2015). Influence of micro/nanofiller alumina on the mechanical behavior of novel hybrid epoxy nanocomposites. *High Performance Polymers*, 27(3), 342-351.
27. George Lubin, *Handbook of composites*, Springer, Boston, MA, <https://doi.org/10.1007/978-1-4615-7139-1>.
28. Pelzl, Bernhard; Wolf, Rainer; Kaul, Bansi Lal (2018). "Plastics, Additives". *Ullmann's Encyclopedia of Industrial Chemistry*. Weinheim: Wiley-VCH. pp. 1–57. doi:10.1002/14356007.a20\_459.pub2.
29. Yevgen Mamunya (2011). Carbon Nanotubes as Conductive Filler in Segregated Polymer Composites-Electrical Properties, *Carbon Nanotubes - Polymer Nanocomposites*, Dr. Siva Yellampalli (Ed.), ISBN: 978-953-307-498-6.
30. *Handbook of Composites*, S.T. Peters, Springer, Boston, MA, <https://doi.org/10.1007/978-1-4615-6389-1>.
31. Vinay SS, Sanjay MR, Siengchin S, Venkatesh CV. Effect of Al<sub>2</sub>O<sub>3</sub> nanofillers in basalt/epoxy composites: Mechanical and tribological properties. *Polymer Composites*. 2021;42:1727–1740. <https://doi.org/10.1002/pc.25927>.

## APPENDIX

- Abstract of the paper has been submitted to International Conference on Material Science & Engineering (ICMSE) 2022 on 30<sup>th</sup> April 2022 and has been accepted.

### Abstract acceptance Inbox x

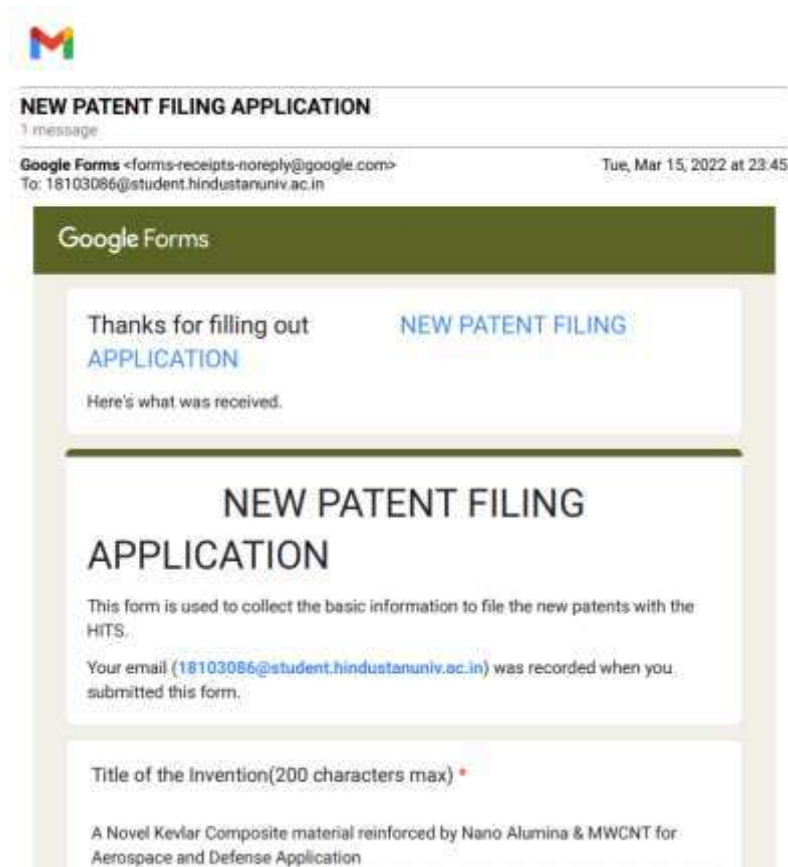
**ICMSE-2022** <icmse2022@easychair.org>

to Rishi ▾

Dear Participant,

We are glad to accept your abstract for ICMSE-2022

- The paper has been checked for plagiarism.
- First copyright patent on the combination of Nano Alumina + MWCNT has been filed from the Institute.



The image shows a screenshot of a Gmail interface. At the top is the Gmail logo. Below it, the email header reads "NEW PATENT FILING APPLICATION" with "1 message" underneath. The sender is "Google Forms <forms-receipts-noreply@google.com>" and the recipient is "To: 18103086@student.hindustanuniv.ac.in". The date and time are "Tue, Mar 15, 2022 at 23:45". The email body contains a "Google Forms" header, followed by "Thanks for filling out NEW PATENT FILING APPLICATION" and "Here's what was received:". Below this is a preview of the form titled "NEW PATENT FILING APPLICATION". The form text states: "This form is used to collect the basic information to file the new patents with the HITS. Your email (18103086@student.hindustanuniv.ac.in) was recorded when you submitted this form." The first question is "Title of the Invention(200 characters max) \*", and the answer provided is "A Novel Kevlar Composite material reinforced by Nano Alumina & MWCNT for Aerospace and Defense Application".

# PLAGIARISM REPORT

---

**Submission date:** 04-May-2022 10:35AM (UTC+0530)

**Submission ID:** 1827851142

**File name:** Re\_Report\_for\_Plug\_Check\_-\_FYP\_Rishi.pdf (2.24M)

**Word count:** 13876

**Character count:** 64983

## Final Report

---

### ORIGINALITY REPORT

---

**17**%

SIMILARITY INDEX

%

INTERNET SOURCES

**17**%

PUBLICATIONS

%

STUDENT PAPERS

---